Ring-opening polymerisation of ε-substituted-ε-caprolactones towards novel, semi-crystalline functional polyesters

by

SIOBHAN GEMMA KILBRIDE

A thesis submitted to the University of Birmingham for the degree of DOCTOR OF PHILOSOPHY

School of Chemistry
College of Engineering and Physical Sciences
University of Birmingham
September 2020

UNIVERSITY OF BIRMINGHAM

Note: Please sign this form and present it to the Bindery with your thesis, so that it can be bound at the front of the Library deposit copy

RESEARCH THESIS
Author's Declaration

Full name (block capitals, surname first): KILBRIDE, SIOBHAN GEMMA

Full title of thesis/dissertation (block capitals): RING-OPENING POLYMERISATION OF ε-SUBSTITUTED-ε-CAPROLACTONES TOWARDS NOVEL, SEMI-CRYSTALLINE FUNCTIONAL POLYESTERS

College/School/Department (block capitals): SCHOOL OF CHEMISTRY, COLLEGE OF ENGINEERING AND PHYSICAL SCIENCES

Date of award of degree (leave blank):

1. I understand that one printed and one electronic copy of my thesis/dissertation (the Work) will be deposited in the University Library (the Library) and in a suitable electronic repository, for permanent retention.
2. Without changing the content, the Library or any third party with whom it has an agreement to do so, may convert either copy into a format or medium for the purpose of long-term retention, accessibility and preservation.
3. The Library will publish, and/or arrange with appropriate third parties for the non-exclusive publication of, a bibliographic description of the thesis/dissertation, and the author's abstract.
4. Unless arrangements are made to the contrary, (see paragraph 6. below), the Library is authorised to make the Work available for consultation in the Library, and via a recognised inter library loans system. The Library is authorised to make the electronic copy of the Work freely accessible to individuals and institutions - including automated agents - via the Internet.
5. Rights granted to the University of Birmingham through this agreement are entirely non-exclusive. I retain all my rights in the Work in its present version or future derivative works.
6. I understand that I may apply to the University to retain the right to withhold access to the content of my thesis/dissertation. Access to the paper version may be withheld for a period which shall not normally exceed four calendar years from the congregation at which the degree is conferred. The actual length of the period will be specified in the application, together with the precise reasons for making that application. The electronic copy may be withheld from dissemination via the web or other networks for any period.
7. I have obtained permission for any use made of substantial amounts of published or unpublished copyright material (text, illustrations, etc) where the rights are owned by a third party, other than as permitted under either The Copyright Designs and Patents Act 1988 (as modified by any related or successor legislation) or the Terms and Conditions of any Licence governing its use.
8. The content of the copies I shall deposit with the Library will be the final version of my thesis, as approved by the Examiners.
9. I understand that the Library and administrators of any electronic theses repository do not hold any obligation to take legal action on behalf of myself, or other rights holders, in the event of a breach of intellectual property rights, or any other right, in the material deposited.
10. I understand that, in the event of my thesis/dissertation being not approved by the Examiners, this declaration will become null and void.

Signature:  **Date:** 14 SEP 2020

For Library use (please leave blank):

Classmark: **Accession number:** **Control number:**

eTheses Repository url:

Table of Contents

List of figures

List of schemes

List of tables

List of abbreviations

[M]	Concentration of cyclic monomer
AMM	Activated monomer mechanism
ATRP	Atom transfer radical polymerisation
BINOL	Binaphthol
BnOH	Benzyl alcohol
CDSA	Crystallisation-driven self-assembly
CRP	Controlled radical polymerisation
DASA	Donor-acceptor Stenhouse adducts
DBTDL	Dibutyltin dilaurate
DBU	1,8-Diazabicyclo[5.4.0]undec-7-ene
$Đ_M$	Dispersity
DMAP	4-(Dimethylamino)pyridine
DP	Degree of polymerisaton
DPP	Diphenyl phosphate
DSC	Differential scanning calorimetry
ee	Enantiomeric excess
ELSD	Evaporative light scattering detector
FTIR	Fourier transform infrared
GC	Gas-chromatography
GC-MS	Gas chromatography-mass spectrometry
H_0	Hammett acidity
HCl	Hydrochloric acid
HOTf	Trifluoromethanesulfonic acid
HPLC	High-performance liquid chromatography
HRMS	High resolution mass-spectrometry
LA	Lactide

LDA	Lithium diisopropylamide
LLA	L-Lactide
MAC	Methyl allyl carbonate
MALDI	Matrix-assisted laser desorption ionisation
*m*CPBA	*meta*-Chloroperoxybenzoic acid
M_n	Number average molecular weight
MSA	Methanesulfonic acid
NHC	*N*-Heterocyclic carbene
NMR	Nuclear magnetic resonance
PCL	Poly(ε-caprolactone)
PDL	Poly(ε-decalactone)
P_i	Probability of an isotactic diad
PLA	Polylactide
PLLA	Poly(L-lactide)
ppm	Parts per million
PVL	Poly(δ-valerolactone)
PεSεL	Poly(ε-substituted-ε-caprolactone)
R	Gas constant
ROP	Ring-opening polymerisation
SEC	Size-exclusion chromatography
T	Temperature
TBD	1,5,7-triazabicyclo[4.4.0]dec-5-ene
TCE-d_2	Tetrachloroethane-d_2
T_g	Glass transition temperature
TRIP	Tris(isopropyl)
αBnCL	α-Benzyl-ε-caprolactone
αClεCL	α-Chloro-ε-caprolactone
γBrεCL	γ-Bromo-ε-caprolactone
γMeCL	γ-Methyl-ε-caprolactone

ΔG_p	Gibbs free energy of polymerisation
$\Delta H°_p$	Standard enthalpy of polymerisation
$\Delta H°_p$	Standard entropy of polymerisation
δVL	δ-Valerolactone
εBnCL	ε-Benzyl-ε-caprolactone
εCL	ε-Caprolactone
εDL	ε-Decalactone
εHL	ε-Heptalactone
εSεL	ε-Substituted-ε-caprolactone
λ_{max}	Wavelength of maximum absorption

Firstly, I would like to thank my supervisor Professor Andrew Dove, your guidance and assistance over the past three years has been invaluable. Throughout my PhD journey you have motivated me to become the chemist that I am today.

Next, a massive thank you has to go to members of the Dove and O'Reilly groups, both past and present. Having the opportunity to be surrounded by such fantastic scientists has been an experience that will be tough to beat. Moreover, it's safe to say their friendly faces and words of advice have made my PhD achievable. The warmest of thank you goes to Chiara, Kayla, Weems, Sètuhn, Josh, Lucy, Connor, and Laura for the morning coffee catchups, the many (many) evenings spent at Las Iguanas, and for never complaining when I'd drag you along to Selly Oaks finest establishment that is The Goose for many a rememberable night. Oh, and it would be rude of me if I didn't give one more very, *very* special shoutout to the move, flood, and COVID-19 pandemic for keeping everyday a little different, and making me into a more resilient person

I don't think I could write an acknowledgements section without saying thank you to my mum and dad, Paula and Karl. I can't put into words how much you have both sacrificed to get me to where I am today, and I will be eternally grateful for this and can only hope that I can one day pay you back for the selflessness you have displayed towards me throughout my entire life. For an endless supply of memes and TikToks to get me through the tougher days, my sister Chloe has always known how to put a smile on my face when all else has failed. And finally, Thai, Deano, Dexter, and Luna, I can only hope that I have become the human that you all think I am when you greet me at the door with tails wagging at a million miles a minute.

Abstract

This thesis investigates the synthesis of stereoenriched poly(ε-substituted-ε-caprolactones) based on organocatalytic methods. Moreover, the investigation into orthogonally controlled switchable catalysis for ring-opening polymerisation (ROP) is also explored.

Chapter one reviews how substituent placement on a cyclic monomer effects the thermodynamics of the polymerisation. Moreover, an overview of organocatalysts for ROP, including those that display stereoselectivity during the polymerisation, is presented.

Chapter two describes the enantioenriched synthesis and subsequent functionalisation of a ε-substituted-ε-caprolactone (εSεL) monomer. The effect of functionality on the polymerisation is then reviewed. Following this, the thermal properties of the resulting polymer was then analysed.

Chapter three describes the screening of a range of chiral binaphthol-based phosphoric acids as stereoselective catalysts for the ROP of a variety of racemic εSεLs. The steric and electronic properties of the catalysts are investigated to understand how these influence the polymerisation. Moreover, the microstructure of the polymer is evaluated by ^{13}C NMR spectroscopy, and the thermal properties of the resulting polymers are analysed.

Chapter four summarises donor-acceptor Stenhouse adducts as switchable catalysts for the ROP of cyclic esters using light and heat to control the ON and OFF states of the polymerisation.

Chapter five describes the key findings of chapters two to four and presents opportunities for future investigations in the area of research of this thesis.

Chapter six provides the experimental protocols and characterisation data of the compounds and materials prepared in this thesis.

1. Chapter One

Introduction

1.1. Introduction

As the first commercial plastic, Bakelite was first synthesised in the early 1900's by Baekeland[1] and revolutionised the world as a result of its electrical non-conductivity, light-weight, durable, and heat-resistant properties. This breakthrough lead to a radical transformation in industrial plastic production, and despite its large-scale production only dating back to the 1950s, picturing a world without plastics seems near to impossible. Plastics, otherwise known as polymers, have significantly transformed the way we live our day-to-day lives, with plastics now replacing traditional materials such as metal, glass, and wood. The global production of plastics has drastically grown from 1.5 million tonnes in 1950, to 359 million tonnes in 2018.[2, 3] Despite this, plastics of a non-degradable nature have become undesirable for several applications regarding environmental concerns. To avoid a global crisis, there is an increasing need to encourage sustainable and degradable plastics, however, sustainable polymers only constitute <10% of the commercial plastics market.[4]

To slow down the build-up of plastic waste, degradable polymers such as polyesters have quickly become one of the most economically important and widely used synthetic polymers.[5] Polyesters can easily be of processed through melt spinning, injection/blow moulding, and film extrusion leading to their wide usage as packaging materials, textiles *etc*. Moreover, most commodity polyesters are derived from renewable sources such as corn and potato starch. As a consequence of the ester linkages in the polymer backbone, polyesters can be readily degraded *via* hydrolytic or enzymatic pathways into non-toxic small molecules, making polyesters ideal for biological applications. Polyesters can be synthesized through a variety of methods including polycondensation, ring-opening polymerisation (ROP), and free-radical

polymerisation. Whilst being the most commonly used industrial method, polycondensation between diols and diacids provide little control over polymer molecular weights and dispersities, and monomer conversion. Moreover, polycondensations often require harsh polymerisation conditions such as high temperatures and requiring long reaction times to obtain polymers of high molecular weights. As such, alternative methods are preferred to produce polyesters with predictable molecular weights and narrow dispersities. Methods such as ROP provide pathways to predictable and higher molecular weights with narrow dispersities and control over chain-end fidelity meaning research has turned towards ROP for polyester production.

1.2. Ring-opening polymerisation

A polymerisation where a cyclic monomer is polymerised to form a polymer consisting of acyclic repeat units is defined as a ring-opening polymerisation. As an example of a chain-growth polymerisation, most ROP's can be defined as controlled polymerisations which must meet the following criteria:[6]

First order polymerisation kinetics

For a polymerisation to be considered first-order in monomer the relationship between the logarithm of monomer concentration ($\ln([M]_0/[M]_t$) and time must be linear (Figure 1.1a). However, a deviation from linearity such as if the plot curves downwards indicates a decrease in the concentration of the propagating species which suggests either chain termination or other side-reactions hindering the generation of active chain-ends (such as catalyst death) (Figure 1.1b); an upwards curvature indicates an

increase in the concentration of the propagating species, which suggests slow initiation (Figure 1.1c).

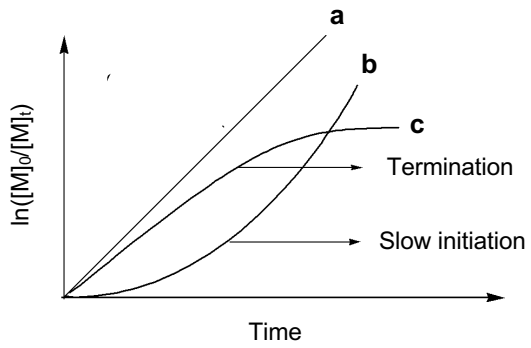

Figure 1.1. Graph of showing a) the linear relationship between $\ln([M]_0/[M]_t)$ against time confirming first-order polymerisation kinetics b) a downwards curvature which indicates a decrease in propagating species and c) an upwards curvature which indicates an increase in propagating species. Adapted from Matyjaszewski and co-workers.[6]

Predictable degrees of polymerisation

Through control of $[\text{monomer}]_0$:$[\text{initiator}]_0$ it is possible to control the degree of polymerisation (DP); moreover, the number-average molecular weight (M_n) should be a linear function of conversion throughout the polymerisation. For these conditions to be met, initiation must be fast enough so that all chains start to grow simultaneously and the number of growing chains remains constant throughout (*i.e.* no chain transfer).

Narrow molecular weight distribution

To obtain a narrow molecular weight distribution (dispersity, $Đ_M$) the following criteria is required:

a) Rate of initiation is at least comparable to the rate of propagation to allow polymer chains to grow simultaneously.

b) Chain transfer and termination must be negligible.

c) Rate of propagation is faster than the rate of depolymerisation to ensure polymerisation is favoured.

Cyclic monomers that are capable of undergoing ROP include, but are not limited to, epoxides,[7, 8] cyclic esters (lactones),[9-12] cyclic phosphates,[13] cyclic siloxanes,[14] and cyclic amides (lactams)[15] *etc.* As a consequence of the large structural diversity of monomers capable of undergoing ROP, there are a range of mechanisms which can occur including coordination, ionic, and enzymatic. However, the ease of polymerisation of a cyclic monomer depends upon thermodynamic factors.

1.2.1. Thermodynamics of a ring-opening polymerisation

The thermodynamics of a ring-opening polymerisation has a strong influence on whether a cyclic monomer will polymerise to yield a linear polymer. Therefore, the polymerisability of a given cyclic monomer is dependent upon the sign of the Gibbs free energy of the polymerisation, which can be defined as:

$$\Delta G_{\mathrm{p}} = \Delta H_{\mathrm{p}}^{\circ} - T\left(\Delta S_{\mathrm{p}}^{\circ} + R\ln[M]\right)$$

where ΔG_{p} is the Gibbs free energy, $\Delta H_{\mathrm{p}}^{\circ}$ is the standard enthalpy of polymerisation, T is the temperature, $\Delta S_{\mathrm{p}}^{\circ}$ is the standard entropy of polymerisation, R is the gas constant, and [M] is the concentration of the cyclic monomer. In accordance with the general rules of thermodynamics, for a polymerisation to be possible the Gibbs free energy must be below zero ($\Delta G_{\mathrm{p}} < 0$). Ideally, for ROP to occur $\Delta H_{\mathrm{p}}^{\circ}$ must be negative ($\Delta H_{\mathrm{p}}^{\circ} < 0$) and $\Delta S_{\mathrm{p}}^{\circ}$ must be positive ($\Delta S_{\mathrm{p}}^{\circ} > 0$). However, if both $\Delta H_{\mathrm{p}}^{\circ}$ and $\Delta S_{\mathrm{p}}^{\circ}$ are positive or negative, temperature and monomer concentration become critical to the polymerisability of a cyclic monomer.

The driving force behind most polymerisations of cyclic monomers results from the release of the monomeric ring strain as a consequence of the deviation from ideal bond angles, and nonbonding interactions between substituents such as angular strain (perturbation of valence angles and inter-atomic distances), conformational perturbation (difference in energy between conformations), and transannular strain (unfavourable interactions of ring substituents on non-adjacent carbons). For a system where monomer-solvent-polymer interactions are negligible, enthalpy can be a representation of monomer ring strain. As such, the ROP of small and medium sized cyclic monomers is usually enthalpically favoured ($\Delta H^{\circ}_{p} < 0$). Conversely, a loss in the translational degrees of freedom leads to a decrease in entropy ($\Delta S^{\circ}_{p} < 0$) and the polymerisation is only energetically allowed when $|\Delta H^{\circ}_{p}| > -T(\Delta S^{\circ}_{p} + R\ln[M])$ is satisfied. As such, the most polymerisable monomers are those with the highest ring strain (3- and 4-membered rings) with ring strain quickly decreasing with increasing ring size (5-membered cyclic esters are the most resistant to polymerisation) as shown with cycloalkanes (Figure 1.2).

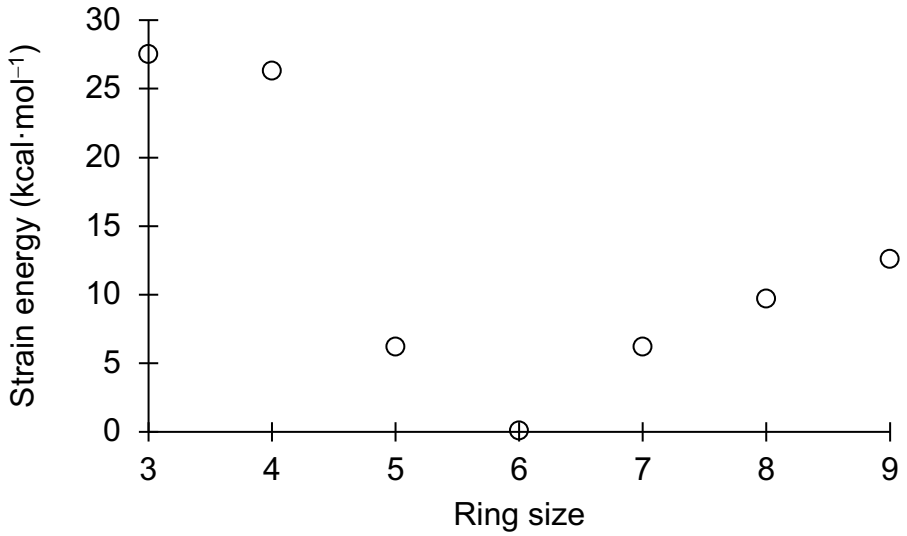

Figure 1.2. Ring strain of common cycloalkanes. Adapted from Anslyn and Dougherty.[16]

1.2.1.1. Substitution pattern effects

The ring-opening polymerisation of a lactone to yield a linear polyester is an example of an isodesmic reaction, where the types of bonds broken during a reaction are the same as those created, this means that differences in the standard enthalpy of the polymerisation are a direct comparison to lactone ring strain. Generally, alkyl substituted lactones possess higher ring-strain compared to their non-substituted counterparts as a result of increased unfavourable interactions such as transannular ring-strain. A recent study by Hillmyer and co-workers[17] investigating the effect of position and length of *n*-alkyl substituents on the ROP of δ-valerolactone (δVL) found that the ROP of substituted δVL was two to three times more entropically disfavoured compared to the ROP of δVL. The change in entropy of a polymerisation is the sum of rotational, vibrational, and translational components. Introducing a side chain decreases the rotational component of entropy through an increase of rigidity in the polymer,[18] rendering the polymerisation of substituted δVL's more thermodynamically

disfavoured. Moreover, the placement of the alkyl substituent on the δVL ring has a higher impact on ring strain (ΔH°_{p}) than the length of the *n*-alkyl substituent.[19] Comparing the placement of a methyl substituent on the δVL ring from the α- to δ-position provided an associated increase in monomer ring strain. Moreover, as the entropic change related to medium-sized lactones is generally unfavourable ($\Delta S^{\circ}_{p} < 0$), the ROP of δ-methyl-δ-valerolactone is more thermodynamically favoured in comparison to α-methyl-δ-valerolactone as a result of the increased monomer ring-strain arising from substituent placement. Overall, this highlights how discrete control over substituent placement can help in favouring polymerisation through manipulation of thermodynamics.

1.2.2. Catalysis for ring-opening polymerisation

Careful catalyst selection is essential to control the physical-chemical properties of the resulting polymer and also to provide cost-effective manufacturing.[20] During the polymerisation a catalyst can influence the resulting polymer stereochemistry and crystallinity, molecular weight, dispersity, and chain composition. This has led to an in-depth understanding of polymerisation catalysts which can generally be split in to three categories; metallic,[21, 22] enzymatic,[23, 24] and organo-based.[25, 26]

1.2.2.1. Metal-based catalysts

Metallic-based complexes, including organometallic and metal alkoxides, are one of the most utilised catalysts for the ROP of lactones as a result of their ease of tuning the ligand and metal centre to optimise polymerisation conditions. Whilst metal-based catalysts produce well-defined polymers, the polymers are usually contaminated with a trace amount of metal impurities which are often difficult to remove leading to major limitations for biomedical and microelectronic related applications.[27, 28] One example is

stannous 2-ethylhexanoate ($Sn(Oct)_2$), which has been demonstrated to effectively polymerise a range of cyclic esters,[29, 30] to yield well-defined polyesters alongside high polymerisation rates. Yet the complete removal of $Sn(Oct)_2$ from the final material is practically impossible.[31] Moreover, metal-based catalysts often require the use of extremely pure monomers and Schlenk conditions leading to increased costs required to produce a controlled polymer.

1.2.2.2. Enzyme catalysts

Derived from natural resources, enzymes have gained increasing attention and can realistically be seen as a more suitable alternative to toxic metal-based catalysts. Enzyme catalysts, such as lipases[32, 33] and proteases,[34] often require mild polymerisation conditions (temperature, pressure, and pH),[35] and can exert high levels of regio- and stereoselectivities. Moreover, enzymes are commonly immobilised on resin beads meaning removal *via* simple gravity filtration is uncomplicated compared to metal-based catalysts. Yet, enzyme catalysed polymerisations often require water as the solvent since organic solvents often lead to enzyme deactivation,[31] increasing the risk of side-reactions during the polymerisation. Additionally, enzymes are only effective for the polymerisation of medium-sized lactones; the polymerisation of larger lactones (> 7-membered lactones) leads to the formation of only oligomers, even after extended reaction times.

1.2.2.3. Organocatalysts

Since the first report in the early 2000s, interest in organocatalysis for the ROP of cyclic esters has grown exponentially.[25, 36-38] Organocatalysis is now a realistic alternative to more traditional methods for ROP such as organometallic catalysis and metal alkoxide initiators which often leave behind metal contaminants in the resultant polymers. In

comparison to metal-based catalysts, the recognition of organocatalysts has surged in recent years as a consequence of their commercial availability, decreased toxicity, increased stability under ambient conditions, and ease of removal from polymers *via* simple precipitation methods. Most organocatalysed polymerisations proceed in a controlled manner yielding polymers with narrow dispersities, good end-group fidelity, and experimental molecular weights in good agreement with calculated values making them a suitable replacement for metal-based ROP catalysts.

The first example of an organocatalysed ROP was reported in 2001 by Hedrick and co-workers for the ROP of lactide.[36] It was discovered that the use of strongly basic amines such as 4-(dimethylamino)pyridine (DMAP) and 4-pyrrolidinopyridine could be used as powerful alternatives to more traditional organometallic catalysts such as tin, aluminium, and lanthanide alkoxides.[21, 39, 40] Under ambient conditions polylactide (PLA) was synthesized with predictable molecular weights and narrow dispersities ($Đ_M$ ≤ 1.16) whilst maintaining reasonable reaction times (≤ 96 h). Since this pioneering work, considerable research has been devoted to expanding the breadth of basic/nucleophilic organocatalysts for ROP to include *N*-heterocyclic carbenes,[10] phosphazenes,[41] guanidines,[42] and thiourea/amines[43] (Figure 1.3).

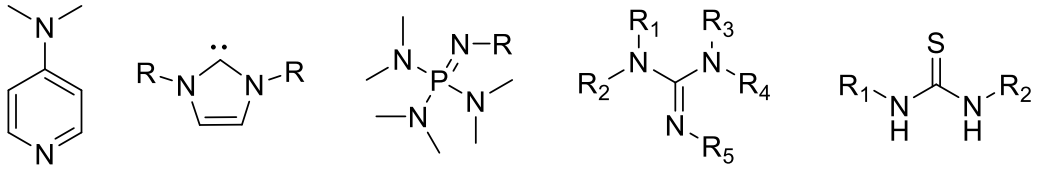

Figure 1.3. Organocatalysts applied in ring-opening polymerisation: a) 4-dimethylaminopyridine, b) general structure for a *N*-heterocyclic carbene, c) general structure of a phosphazene base, d) general structure of a guanidine, and e) general structure of a thiourea.

Conversely, in comparison to basic organocatalysts, the field of Brønsted acid organocatalysts for ROP is less developed. Strong organic acids such as methanesulfonic acid,[44] trifluoromethanesulfonic acid,[45] and trifluoromethanesulfonimides[46] have been shown to be effective catalysts for the ROP of cyclic esters to produce well-defined polyesters. However, it was found that there is no simple correlation between acidity and catalytic activity.[47] Comparing the activity of hydrochloric acid (HCl) (Hammett acidity $H_0 \sim -8$), trifluoromethanesulfonic acid (HOTf) ($H_0 \sim -14$), and methanesulfonic acid (MSA) ($H_0 \sim -1$) for the ROP of ε-caprolactone (εCL), it was found that the least acidic MSA was the most active, with high monomer conversions achieved in short reaction times (> 98% monomer conversion in 2 h). Conversely, HCl only achieved low monomer conversions even after extended reaction times (22 % in 24 h). Moreover, MSA displayed good control during the polymerisation to achieve polymers with narrow dispersities ($Đ_M = 1.07$) and good correlation between theoretical and observed molecular weights.

Further expanding the field of Brønsted acid ROP catalysts, weak acids such as phosphoric acids have also been demonstrated to exert good control over cyclic ester

polymerisation to yield polymers with predictable molecular weights and narrow dispersities, even after extended reaction times.[48-50] The structure of phosphoric acids are easily tuneable to allow for optimisation of selectivity and activity during the polymerisation. A cheap, chemically stable, and commercially available catalyst, diphenyl phosphate (DPP) (pK_a = 2 – 4) was first reported in 2011 by Kakuchi and co-workers for the controlled ROP of δVL and εCL (Scheme 1.1.).[51] Using 3-phenyl-1-propanol as initiator, DPP catalysed the ROP of δVL and εCL to high conversions (> 95%) within short reaction times (< 8 h) at ambient temperatures.

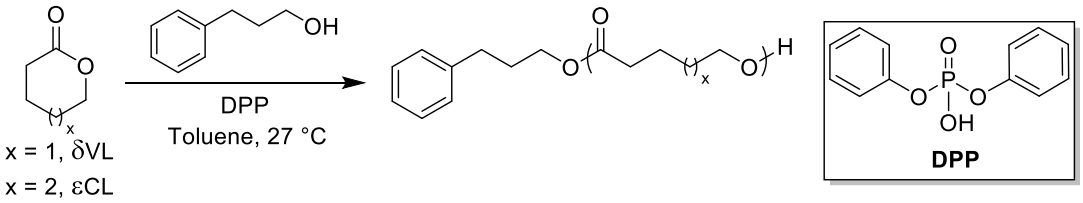

Scheme 1.1. Ring-opening polymerisation of δ-valerolactone and ε-caprolactone using diphenyl phosphate as the catalyst. Adapted from Kakuchi and co-workers.[51]

It is proposed that phosphoric acid catalysed polymerisations proceed according to the activated monomer mechanism (AMM) (Scheme 1.2.).[48] The first stage of an AMM involves protonation of the carbonyl oxygen of the monomer to produce the activated species, which is then more electrophilic and open to attack by the initiating alcohol. The corresponding ring-opening reaction leads to a linear ester with an alcohol chain-end which can then go on to react with another activated monomer, leading to chain extension. Computational experiments have proven that in addition to activated monomer, phosphoric acids such as DPP can act as a bifunctional catalyst during the ROP of cyclic esters, activating both the monomer and initiator *via* hydrogen bonding.[49] Polymerisations that follow a AMM can be considered a controlled polymerisation as

chain-growth occurs in the absence of significant chain-transfer and termination leading to polymers with well-defined molecular weights and narrow dispersities ($Đ_M \leq$ 1.3).

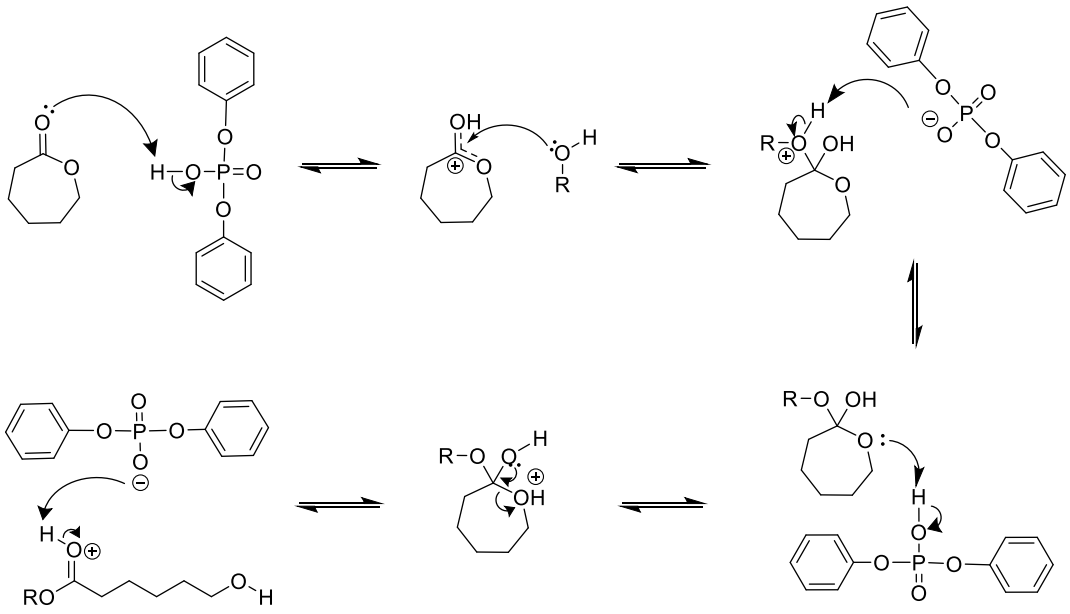

Scheme 1.2. Proposed activated monomer mechanism for the ring-opening polymerisation of ε-caprolactone catalysed by diphenyl phosphate.

1.2.2.4. Stereoselective catalysis

Chirality is ubiquitous throughout nature and chiral polymers can be found in biologically active substances such as DNA, RNA, proteins, *etc*. for which their chiral nature is essential. However, achieving synthetic chiral polymers that can rival nature has challenged polymer chemists for many decades.[52, 53] Synthetic chiral polymers possess physical and thermomechanical properties that differ to their achiral counterparts, and the correlation between the physical properties of a polymer and its main-chain stereochemistry was first predicted in 1929 by Staudinger *et al.*[54] However, the first stereoregular synthetic polymer wasn't reported until 1947 by McKinley and

co-workers who attributed the semi-crystalline properties of a poly(isobutyl vinyl ether) material to the tacticity of the polymer backbone.[55] Stereoregular polymers are often defined as isotactic, where neighbouring stereocentres have the same configuration (Figure 1.4a), or syndiotactic, where neighbouring stereocentres adopt alternating configurations (Figure 1.4b). Stereoregular polymers can solidify in to crystalline or semi-crystalline phases as a result of their long-range order; however, atactic polymers (random distribution of stereocentres along the polymer backbone) tend to solidify to form amorphous glasses, which indicates the absence of crystallinity. Generally, isotactic polymers have superior thermal properties over their atactic and syndiotactic equivalents (higher melting and crystallisation temperatures).[9] One example is commercial polypropylene which is typically isotactic and is used to make dish-washer safe food containers as a result of its high melting point (160 °C); conversely, atactic polypropylene is a waxy and slightly tacky solid possessing a low melting point (< 0°C).

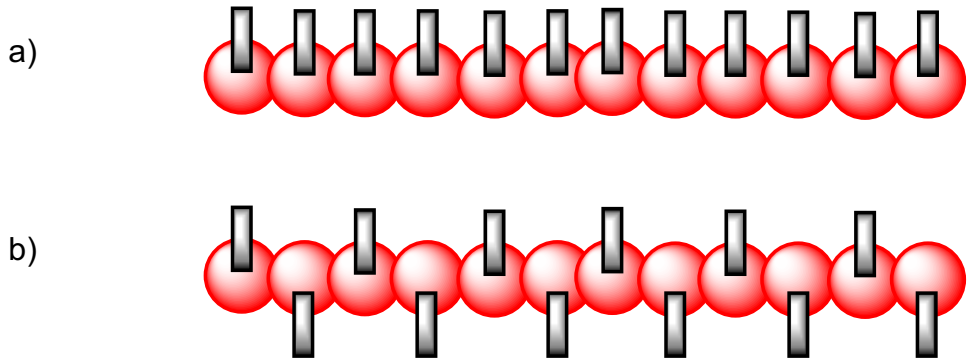

Figure 1.4. Examples of stereoregular polymers: a) isotactic and b) syndiotactic.

There are two main routes to exert control over the tacticity of the polymer backbone. The first is through the polymerisation of a stereopure monomer, where the polymerisation proceeds with retention of stereochemistry (Scheme 1.3a), often to

yield an isotactic polymer. Alternatively, the most employed method of synthesising a stereoregular polymer is through the stereoselective polymerisation of a racemic monomer, that results in polymers possessing a patterned microstructure (Scheme 1.3b). Stereoselective polymerisations can be mediated by two different mechanisms, chain-end control, and enantiomorphic site control. In the former case, the chirality of the next inserted monomer is determined by the propagating chain-end and is often witnessed for sterically bulky catalysts. In contrast, with enantiomorphic site control, the chirality of the next inserted monomer is determined by the chirality of the catalyst.

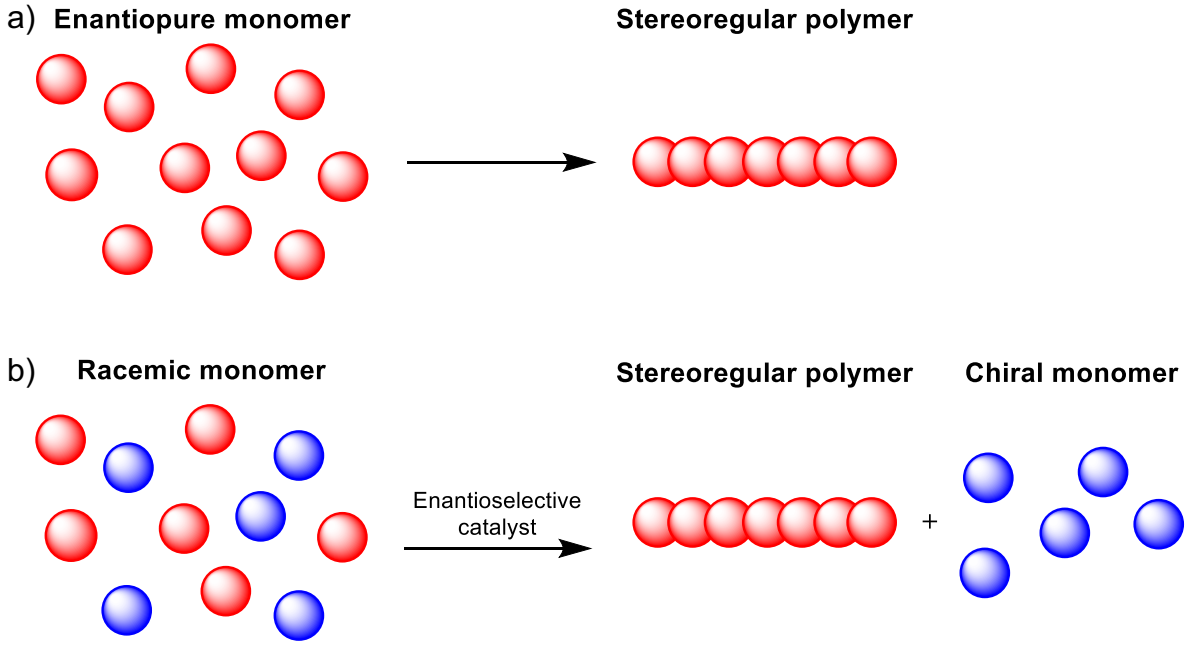

Scheme 1.3. a) Polymerisation of an enantiopure monomer and b) an example of a stereoselective polymerisation of a racemic monomer.

A high percentage of reported stereoselective polymerisations of cyclic (di)esters report the use of an organometallic initiator/catalyst.[56-59] As highlighted earlier, the use of metal-based catalysts can be unfavourable and largely depends on the final application of the material. Despite the abundance of known chiral organic catalysts

known within organic chemistry,[60-62] stereoselective organocatalysts for ROP remains underexplored. However, in recent years examples of organocatalysed stereoselective ROP of cyclic esters have been reported, using either chiral or achiral catalysts. Sterically encumbered *N*-heterocyclic carbenes (NHC) were demonstrated to be the first example of an stereoselective organocatalyst for the ROP of *racemic* and *meso*-lactide displaying modest isoselectivities whilst maintaining good control over the polymerisation.[63] Upon lowering the polymerisation temperature to −70 °C, a considerable increase in enantioselectivity was observed as a result of enhanced kinetic resolution (probability of forming a isotactic diad, P_i, of 0.83 and 0.90, respectively) . Interestingly, it was found that both chiral and achiral NHCs yielded similar levels of enantioselectivity which suggested a chain-end control mechanism.

Chiral organocatalysts such (*R*)-binaphthol phosphoric acids,[64] thiourea-amines,[65] and β-isocupreidine/thiourea/chiral binaphthylamine[66] have been reported as efficient stereoselective catalysts for the ROP of cyclic (di)esters with high levels of isoselectivity (P_i = 0.86, 0.88, and 0.88 at 75, 25, and 25 °C, respectively). However, Mecerreyes and Cossío reported a co-catalytic system of a densely substituted proline in combination with 1,8-diazabicyclo[5.4.0]undec-7-ene (DBU) polymerised *rac*-lactide to yield a highly isotactic polymer (P_i = 0.96) at 25 °C. The *endo*-isomer was found to preferentially polymerise D-lactide whilst the *exo*-isomer preferentially polymerised L-lactide. This stereoselectivity of incoming monomer based on the chirality of the catalyst is in line with an enantiomorphic site control mechanism. Moreover, as the polymerisations approached 40% the polymerisation slowed down substantially, with the polymerisation stopping close to a 50% conversion, highlighting the high degree of stereoselectivity of the catalyst once the preferential monomer had been consumed.

Whilst the field of organocatalysed stereoselective polymerisations has grown in terms of effective catalysts, the breadth of monomer variety remains limited with most reports focusing on polylactide synthesis.

1.3. ε-Substituted-ε-caprolactones

As the field of material science advances and expands, the design and synthesis of functional polymers is becoming ever more essential to keep pace with industrial demands. However, many commodity polymers are non-degradable and petrochemically derived. Conversely, biodegradable polymers are quickly emerging as a more sustainable alternative to current commercial non-degradable plastics. An example of a well-known biodegradable polymer is poly(ε-caprolactone) (PCL), first synthesised by Carothers *et al.* in the early 1930s.[5] Owing to its inherent semi-crystallinity, PCL is readily used in a range of different applications, from the development of 3D scaffolds for tissue engineering,[67] where the polymers' semi-crystallinity regulates mechanical properties and degradation rates,[68] to advanced nanoparticle design methodologies such as crystallisation-driven self-assembly (CDSA) where the crystalline core directs the size and morphology of the resultant particle.[69]

Despite this, the lack of side-chain functionality in PCL prevents the introduction of small molecules to the core of assembled particles, particularly those obtained *via* CDSA, which show promise for targeted drug delivery and *in vivo* imaging applications.[70] To access functionalised PCL-based crystallisation-driven self-assemblies, two primary approaches have been proposed. The first is the chemical modification of pre-synthesised semi-crystalline PCL, through deprotonation at the α-position of the carbonyl of the polyester backbone by a strong non-nucleophilic

base such as lithium diisopropylamide (LDA), followed by the reaction with a suitable electrophile (Scheme 1.4, route A).[71, 72] However, this method can lead to decreased polymer molecular weights and an increase in polymer dispersities as a result of cleavage of the polymer backbone. Alternatively, the synthesis of a functionalised semi-crystalline PCL can also be realised through the polymerisation of a functional εCL monomer possessing a reactive moiety, followed by post-polymerisation functionalisation. The second method is preferable as pre-functionalisation of the monomer eliminates the need for post-polymerisation reactions requiring strong bases, thus minimising polymer degradation. Moreover, careful choice of the starting monomer allows for a range of control over the placement of the functional group along the polymer backbone. Selective choice of the starting monomer also opens a range of functionalities available for small molecule attachment such as fluorescent tags.[73,70]

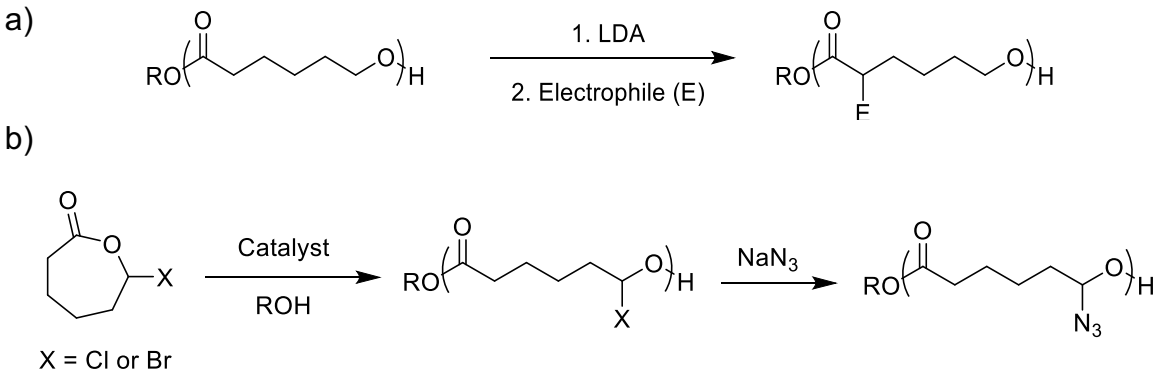

Scheme 1.4. a) Post-polymerisation functionalisation of PCL at the α-position through a strong non-nucleophilic base and electrophile b) ROP and post-polymerisation functionalisation of a halogenated εCL monomer.

Placing substituents at the ε-position of εCL is advantageous as this introduces steric hindrance in close proximity to the ring-opening centre and helps to prevent

transesterification.[74] Transesterification (inter- and intramolecular) is an inherent risk of ROP causing a decrease in molecular weights and a broadening of dispersities. Moreover, as a result of increased dispersities, transesterification side reactions led to a disruption in long-range order in the polymer microstructure, hindering crystallinity.

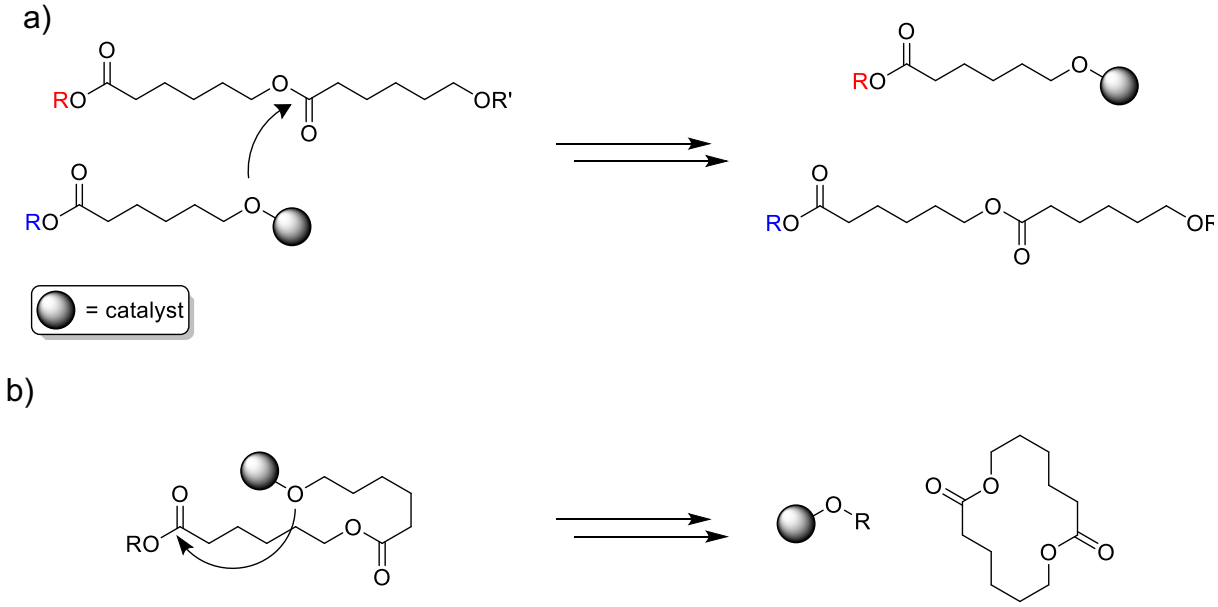

Scheme 1.4. a) intermolecular and b) intramolecular transesterification side reactions during the ring-opening polymerisation of a cyclic ester.

Despite this, the ROP of ε-substituted-ε-caprolactones (εSεLs) is a largely understudied area. Most reports in this area focus on the ROP of the naturally derived (–)-menthide, dihydrocarvide, and carvomenthide (Figure 1.5),[75] however, all these monomers are also substituted at the γ-position and provide little opportunity for post-polymerisation functionalisation. Moreover, monomer synthesis requires the use of expensive metal catalysts and the use of hydrogen gas which can lead to safety issues.

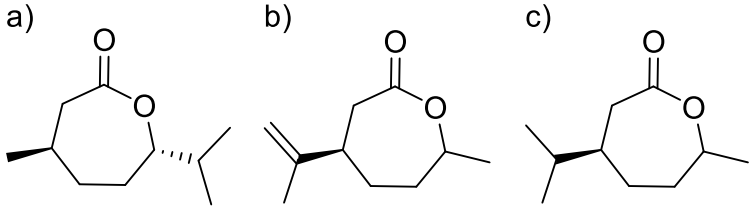

Figure 1.5. a) (–)-Menthide, b) dihydrocarvide and c) carvomenthide.

1.3.1. Synthesis of ε-substituted-ε-caprolactones

Functionalised εCL monomers can be synthesised through the Baeyer-Villiger ring-expansion of a cyclohexanone precursor, leading to a wide variety of functionalised εCL monomers available for ROP. The most common route for Baeyer-Villiger ring expansion is through the application of *meta*-chloroperoxybenzoic acid (*m*-CPBA) as the oxidising agent, which is tolerant to a wide range of functional groups.[76-79]

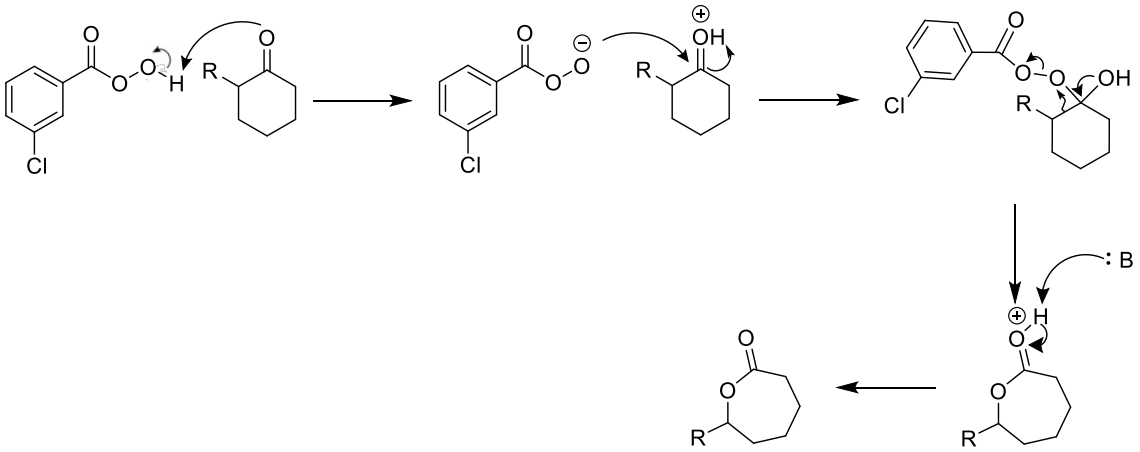

Scheme 1.5. Mechanism for Baeyer-Villiger oxidation of 2-substituted cyclohexanone using *m*-CPBA.

1.3.2. Ring-opening polymerisation of ε-substituted-ε-caprolactones

One way to modulate a materials final properties is through the copolymerisation of two complementing monomers. The ability to create copolymers with varying molecular weights, architectures, and compositions has led to the creation of a large library of new materials with unique properties. In recent years, the copolymerisation of *rac*-ε-decalactone (εDL), a naturally occurring monomer, has gained increasing attention as an alternative to εCL as an amorphous alternative with increased hydrophobicity.[80, 81] Moreover, exchanging the semi-crystalline PCL core in a poly(ethylene glycol)-PCL assembly with amorphous poly(ε-decalactone) (PDL) leads to an increase in core volume relative to that of a semi-crystalline core allowing for an increased drug loading capacity.[80] Alternatively, with the aim of introducing flexibility to the main chain of the rigid poly(L-lactide), L-lactide (LLA) was copolymerised with εDL as a result of its amorphous nature and low glass-transition temperature (T_g) (–52 °C) (Scheme 1.6).[82] The sequential addition of LLA to a macroinitiator of PDL yielded a triblock copolymer with a low degree of transesterification, whereas the simultaneous monomer addition provided a random copolymer. Comparing the thermal properties of the triblock and random copolymers, both copolymers gave two T_g's corresponding to the separate εDL and LLA sections, and a melting temperature comparable to that of poly(L-lactide) (PLLA). Moreover, both copolymers exhibited increased strain-at-break values compared to PLLA, with the triblock showing a 250-fold increase owing to the central PDL block and 150-fold increase for the random copolymer. As such, the copolymerisation of εSεLs with more crystalline monomers presents a simple approach to modulate the amorphous nature of the final material creating the opportunity for the synthesis of new materials with tuneable properties.

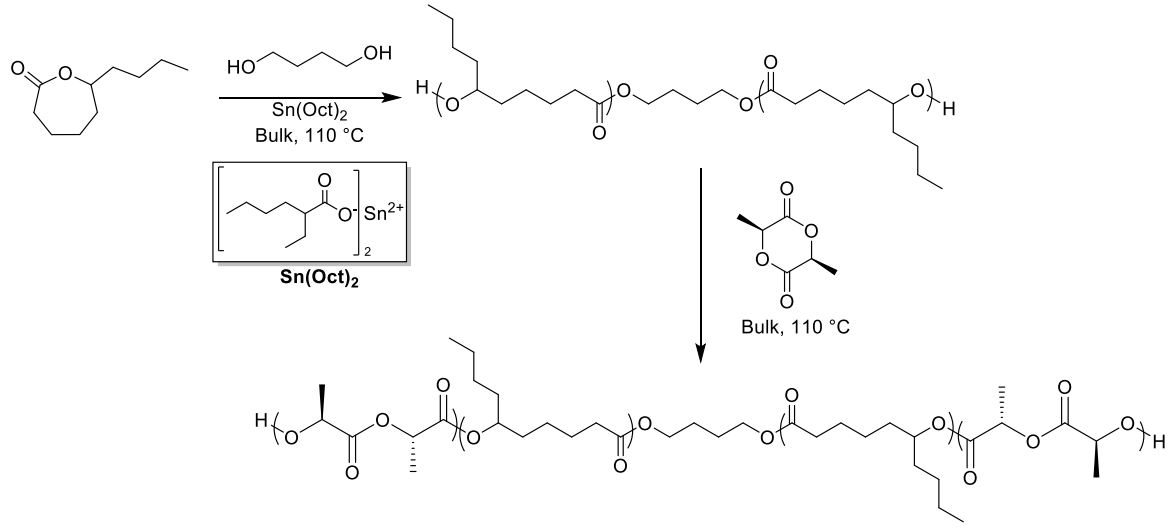

Scheme 1.6. Copolymerisation of ε-decalactone with L-lactide using $Sn(Oct)_2$ as catalyst. Adapted from Albertsson and co-workers.[82]

Alternatively, one of the few examples of a homopolymerisation of an εSεLs was reported by Peeters *et al.* investigating the stereoselective activity of Novozym-435 towards the ROP of methyl-substituted ε-caprolactones.[83] Interestingly, whilst Novozym-435 was effective for the ROP of β-, γ-, and δ-methyl-ε-caprolactone, no propagation was observed for ε-methyl-ε-caprolactone (εHL).[83] Upon ring-opening, εHL forms a secondary alcohol with an (*S*)-configuration, and in line with the Kazlauskas' rule,[84] (*S*)-secondary alcohols are extremely slow to react with lipase-based catalysts, meaning that the stereoconfiguration of the terminal alcohol prevents propagation on a reasonable time scale. To overcome this Meijer and co-workers, inspired by dynamic kinetic resolution, epimerised the terminal alcohol *in situ* using a ruthenium-based catalyst (Scheme 1.7).[85] Upon the reaction between εHL and benzyl alcohol as initiator, in the presence of Novozym-435 εHL ring-opened to yield the secondary (*S*)-alcohol, however epimerisation of the (*S*)-alcohol provided a 1:1 ratio of the (*R*)- and (*S*)-alcohol isomers. Further addition of εHL displayed a 50%

consumption of additional monomer by the secondary (*R*)-alcohol. Epimerisation and propagation was then repeated for a further 5 cycles. The product was then degraded by methanolysis and analysed by chiral gas-chromatography which displayed a 92% (*R*)-configuration. Yet despite the high degree of isotacticity obtained by enzyme catalysis, a two-stage tandem process was required using an organometallic catalyst and after many cycles only oligomers were obtained (DP = 3).

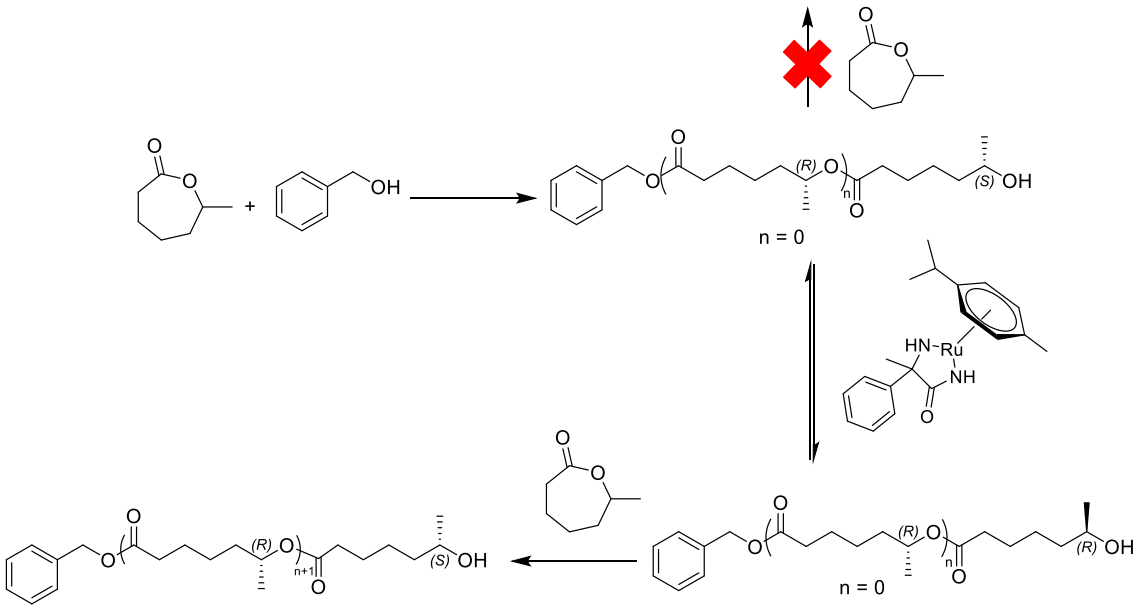

Scheme 1.7. Novozym-435 catalysed ROP of εHL using a ruthenium-based epimerisation catalyst reported by Meijer and co-workers.[85]

The selectivity of an enzyme catalyst is fixed by the nature of the enzyme meaning only one enantiomer can be polymerised on an observable timescale. Conversely, the enantioselective behaviour of organometallic catalysts can easily be controlled through selective design of the ligand coordinated to the metal centre. As such, Feijen and co-workers compared the ROP of εCL, εHL, and γ-methyl-ε-caprolactone (γMeCL) using a chiral salen aluminium-based catalyst (Scheme 1.8) to understand how substitution placement affected the polymerisation. At 90 °C polymerisations

proceeded in a controlled manner with varying rates of polymerisation (εCL > γMeCL > εHL). Upon lowering the temperature to 70 °C the ROP of εCL and γMeCL proceeded, albeit at a slower rate whereas no polymerisation was witnessed for εHL (εCL > γMeCL >>> εHL), thought to be a consequence steric hindrance, highlighting the effect of substituent placement. Yet despite the decreased rate in polymerisation, the (*R,R*)-stereoisomer of the catalyst preferentially polymerised (*R*)-εHL from *rac*-εHL to achieve an enantiomeric excess of 18% at a 40% monomer conversion, at 90 °C whilst no stereoselectivity was witnessed for γMeCL, likely as a result of the closer proximity of the ε-substituent over γ-substituent to the chiral catalyst. However, the thermal properties of the stereo-enriched polymer were never evaluated. To date, little focus has gone into the stereoselective ROP of εSεLs, particularly using organocatalysts, and the thermal properties of the resulting stereo-enriched polymer, particularly regarding polymer semi-crystallinity.

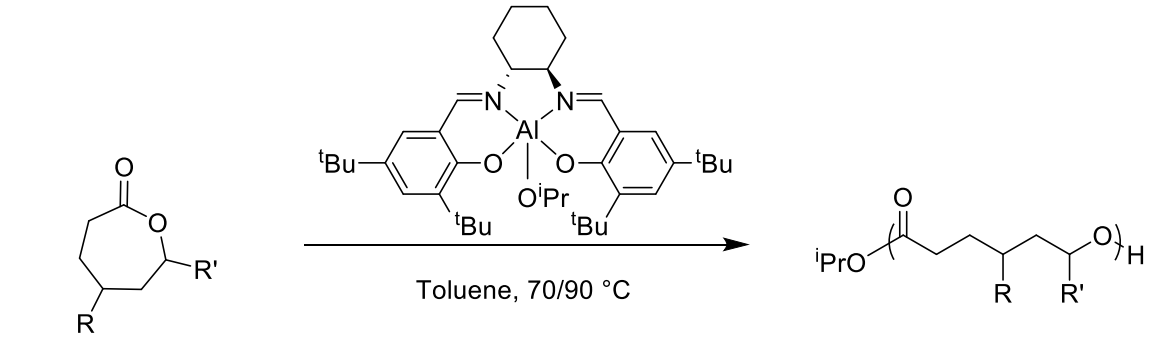

εCL: R = H, R' = H
γMeCL: R = Me, R'=H
εHL: R = H, R' = Me

Scheme 1.8. Polymerisation of εCL, γMeCL, and εHL using a chiral salen aluminium catalyst.

1.4. Conclusions

Biodegradable polyesters have played a crucial role in providing a sustainable approach to polymer science and have as such experienced a revival in the biomedical community. The synthesis of polyesters *via* ROP has been the preferred method by polymer scientists as a result of controlled polymerisations leading to polymers with narrow dispersities and predictable molecular weights with good end-group fidelity. The field of organocatalysis towards ROP has experienced a renaissance and thus a range of catalysts have been developed that require less rigorous conditions than their metal-based equivalent. Furthermore, advancement in stereoselective organocatalysis, both chiral and achiral, has led to a large expansion in organocatalysts that display a high degree of stereoselectivity towards a wide range of monomers so organocatalysis can now be seen as a realistic alternative to metal-based catalysts.

Despite their resistance to transesterification, research into the ROP of εSεLs is an under explored area with most reports focussing on the polymerisation of a limited scope of monomers. Polymers from racemic εSεLs are ideal candidates for copolymerisation with current crystalline materials to provide the ability to tune final material properties because of their amorphous nature. Employing mild conditions, enzyme catalysis provides a high degree of stereoselectivity but fails to yield high molecular weight polymers, instead only oligomers are provided. Moreover, a complicated two stage tandem synthesis is required to obtain stereopure oligomers as a result of the (*S*)-secondary alcohol that is unique to εSεLs. More traditional catalysts display good control over the polymerisation of εSεLs to yield polymers with predictable molecular weights and narrow dispersities. However to achieve stereoselectivity during

the polymerisation of substituted ε-caprolactones, selective placement of the pendant group is essential. The close proximity of the substituent to the ring-opening centre as found in εSεLs is ideal for stereoselectivity to occur, albeit at the cost of increased polymerisation times.

Overall, the polymerisation of εSεLs provides a unique opportunity to create new functional materials with control over stereochemistry of the resulting polymer. The synthesis of semi-crystalline functionalised poly(ε-substituted-ε-caprolactones) and their corresponding thermal properties has yet to be explored.

1.5. References

1. L. H. Baekeland, *Journal of Industrial & Engineering Chemistry*, 1909, **1**, 149-161.
2. PlasticsEurope, *The Compelling Facts About Plastics: An Analysis of Plastic Production, Demand and Recovery for 2006 in Europe* PlasticsEurope, 2006.
3. PlasticsEurope, *Plastics – the Facts 2019*, PlasticsEurope, 2019.
4. M. Peplow, *Nature*, 2016, **536**, 266-268.
5. W. H. Carothers, G. L. Dorough and F. J. van Natta, *J. Am. Chem. Soc.*, 1932, **54**, 761-772.
6. J. Qui, K. Charleux and K. Matyjaszewski, *Polimery*, 2001, **46**, 453-460.
7. S. Asano, T. Aida and S. Inoue, *J. Chem. Soc., Chem. Commun.*, 1985, 1148-1149.
8. X. Kou, Y. Li, Y. Shen and Z. Li, *Macromol. Chem. Phys.*, 2019, **220**, 1900416.
9. C. M. Thomas, *Chem. Soc. Rev.*, 2010, **39**, 165-173.
10. E. F. Connor, G. W. Nyce, M. Myers, A. Mock and J. L. Hedrick, *J. Am. Chem. Soc.*, 2002, **124**, 914-915.
11. F. Nederberg, E. F. Connor, T. Glausser and J. L. Hedrick, *Chem. Commun.*, 2001, 2066-2067.
12. J. Payne, P. McKeown, M. F. Mahon, E. A. C. Emanuelsson and M. D. Jones, *Polym. Chem.*, 2020, **11**, 2381-2389.
13. T. Steinbach, S. Ritz and F. R. Wurm, *ACS Macro Lett.*, 2014, **3**, 244-248.
14. M. Rodriguez, S. Marrot, T. Kato, S. Stérin, E. Fleury and A. Baceiredo, *J. Organomet. Chem.*, 2007, **692**, 705-708.

15. M. Winnacker, S. Vagin, V. Auer and B. Rieger, *Macromol. Chem. Phys.*, 2014, **215**, 1654-1660.

16. E. V. Anslyn and D. A. Dougherty, *Modern Physical Organic Chemistry* University Science Books, 2006.

17. D. K. Schneiderman and M. A. Hillmyer, *Macromolecules*, 2016, **49**, 2419-2428.

18. H. Sawada, *J. Macromol. Sci., Part C*, 1969, **3**, 313-338.

19. M. A. F. Delgove, A. A. Wróblewska, J. Stouten, C. A. M. R. van Slagmaat, J. Noordijk, S. M. A. De Wildeman and K. V. Bernaerts, *Polym. Chem.*, 2020, **11**, 3573-3584.

20. C. K. Williams and K. Nozaki, *Inorg. Chem.*, 2020, **59**, 957 - 959.

21. H. R. Kricheldorf, M. Berl and N. Scharnagl, *Macromolecules*, 1988, **21**, 286-293.

22. H. Li, R. M. Shakaroun, S. M. Guillaume and J. F. Carpentier, *Chem. Eur. J.*, 2020, **26**, 128-138.

23. R. K. Srivastava and A. C. Albertsson, *Biomacromolecules*, 2006, **7**, 2531-2538.

24. W. He, Z. Fang, N. Zhu, D. Ji, Z. Li and K. Guo, *Biocatal. Biotransform.*, 2015, **33**, 150-155.

25. A. P. Dove, *ACS Macro Lett.*, 2012, **1**, 1409-1412.

26. M. K. K. J. Shin, J. L. Hedrick and R. M. Waymouth, 2010, **43**, 2093 - 2107.

27. A. C. Albertsson and I. K. Varma, *Biomacromolecules*, 2003, **4**, 1466-1486.

28. J. L. Hedrick, T. Magbitang, E. F. Connor, T. Glauser, W. Volksen, C. J. Hawker, V. Y. Lee and R. D. Miller, *Chem. Eur. J.*, 2002, **8**, 3308-3319.

29. G. Schwach, J. Coudane, R. Engel and M. Vert, *J. Polym. Sci., Part A: Polym. Chem.*, 1997, **35**, 3431-3440.

30. C.-M. Dong, K.-Y. Qiu, Z.-W. Gu and X.-D. Feng, *Macromolecules*, 2001, **34**, 4691-4696.

31. I. K. Varma, A. C. Albertsson, R. Rajkhowa and R. K. Srivastava, *Prog. Polym. Sci.*, 2005, **30**, 949-981.

32. K. S. Bisht, L. A. Henderson, R. A. Gross, D. L. Kaplan and G. Swift, *Macromolecules*, 1997, **30**, 2705-2711.

33. A. Kumar, B. Kalra, A. Dekhterman and R. A. Gross, *Macromolecules*, 2000, **33**, 6303-6309.

34. L. Zhang, X. Deng and Z. Huang, *Biotechnol. Lett*, 1996, **18**, 1051-1054.

35. S. Kobayashi, H. Uyama and S. Kimura, *Chem. Rev.*, 2001, **101**, 3793-3818.

36. F. Nederberg, E. F. Connor, M. Möller, T. Glauser and J. L. Hedrick, *Angew. Chem. Int. Ed.*, 2001, **40**, 2712-2715.

37. M. K. K. Waymouth, S. Eun Ji, L. H. James and M. Robert, *Macromolecules*, 2010, **43**, 2093 - 2107.

38. N. E. Kamber, W. Jeong, R. M. Waymouth, R. C. Pratt, B. G. G. Lohmeijer and J. L. Hedrick, *Chem. Rev.*, 2007, **107**, 5813-5840.

39. P. Degée, P. Dubois, R. Jérŏme, S. Jacobsen and H.-G. Fritz, *Macromol. Symp.,* 1999, **144**, 289-302.

40. B. J. O'Keefe, M. A. Hillmyer and W. B. Tolman, *J. Chem. Soc., Dalton Trans.*, 2001, 2215-2224.

41. L. Zhang, F. Nederberg, R. C. Pratt, R. M. Waymouth, J. L. Hedrick and C. G. Wade, *Macromolecules*, 2007, **40**, 4154-4158.

42. B. G. G. Lohmeijer, R. C. Pratt, F. Leibfarth, J. W. Logan, D. A. Long, A. P. Dove, F. Nederberg, J. Choi, C. Wade, R. M. Waymouth and J. L. H. Hedrick, *Macromolecules*, 2006, **39**, 8574-8583.

43. A. P. Dove, R. C. Pratt, B. G. G. Lohmeijer, R. M. Waymouth and J. L. Hedrick, *J. Am. Chem. Soc.*, 2005, **127**, 13798-13799.

44. A. Couffin, D. Delcroix, B. Martín-Vaca, D. Bourissou and C. Navarro, *Macromolecules*, 2013, **46**, 4354-4360.

45. A. Couffin, B. Martín-Vaca, D. Bourissou and C. Navarro, *Polym. Chem.*, 2014, **5**, 161-168.

46. K. Makiguchi, S. Kikuchi, T. Satoh and T. Kakuchi, *J. Polym. Sci., Part A: Polym. Chem.*, 2013, **51**, 2455-2463.

47. S. Gazeau-Bureau, D. Delcroix, B. Martín-Vaca, D. Bourissou, C. Navarro and S. Magnet, *Macromolecules*, 2008, **41**, 3782-3784.

48. D. C. Batiste, M. S. Meyersohn, A. Watts and M. A. Hillmyer, *Macromolecules*, 2020, **53**, 1795 - 1808.

49. J. Zhao and N. Hadjichristidis, *Polym. Chem.*, 2015, **6**, 2659-2668.

50. K. Makiguchi, C. Asakura, K. Yanai, T. Satoh and T. Kakuchi, *Macromol. Symp.*, 2015, **349**, 74-84.

51. K. Makiguchi, T. Satoh and T. Kakuchi, *Macromolecules*, 2011, **44**, 1999 - 2005.

52. M. Liu, L. Zhang and T. Wang, *Chem. Rev.*, 2015, **115**, 7304-7397.

53. J. J. L. M. Cornelissen, A. E. Rowan, R. J. M. Nolte and N. A. J. M. Sommerdijk, *Chem. Rev.*, 2001, **101**, 4039-4070.

54. H. Staudinger, A. A. Ashdown, M. Brunner, H. A. Bruson and S. Wehrli, *Helv. Chim. Acta*, 1929, **12**, 934-957.

55. C. E. Schildknecht, A. O. Zoss and C. McKinley, *Ind. Eng. Chem.*, 1947, **39**, 180-186.

56. T. M. Ovitt and G. W. Coates, *J. Polym. Sci., Part A: Polym. Chem.*, 2000, **38**, 4686-4692.

57. C. X. Cai, A. Amgoune, C. W. Lehmann and J. F. Carpentier, *Chem. Commun.*, 2004, 330-331.

58. H. Wang, J. Guo, Y. Yang and H. Ma, *Dalton Trans.*, 2016, **45**, 10942-10953.

59. M. R. T. Breteler, Z. Zhong, P. J. Dijkstra, A. R. A. Palmans, J. Peeters and J. Feijen, *J. Polym. Sci., Part A: Polym. Chem.*, 2006, **45**, 429-436.

60. X.-H. Chen, Q. Wei, S.-W. Luo, H. Xiao and L.Z. Gong, *J. Am. Chem. Soc.*, 2009, **131**, 13819-13825.

61. M. Bartók, *Chem. Rev.*, 2010, **110**, 1663-1705.

62. D. Almaşi, D. A. Alonso, E. Gómez-Bengoa and C. Nájera, *J. Org. Chem.*, 2009, **74**, 6163-6168.

63. A. P. Dove, H. Li, R. C. Pratt, B. G. G. Lohmeijer, D. A. Culkin, R. M. Waymouth and J. L. Hedrick, *Chem. Commun.*, 2006, 2881-2883.

64. C. Lv, R. Yang, G. Xu, L. Zhou and Q. Wang, *Eur. Polym. J.*, 2020, **133**, 109792.

65. B. Orhan, M. J. L. Tschan, A.-L. Wirotius, A. P. Dove, O. Coulembier and D. Taton, *ACS Macro Lett.*, 2018, **7**, 1413-1419.

66. J. B. Zhu and E. Y. X. Chen, *J. Am. Chem. Soc.*, 2015, **137**, 12506-12509.

67. E. Nyberg, A. Rindone, A. Dorafshar and W. L. Grayson, *Tissue Engineering Part A*, 2017, **23**, 503-514.

68. M. A. Woodruff and D. W. Hutmacher, *Prog. Polym. Sci.*, 2010, **35**, 1217-1256.

69. M. C. Arno, M. Inam, Z. Coe, G. Cambridge, L. J. Macdougall, R. Keogh, A. P. Dove and R. K. O'Reilly, *J. Am. Chem. Soc.*, 2017, **139**, 16980-16985.

70. M. Elsabahy and K. L. Wooley, *Chem. Soc. Rev.*, 2012, **41**, 2545-2561.

71. S. Ponsart, J. Coudane and M. Vert, *Biomacromolecules*, 2000, **1**, 275-281.

72. M.-H. Huang, J. Coudane, S. Li and M. Vert, *J. Polym. Sci., Part A: Polym. Chem.*, 2005, **43**, 4196-4205.

73. B. Kulkarni and M. Jayakannan, *ACS Biomater. Sci. Eng.*, 2017, **3**, 2185-2197.

74. J. A. Wilson and A. P. Dove, *Biomacromolecules*, 2015, **2015**, 10.

75. J. R. Lowe, W. B. Tolman, M. A. Hillmyer and M. T. Martello, *Polym. Chem.*, 2011, **2**, 702-708.

76. M. Renz and B. Meunier, *Eur. J. Org. Chem.*, 1999, **1999**, 737-750.

77. T. F. Al-Azemi and A. A. Mohamod, *Polymer*, 2011, **52**, 5431-5438.

78. D. Zhang, M. A. Hillmyer and W. B. Tolman, *Biomacromolecules*, 2005, **6**, 2091-2095.

79. N. Berezina, E. Kozma, R. Furstoss and V. Alphand, *Adv. Synth. Catal.*, 2007, **349**, 2049-2053.

80. L. Glavas, P. Olsén, K. Odelius and A.-C. Albertsson, *Biomacromolecules*, 2013, **14**, 4150-4156.

81. L. Glavas, K. Odelius and A.-C. Albertsson, *Polym. Adv. Technol.*, 2015, **26**, 880-888.

82. P. Olsén, T. Borke, K. Odelius and A.-C. Albertsson, *Biomacromolecules*, 2013, **14**, 2883-2890.

83. J. Peeters, A. R. A. Palmas, M. Veld, F. Scheijen, A. Heise and E. W. Meijer, *Biomacromolecules*, 2004, **5**, 1862-1868.

84. R. J. Kazlauskas, A. N. E. Weissfloch, A. T. Rappaport and L. A. Cuccia, *J. Org. Chem.*, 1991, **56**, 2656-2665.

85. B. A. C. van As, J. van Buijtenen, A. Heise, Q. B. Broxterman, G. K. M. Verzijl, A. R. A. Palmans and E. W. Meijer, *J. Am. Chem. Soc.*, 2005, **127**, 9964-9965.

2. Chapter two

Ring-opening polymerisation of enantioenriched ε-substituted-ε-caprolactones

2.1. Introduction

Introducing functionality to semi-crystalline poly(ε-caprolactone) (PCL) *via* the addition of pendant groups can lead to disruption of the polymer chain-packing if poor control is exerted over the stereoregularity of the pendant groups, leading to a loss of polymer crystallinity. As such, to obtain a functionalised PCL sample whilst retaining semi-crystallinity, it is ideal that the starting monomer is of an enantioenriched nature to introduce stereoregularity to the polymer backbone (in the absence of epimerisation).

Following the first report of the Baeyer-Villiger oxidation of α-chloro cyclohexanone to form a mixture of two isomeric lactones, α-chloro-ε-caprolactone (αClεCL) and ε-chloro-ε-caprolactone (in a 95/5 molar ratio), the synthesis of halogenated εCL monomers has become of particular interest due to the numerous post-polymerisation modifications possible.[1-3] To this end, Lenoir *et al.* synthesised and polymerised αClεCL to employ as a macroinitiator for the atom transfer radical polymerisation (ATRP) of methyl methacrylate as a route to graft copolymers.[4] When catalysed by 2,2-dibutyl-2-stanna-1,3-dioxepane, polymerisation rates were found to be faster for the more electron-deficient αClεCL compared to εCL, which lead to more narrow dispersities for poly(α-chloro-ε-caprolactone). Typically, the introduction of functional groups in close proximity to the ring-opening centre retards polymerisation rates as a result of increased steric reactions, however the electron-withdrawing chloro substituent partially activated the carbonyl towards nucleophilic attack, which led to increased polymerisation rates. Alternatively, investigating the application of 1,3-Huisgen cycloadditions on macromolecular structures and the efficiency of “click” reactions, Riva *et al.* converted chloride units in poly(αClεCL-co-εCL) to azide functionalities, followed by a click reaction with functional alkynes (Scheme 2.1, route

A).[5] In the presence of copper iodide and diazobicyclo[5.4.0]undec-7-ene (DBU) the reaction was complete within 2 h, as confirmed by Fourier transform infrared (FT-IR) spectroscopy through the disappearance of the absorption at 2106 cm^{-1} corresponding to the N=N=N stretch of azide groups and the appearance of absorptions at 1650 and 1611 cm^{-1}, indicative of the C=N stretches of triazolines. Importantly, size-exclusion chromatography (SEC) analysis confirmed that no chain degradation occurred during post-polymerisation modifications.

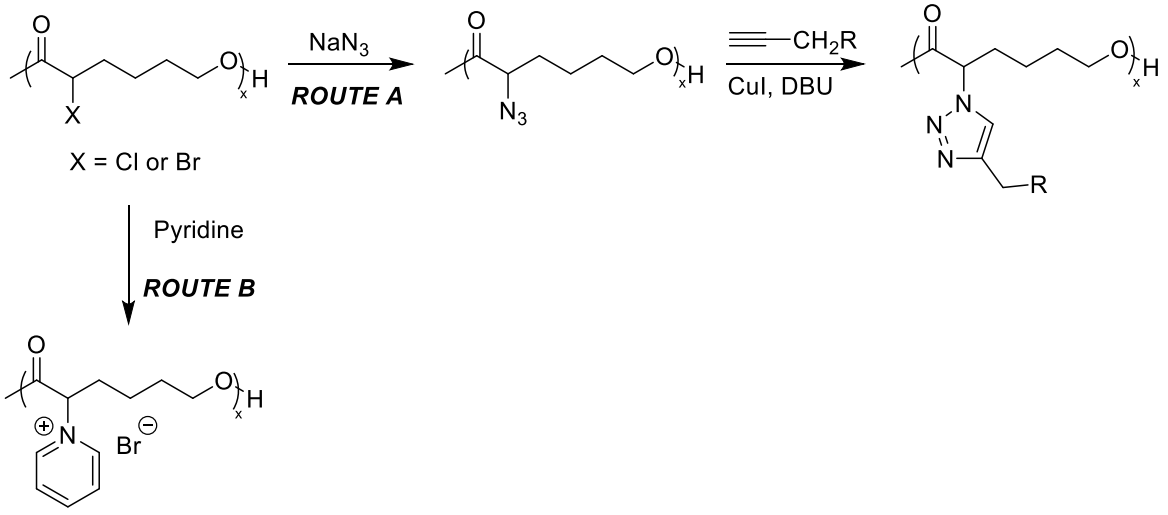

Scheme 2.1. Post-polymerisation functionalisation of halogen-substituted PCL.

The utilisation of γ-bromo-ε-caprolactone (γBrεCL) was first realised by Jérôme and co-workers whilst investigating new routes to functionalised aliphatic polyesters.[6] Following a 4-step reaction pathway for the synthesis of γBrεCL from cyclohexane-1,4-oxide(*cis*-1,4-bromocyclohexanol), the subsequent random copolymerisation with εCL by an aluminium alkoxide catalyst lead to polyesters with predictable molecular weights and narrow dispersities. Successive treatment of the polyester with pyridine provided a quarternized, charged polyester which under physiological conditions was an ideal candidate for non-viral gene delivery (Scheme 2.1, Route B).[7, 8] During the

investigation of pH-sensitive star-shaped polyesters, A_2B and AB_2 copolyesters were synthesised from the copolymerisation of εCL and γBrεCL in the presence of a catalytic amount of tin octanoate. Post-polymerisation substitution of bromide for azide was followed with a reduction to an amine group with the aim of introduce pH-sensitivity. At a pH below 6.4 the copolymer was soluble in water, and following addition of a sodium hydroxide solution the copolymer precipitated out.[9] Conversely, Hegmann and co-workers found that after the copolymerisation of γ-chloro-ε-caprolactone with εCL and lactide, substitution of the halogen atom with azide groups allowed for the attachment of cholesterol molecules to form biocompatible 3D liquid crystal elastomers which were shown to drastically increase cell proliferation compared to conventional materials.[10]

As highlighted above, halogenated ε-caprolactones are a versatile tool for a polymer chemist, allowing for a broad variety of side-chain functionalities to be introduced post-polymerisation. However, none of these previous reports focus on the stereocontrolled synthesis (and corresponding ROP) of a functionalised monomer, and the effects of stereochemistry and substitution on polymer crystallinity has not been investigated. Influencing monomer stereochemistry requires the application of sophisticated catalysts and careful control over reaction conditions adding inherent complexity to the monomer synthesis. Control over the stereochemistry of the monomer pendant group inherently infers control over the tacticity of the resulting polymer. Gaining control over tacticity is essential for the synthesis of semi-crystalline polymers, which often possess mechanical and physical properties that are superior to their atactic counterparts. Furthermore, research on the focus of substitution at the ε-position of εCL remains highly attractive as a result of hindered transesterification

during the polymerisation from increased steric bulk in close proximity to the ring-opening centre, minimising disorder in the polymer microstructure and preventing disruption to crystallinity. Herein, we investigate the synthesis and polymerisation of enantioenriched ε-substituted-ε-caprolactones (εSεLs) and characterise the thermal properties of the resulting polyester.

2.2. Results and Discussion

2.2.1. Monomer synthesis

In search of a versatile monomer, (*S*)-ε-hydroxymethyl-ε-caprolactone, (*S*)-**2**, was initially considered as a result of a wide range of chemical transformations possible from the starting alcohol. The synthesis of (*S*)-**2** was performed following an adapted procedure reported by Chai and co-workers.[11] Initially, the aldol addition between cyclohexanone and formalin was performed at 25 °C using the chiral amino acid L-threonine as an asymmetric catalyst. After 2 weeks at 25 °C, (*S*)-**1** was isolated in good yield (68%) as a colourless and viscous liquid after purification by silica-gel column chromatography. The enantiomeric excess (*ee*) of (*S*)-**1** was analysed by chiral gas-chromatography (GC) which indicated an *ee* of 45%, relatively low in comparison to earlier reports (98% *ee*), however reported reactions were conducted at the lower temperature of 10 °C.[11]

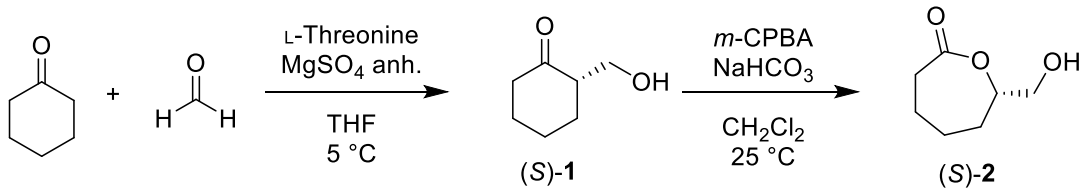

Scheme 2.2. Synthesis of (*S*)-ε-hydroxymethyl-ε-caprolactone from cyclohexanone.

In efforts to increase *ee*, the reaction temperature was lowered from 25 °C to 5 °C. Although this dramatically slowed the rate of reaction, after 4 months the stereopurity of (*S*)-**1** was improved (89% *ee*) albeit at the cost of a decreased yield (44%) from the decreased reaction conversion achieved (Scheme 2.2). Attempts were made at lower temperatures (< 5 °C) to further improve the stereoselectivity. However, the formation of an intermediate iminium species yields water that is crucial to the eventual hydrolysis and regeneration of catalyst species (Scheme 2.3). As such, the reaction was conducted at 0 °C which resulted in a heterogenous reaction due to residual ice particle formation, and led to insufficient stirring of the reaction and a further decrease in reaction rates, this meant that future reactions were then conducted at 5 °C.[12] Following this, a Baeyer-Villiger ring-expansion was performed with *m*-CPBA, after which (*S*)-**2** was recovered in a 72% yield with an 85% *ee*, comparable to the enantiopurity of (*S*)-**1**. The structure of (*S*)-**2** was confirmed by ^{1}H NMR spectroscopy (Figure 2.1).

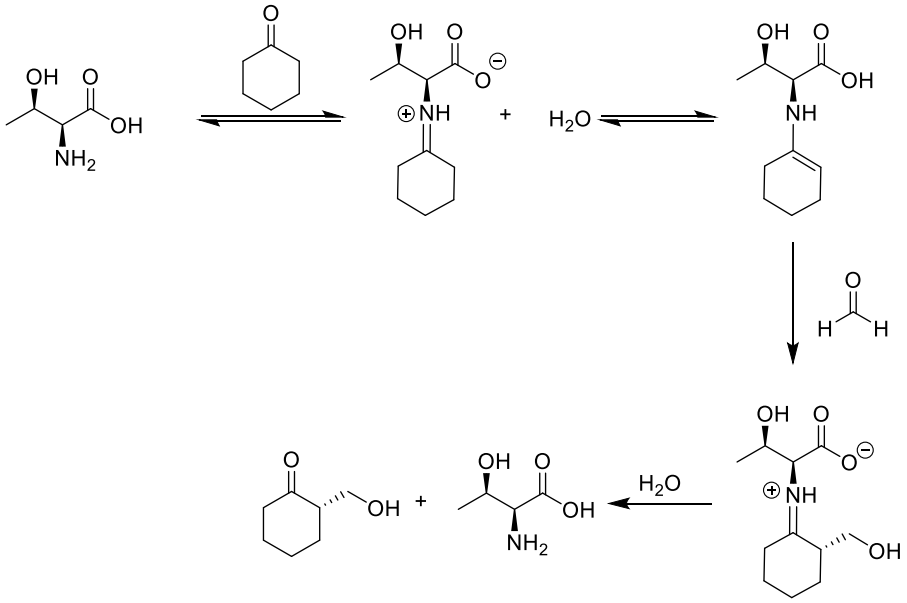

Scheme 2.3. Proposed reaction mechanism for L-threonine catalysed stereoselective Aldol reaction between cyclohexanone and formalin.

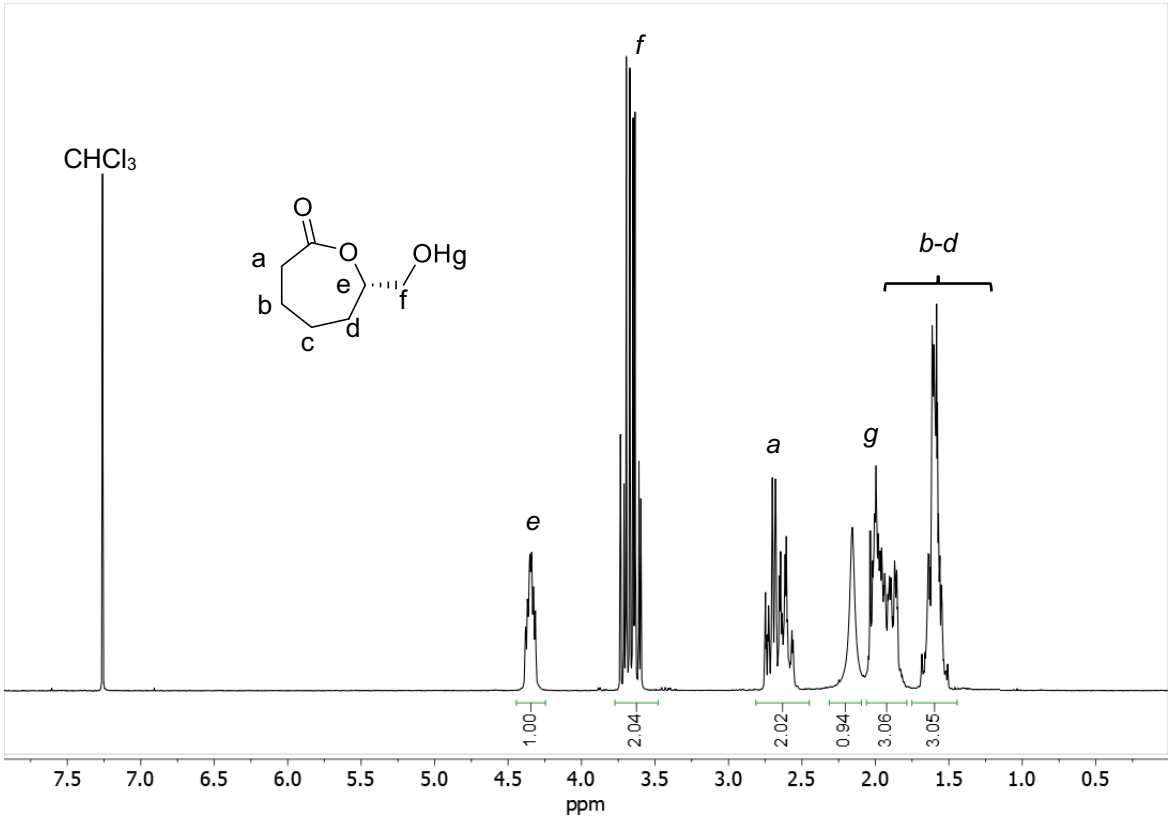

Figure 2.1. ^{1}H NMR spectrum of (*S*)-ε-hydroxymethyl-ε-caprolactone, (*S*)-**2** (400 MHz, 298 K, $CDCl_3$).

2.2.2. Synthesis and polymerisation of (S)-ε-methylacetyloxy-ε-caprolactone

Lactones that contain nucleophilic functional groups, such as a hydroxyl group found in (*S*)-**2,** are likely to self-polymerise to yield hyperbranched polymers.[13, 14] To prevent the formation of hyperbranched polymers, protection of the hydroxyl group was required. As such, the hydroxyl group of (*S*)-**2** was acetylated to yield (*S*)-ε-methylacetyloxy-ε-caprolactone, (*S*)-**3**. It was hypothesised that the deprotection of (*S*)-**3** to reveal (S)-**2** could be achieved through application of a base such as sodium hydroxide. Utilising a method adapted from Cohen and co-workers,[15] (*S*)-**2** was acetylated through the addition of acetic anhydride to yield (*S*)-**3** as a colourless and viscous liquid in moderate yield (56%) with a retention of *ee* (Scheme 2.4). Product formation was confirmed *via* ^{1}H NMR spectroscopy by the downfield shift of the proton signal attributable to C(O)OCHC$\underline{H_2}$OH from δ = 3.69 ppm to δ = 4.14 ppm from deshielding effect of the ester *vs.* the starting alcohol (Figure 2.2). Moreover, the appearance of a singlet at δ = 2.09 ppm which integrated to 3 protons was attributed to C(O)OC$\underline{H_3}$ which further confirmed a successful acetylation of the starting alcohol.

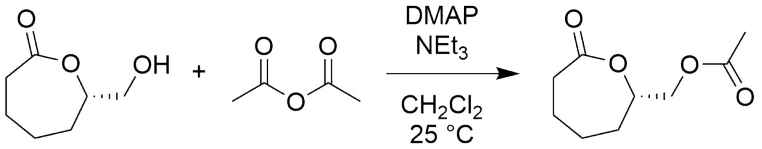

Scheme 2.4. Synthesis of (*S*)-ε-methylacetyloxy-ε-caprolactone, (*S*)-**3**.

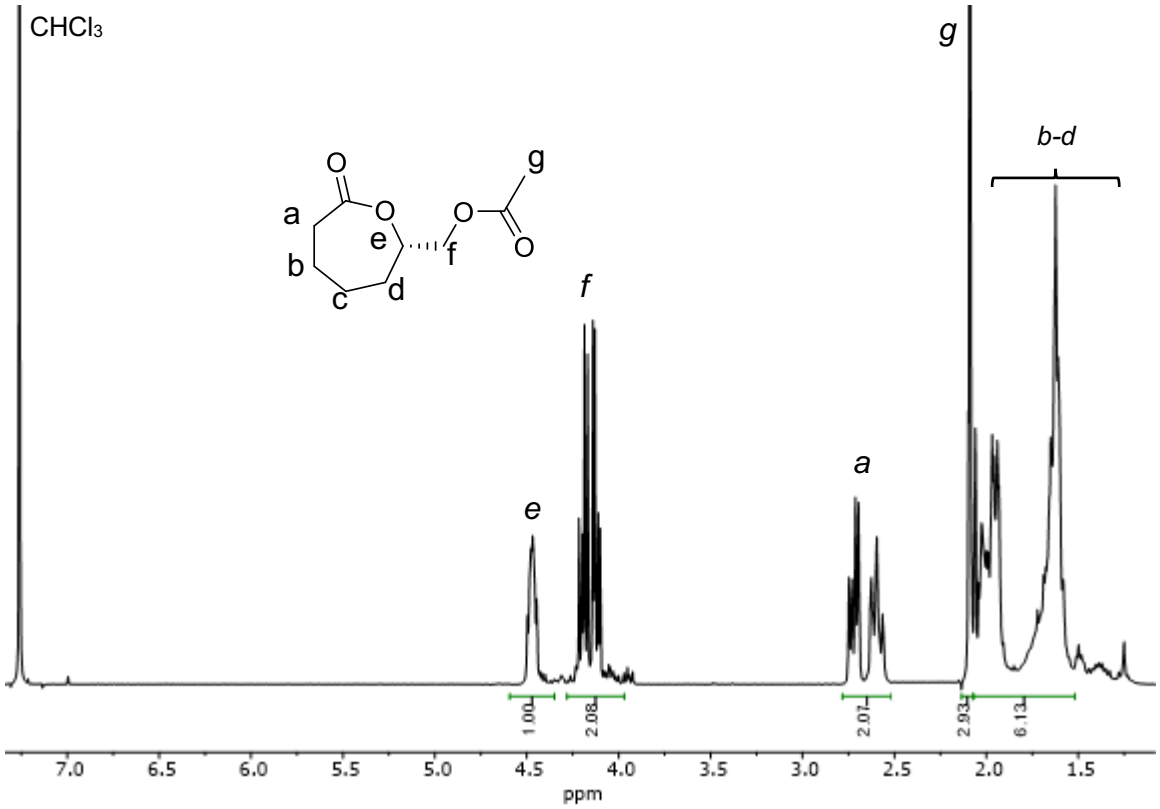

Figure 2.2. ^{1}H NMR spectrum of (*S*)-ε-methylacetyloxy-ε-caprolactone, (*S*)-**3** (400 MHz, 298 K, $CDCl_3$).

Initial polymerisation studies of (*S*)-**3** were performed under Schlenk conditions in benzene-d_6 at 25 °C with a monomer to initiator ratio of $[M]_0$:$[I]_0$ = 100:1 (where $[M]_0$ = 1.5 M) using the commercially available organocatalyst diphenyl phosphate (DPP) (5 mol%) and benzyl alcohol (BnOH) as initiator (Scheme 2.5). Monomer conversion was monitored by ^{1}H NMR spectroscopy, specifically through the disappearance of the proton signal at δ = 4.00 ppm which corresponds to $CH_2C(O)OC\underline{H}$ and the appearance of the equivalent polymer resonance at δ = 5.01 ppm. After 69 h at 25 °C, a 90% monomer conversion was achieved, at which point the polymerisation was quenched through the addition of alkaline resin beads, and subsequently precipitated into cold hexanes.

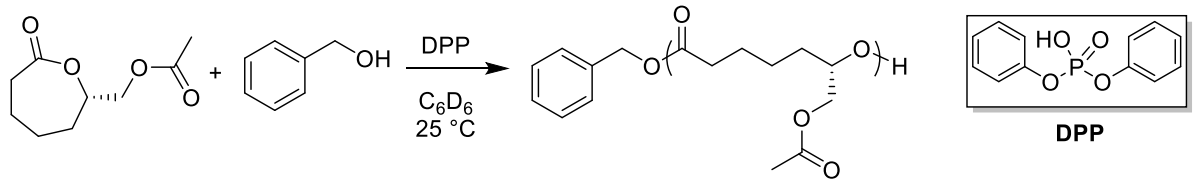

Scheme 2.5. The ROP of (*S*)-**3**, using BnOH as initiator and DPP as the catalyst.

The polymerisation was observed to be first order in monomer concentration as indicated by the linear relationship between $\ln([M]_0/[M]_t)$ and time (Figure 2.3). Molecular weights by SEC were lower than predicted with a multimodal distribution which suggested a lack of control during the polymerisation ($M_{n\ SEC}$ = 10,900 and $M_{n\ theo}$ = 16,300 g·mol^{-1}) (Figure 2.4). Molecular weights by ^{1}H NMR spectroscopy were difficult to ascertain as a result of overlap between the polymer chain-end and backbone resonances in a variety of solvents. The apparent lack of control was thought to be a consequence of transesterification side-reactions caused by the nucleophilic alcoholic chain-end attacking the electrophilic acetyl ester moiety along the polymer backbone. It is thought that the position of the ester side chain on the monomer ring likely plays an important role in determining the rate of side reactions as evidenced by a report describing the ROP of an ester functionalised lactone where the ester pendant group was placed further away from the ring-opening centre.[16] The resulting reported polyesters featuring pendant acetyloxy moieties possessed a monomodal distribution and low to moderate dispersities ($Đ_M$ = 1.23 − 1.42) by SEC. However, it should be noted that the ester group was more sterically encumbered for this example in comparison to (*S*)-**3**, most likely assisted in further prevention of transesterification reactions. As a result of limited control during the polymerisation with DPP, (*S*)-**3** was determined to be unsuitable for further studies.

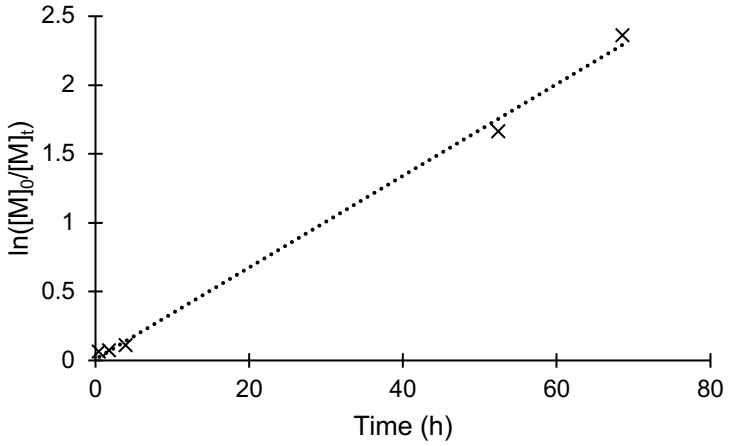

Figure 2.3. Kinetic plot for the ROP of (*S*)-**3** catalysed by DPP. Polymerisation was conducted at 25 °C in benzene-d_6 with [(*S*)-**3**]$_0$:[DPP]$_0$:[BnOH]$_0$ = 100:1:0.05 where [(*S*)-**3**]$_0$ = 1.5 M.

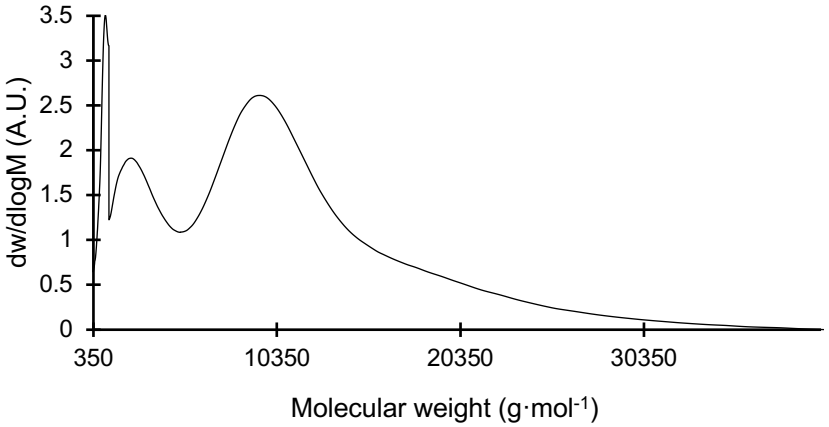

Figure 2.4. Size-exclusion chromatogram of poly((*S*)-ε-methylacetate-ε-caprolactone). Polymerisation was conducted at 25 °C in benzene-d_6 with [(*S*)-**3**]$_0$:[DPP]$_0$:[BnOH]$_0$ = 100:1:0.05 where [(*S*)-**3**]$_0$ = 1.5 M (M_n = 10,900 g·mol^{-1}, $Đ_M$ = 3.2) ($CHCl_3$, RI, calibrated against polystyrene standards).

*2.2.3. Synthesis and polymerisation of (*S*)-ε-methyl-*N*-hexylcarbamate-ε-caprolactone*

In attempts to mitigate nucleophilic attack from the alcohol chain-end and reduce transesterification during polymerisation, the ester group was substituted with a less electrophilic carbamate functionality, (*S*)-**4**, to afford a monomer with a less-reactive pendant group. Under dry and inert conditions, (*S*)-**2** was reacted with a slight excess of hexyl isocyanate in anhydrous THF with a catalytic amount of dibutyltin dilaurate (DBTDL) (Scheme 2.6). After purification *via* neutral alumina gel chromatography, (*S*)-**4** was recovered in 56% yield with a retention of *ee*.

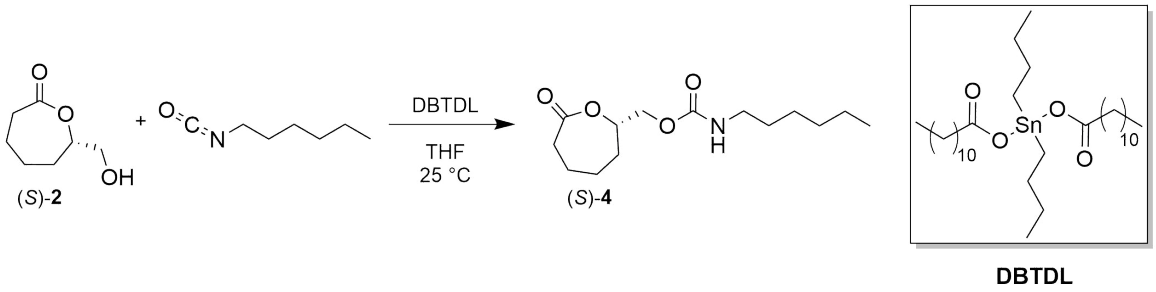

Scheme 2.6. Synthesis of (*S*)-ε-methyl-*N*-hexylcarbamate-ε-caprolactone, (S*)*-**4**, from (*S*)-**2**.

Product formation was monitored *via* ^{1}H NMR spectroscopy through the evolution of a diagnostic resonance at δ = 5.04 ppm, attributable to $CO_2N\underline{H}$, and aliphatic signals (δ = 3.07, 1.39, 1.21, and 0.78 ppm) characteristic of the *N*-hexyl chain of the carbamate unit (Figure 2.5). Additionally, there was a downfield shift in the methylene resonance attributable to C(O)OCHC$\underline{H_2}$ from δ = 3.69 ppm to δ = 4.04 ppm. As expected, this change was smaller than the ester derivative (*S*)-**3** (δ = 4.16 ppm) as the carbamate unit is less electronegative than the ester as a result of the inductive effects.

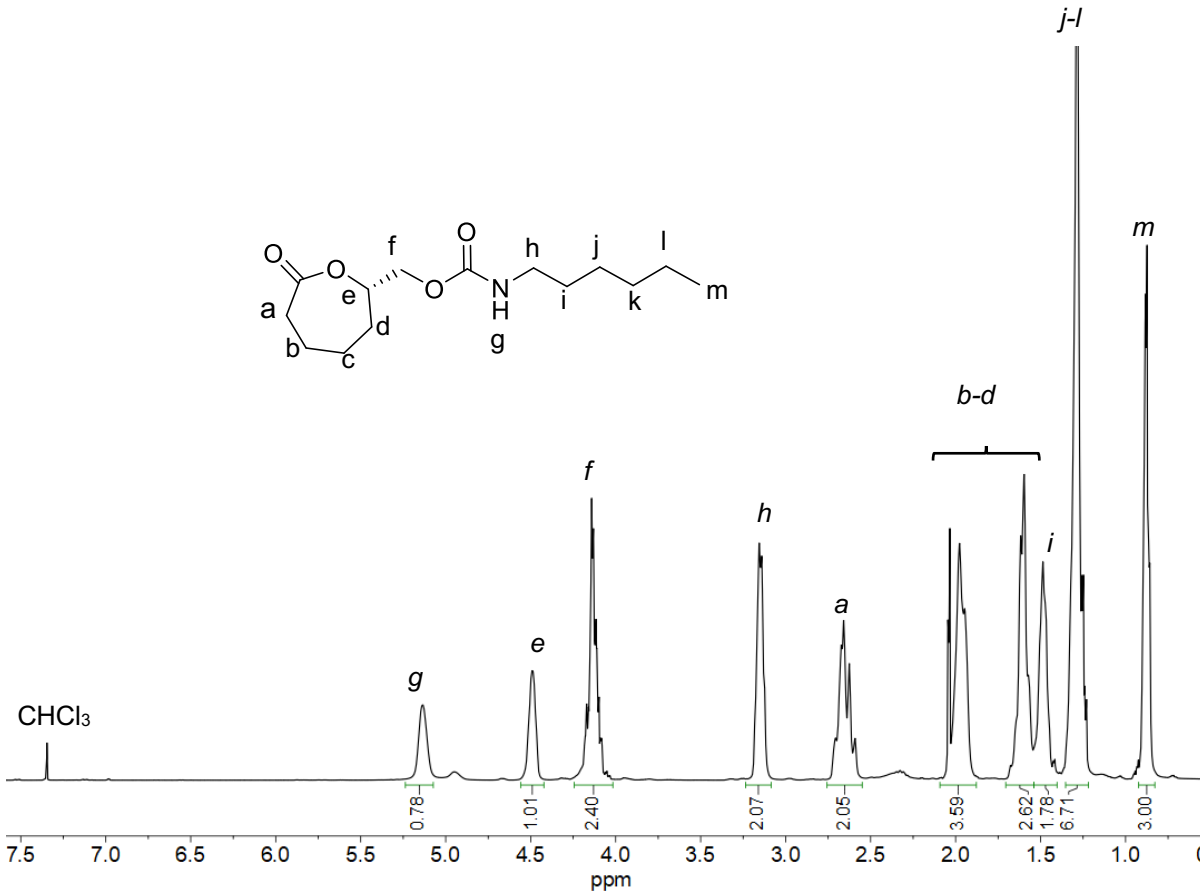

Figure 2.5. ^{1}H NMR spectrum of (*S*)-ε-methyl-*N*-hexylcarbamate-ε-caprolactone, (*S*)-**4** (400 MHz, 298 K, $CDCl_3$).

Initial studies investigated the DPP catalysed ROP of (*S*)-**4** at a $[(S)\text{-}\mathbf{4}]_0/[BnOH]_0/[DPP]_0$ ratio of 50:1:1, where $[(S)\text{-}\mathbf{4}]_0$ = 1 M in benzene-d_6 at 25 °C, showed that BnOH had began to slowly initiate the polymerisation after 45 minutes. This was evidenced through ^{1}H NMR spectrocscopy by the evolution of a singlet at δ = 5.01 ppm, indicative of $PhC\underline{H_2}OC(O)CH_2$, and the dissapearance of a singlet at δ = 4.66 ppm, attributable to $PhC\underline{H_2}OH$ of the unreacted initiator (Figure 2.6, inserts). Moreover, the resonance at δ = 3.93 ppm attributed to $C(O)OC\underline{H}CH_2$ of (*S*)-**4** dissapeared as the reaction progressed. Significant broadening of proton signals suggested formation of a polymeric structure. After 22 h the polymerisation was quenched *via* additon of alkaline resin beads and precipitated into cold hexanes to yield a colourless, tacky semi-solid.

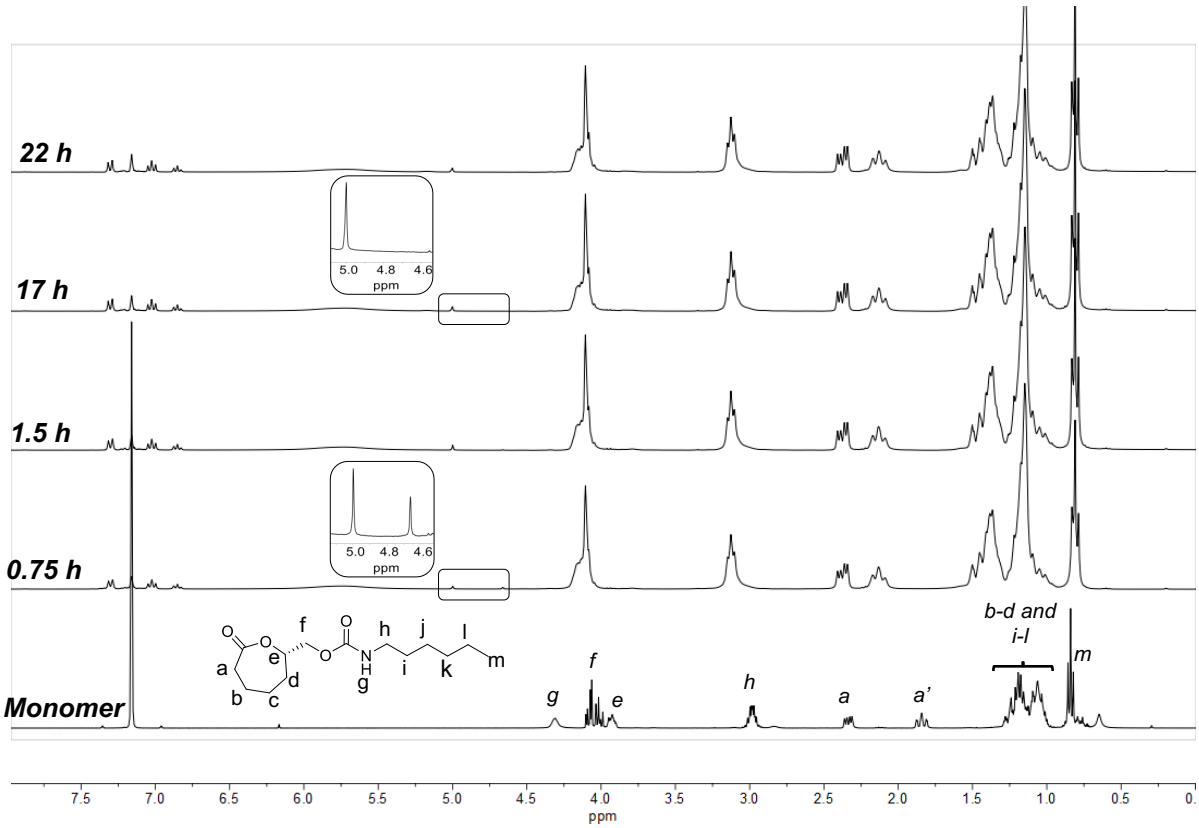

Figure 2.6. ^{1}H NMR spectra of diphenylphosphate catalysed (*S*)-**4** polymerisation at 25 °C (300 MHz, C_6D_6, 298 K).

Interestingly, despite the indication of a successful polymerisation by ^{1}H NMR spectroscopy, the molecular weight of the isolated product was significantly lower than the theoretical molecular weight ($M_{n\ theo}$ = 13,500 g·mol^{-1}) by SEC ($M_{n\ SEC}$ = 400 g·mol^{-1}) (Figure 2.7). Taking into account the indication of complete monomer initiation by ^{1}H NMR spectroscopy, in combination with the low molecular weight by SEC ,it was hypothesised that BnOH ring-opened a single molecule of (*S*)-**4** but this new species did not continue to propagate to form a polymer. This lack of propagation was thought to be a consequence of intramolecular hydrogen bonding between the alcohol chain-end and the carbonyl moiety of the carbamate unit to form a relatively stable 7-membered chelate (energetically comparable to the 7-membered lactone monomer) (Figure 2.8). Moreover, it was postulated that the apparent shift and broadening of

resonances seen by ^{1}H NMR spectroscopy could be a result of extended hydrogen bonding throughout the system. As such, the broad resonance at δ = 4.11 ppm (attributable to C(O)OCHC$\underline{H_2}$ of the monomer) displayed an integration of 3 protons instead of the expected integration of 2 protons which suggested that there was another proton resonance hidden beneath. It was hypothesised this this extra proton at δ = 4.11 ppm could be attributed to the overlap of peaks from a downfield shift of the resonance corresponding to C(O)OC$\underline{H}$CH$_2$ thought to be a consequence of increased hydrogen bonding in close proximity to the proton, which would create a deshielding effect and thus a downshield shift.

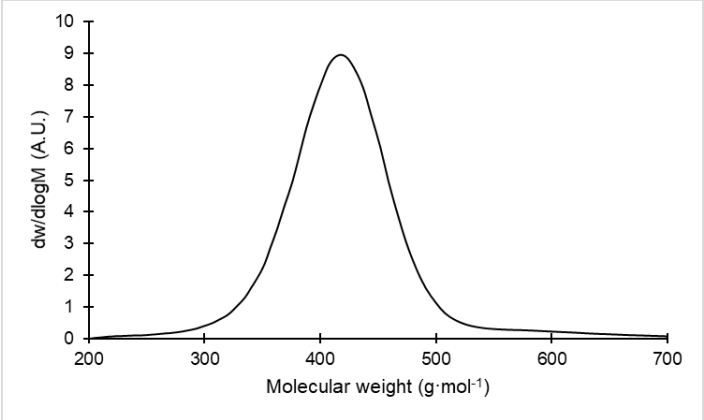

Figure 2.7. Size-exclusion chromatogram of product from ROP of (*S*)**-4** catalysed by DPP (M_n = 400 g·mol^{-1} and $Đ_M$ = 1.02). Polymerisation was conducted at 25 °C in benzene-d_6 with [(*S*)-**4**]$_0$:[DPP]$_0$:[BnOH]$_0$ = 50:1:1 where [(*S*)-**4**]$_0$ = 1.0 M ($CHCl_3$, RI, calibrated against polystyrene standards).

Consequently, the polymerisation was repeated at higher temperatures (70 °C) in hopes this would overcome the intramolecular hydrogen bonding. After 330 h at 70 °C, the polymerisation had reached a 55% monomer conversion by ^{1}H NMR spectroscopy. Comparison of ^{1}H NMR spectra from the DPP-catalysed ROP of (*S*)-**4** at 25 °C and 70 °C displayed the evolution of broad polymer peaks (δ = 2.24, 2.54 and 4.32 ppm)

(Figure 2.9) for the polymerisation at 70 °C which were not witnessed at 25 °C, which suggested polymer propagation successfully overcame the competing internal hydrogen bonding.

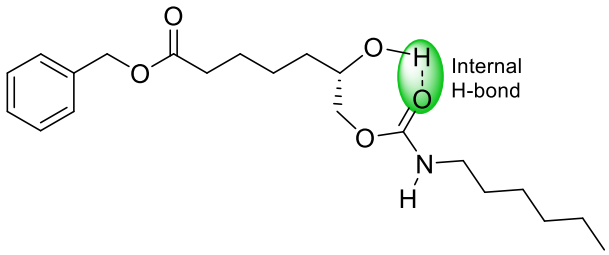

Figure 2.8. Proposed species, after monomer is initially ring-opened, depicting intramolecular hydrogen bonding between the alcohol chain-end and the carbamate carbonyl that may inhibit further propagation.

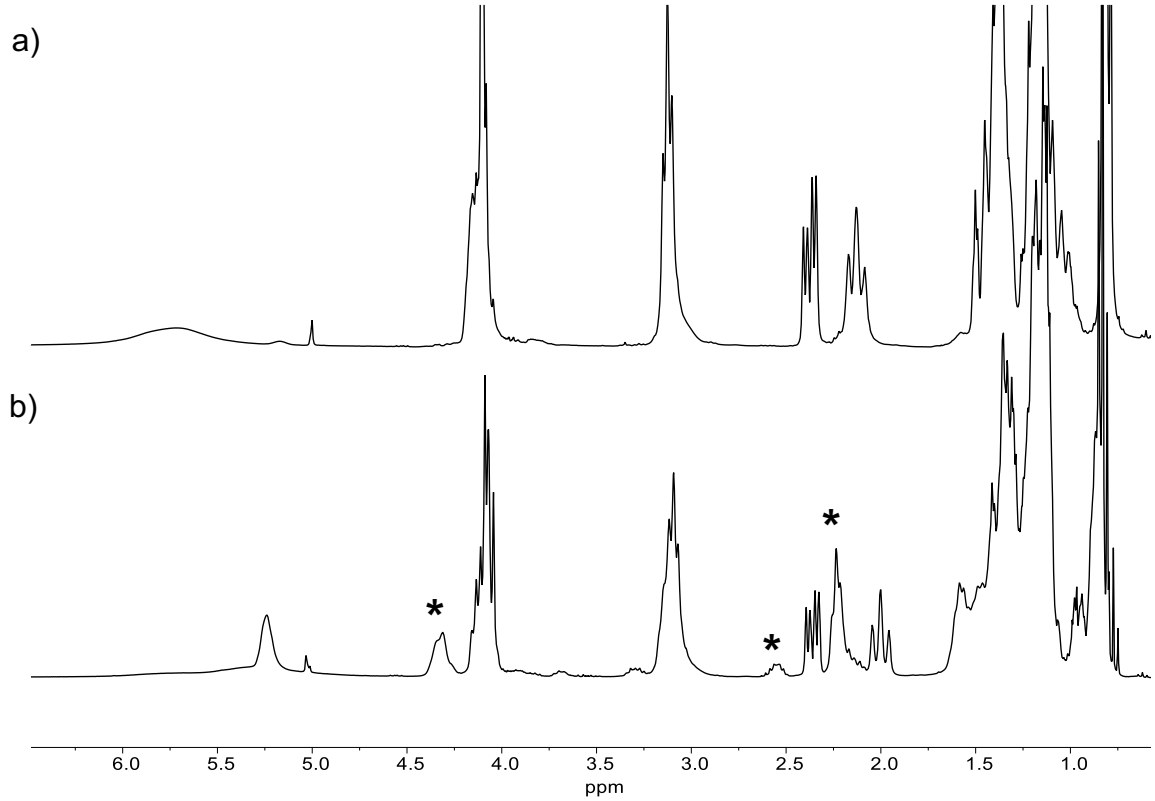

Figure 2.9. ^{1}H NMR spectra comparing the DPP catalysed polymerisation of (*S*)-**4** at a) 25 °C and b) 70 °C where * indicates the evolution of new polymer peaks (300 MHz, C_6D_6, 298 K).

After this point, the reaction mixture was quenched through the addition of alkaline resin beads and precipitated into cold hexanes. The kinetic plot of the polymerisation showed a non-linear relationship between $\ln([M]_0/[M]_t)$ and time (Figure 2.10) which suggested the polymerisation was not controlled. The negative curvature of the plot was suggestive of termination, possibly through intramolecular hydrogen bonding which became competitive with propagation as monomer concentration decreased. A lack of control during the polymerisation was further supported by poor correlation between theoretical molecular weight ($M_{n\ theo}$ = 10,900 g·mol^{-1}) and molecular weights obtained *via* ^{1}H NMR spectroscopy ($M_{n\ NMR}$ = 13,700 g·mol^{-1}) and SEC analysis (M_n

$_{SEC}$ = 4,300 g·mol^{-1}). Moreover, SEC analysis also revealed a broad dispersity ($Đ_M$ = 1.42) which further corroborated an uncontrolled polymerisation.

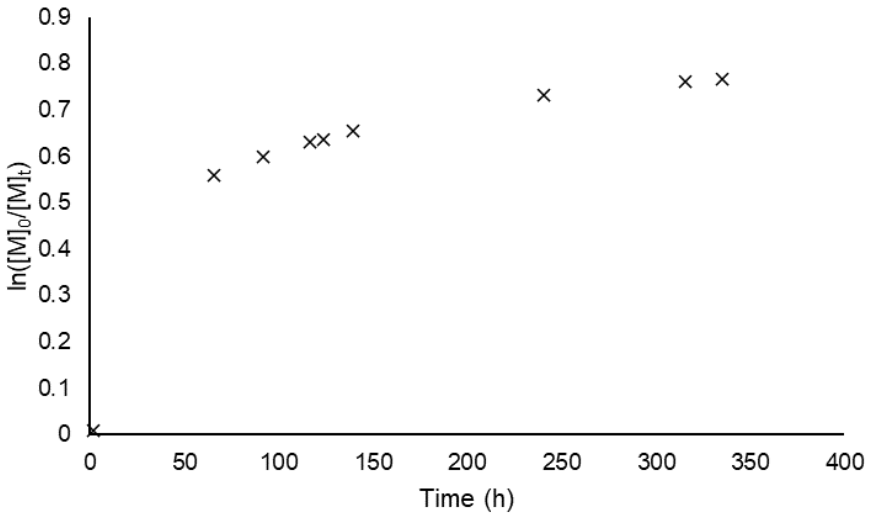

Figure 2.10. Kinetic plot for the ROP of (*S*)-**4** catalysed by DPP at 70 °C. Polymerisation was conducted at 70 °C in benzene-d_6 with [(*S*)-**4**]$_0$/[DPP]$_0$/[BnOH]$_0$ = 50:1:1 where [(*S*)-**4**]$_0$ = 1.0 M.

2.2.4. Synthesis and polymerisation of (S)-ε-methylbromo-ε-caprolactone

After issues that concerned unfavourable interactions between electrophilic pendant groups and the nucleophilic alcohol chain-end, we instead turned our attentions towards halogenated monomers in order to mitigate competitive side-reactions. As highlighted earlier, the introduction of a halogen atom into the monomer allows for post-polymerisation functionalisation through the introduction of an azide moiety to the polymer. From here, well-known azide-alkyne click chemistry opens the possibility of the attachment of small molecules for visualisation and probing strategies.[17] Yet none of these reports concerned the effect of stereochemistry at the functional centre and

its effect on polymer crystallinity and thermomechanical polymer properties. To this end, (*S*)-ε-methylbromo-ε-caprolactone, (*S*)-**5**, was synthesised in 49% yield from the alcohol (*S*)-**2** through an Appel reaction (Scheme 2.7).[11]

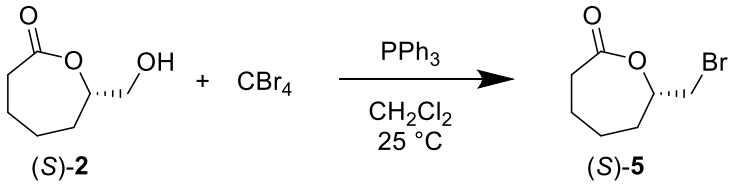

Scheme 2.7. Synthesis of (*S*)-ε-methylbromo-ε-caprolactone, (S*)*-**5**, from (*S*)-**2**.

Using ^{1}H NMR spectroscopy, the formation of the halogenated derivative was determined *via* the disappearance of the broad singlet attributable to the hydroxyl group of (*S*)-**2** (δ = 2.21 ppm). However, as a consequence of the similar electronegativities of oxygen and bromine, no other diagnostic changes were visible *via* NMR spectroscopy (Figure 2.11). FT-IR analysis corroborated the formation of (*S*)-**5** through the appearance of a C–Br stretch at 743 cm^{-1} and the absence of an alcohol group as no characteristic O–H stretch was detected in the 3500 - 3200 cm^{-1} region (Figure 2.12). Retention of stereochemistry was also confirmed by chiral GC and (*S*)-**5** was determined to possess an *ee* of 85% which confirmed the absence of epimerisation during the reaction.

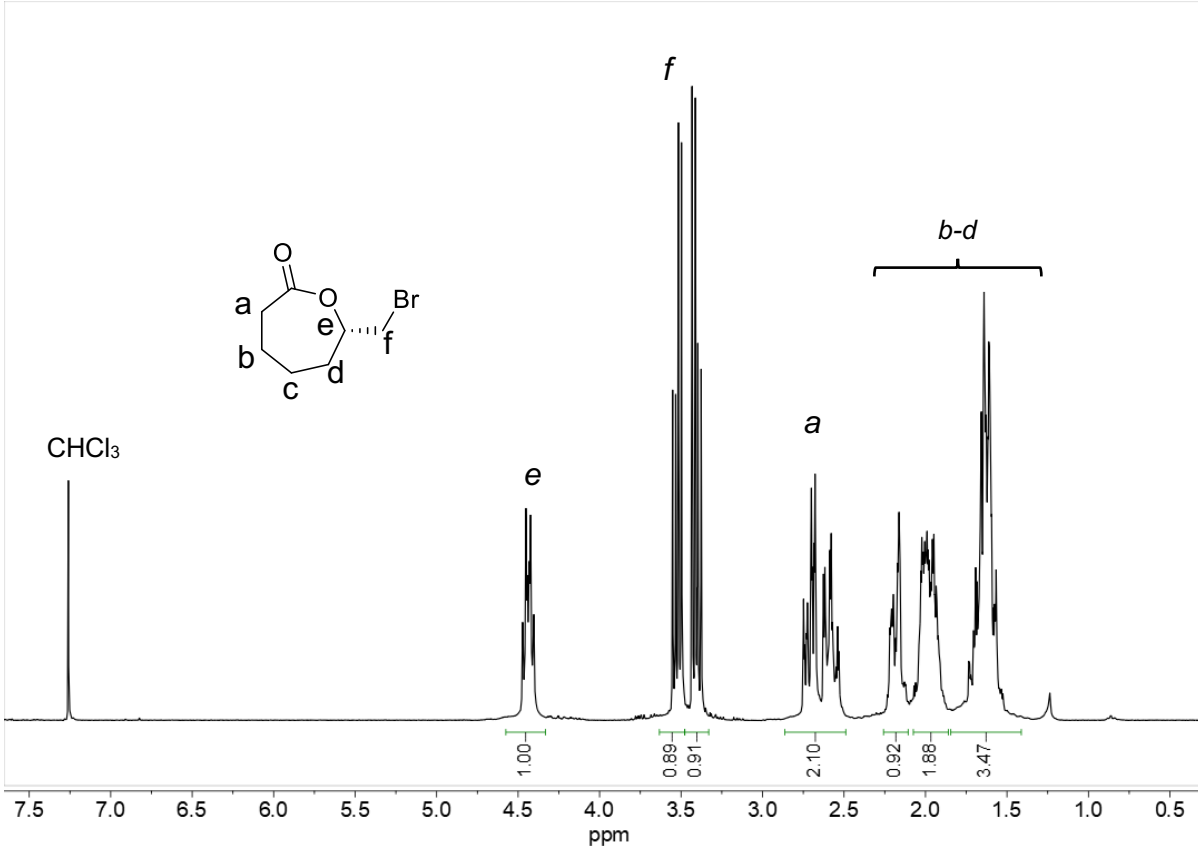

Figure 2.11. ^{1}H NMR spectrum of (*S*)-ε-methylbromo-ε-caprolactone, (*S*)-**5** (400 MHz, 298 K, $CDCl_3$).

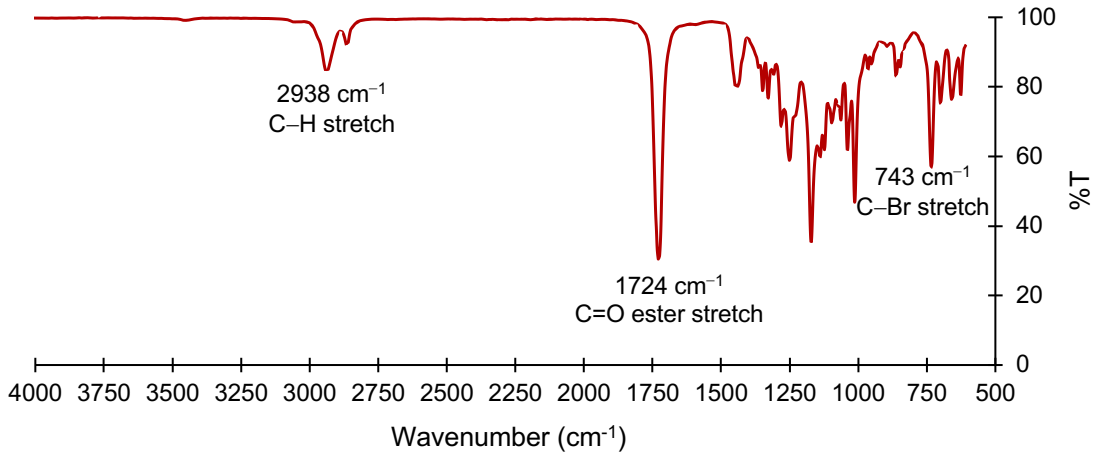

Figure 2.12. FT-IR spectrum of (*S*)-**5**.

The ROP of (*S*)-**5** was investigated at an initial [(*S*)-**5**]$_0$/[BnOH]$_0$/[DPP]$_0$ ratio of 50:1:1 where [(*S*)-**5**]$_0$ = 1 M in benzene-d_6 at 45 °C. The polymerisation was monitored by ^{1}H NMR spectroscopy through the disappearance of the multiplet resonance at δ = 3.79 ppm which corresponded to C(O)OC*H*CH$_2$ and the appearance the equivalent polymer signal at δ = 4.95 ppm. An 80% monomer conversion was eventually reached after 820 h at 45 °C, at which point the polymerisation was quenched through the addition of alkaline resin beads and subsequently precipitated into cold hexanes. The kinetics of the polymerisation were investigated, which showed a linear increase of ln([M]$_0$/[M]$_t$) over time which suggested the polymerisation proceeded in a controlled manner (Figure 2.13). This conclusion was further supported by good correlation between theoretical molecular weight ($M_{n\ calc}$= 8,300 g·mol^{-1}) and molecular weights obtained by ^{1}H NMR spectroscopy ($M_{n\ NMR}$ = 9,200 g·mol^{-1}) and SEC ($M_{n\ SEC}$ = 9500 g·mol^{-1}) (Figures 2.14-15). Additionally, SEC analysis of the polymer showed a monomodal distribution with a narrow dispersity ($Đ_M$ = 1.12) (Figure 2.15).

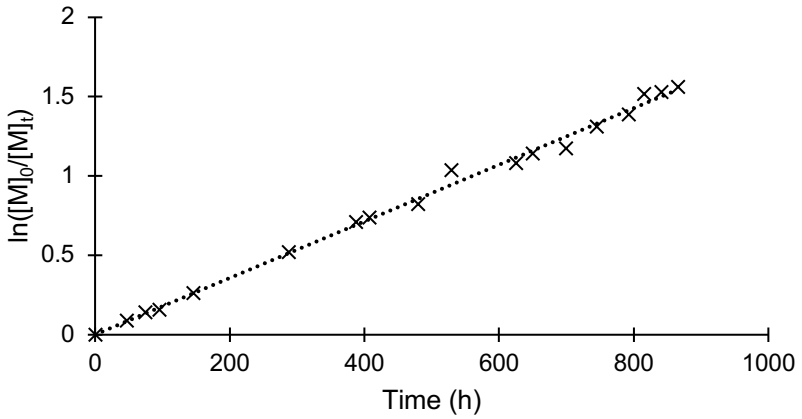

Figure 2.13. Kinetic plot for the ROP of (*S*)-**5**. Polymerisation was conducted at 45 °C in benzene-d_6 with [(*S*)-**5**]$_0$/[DPP]$_0$/[BnOH]$_0$ = 50:1:1 where [(*S*)-**5**]$_0$ = 1 M.

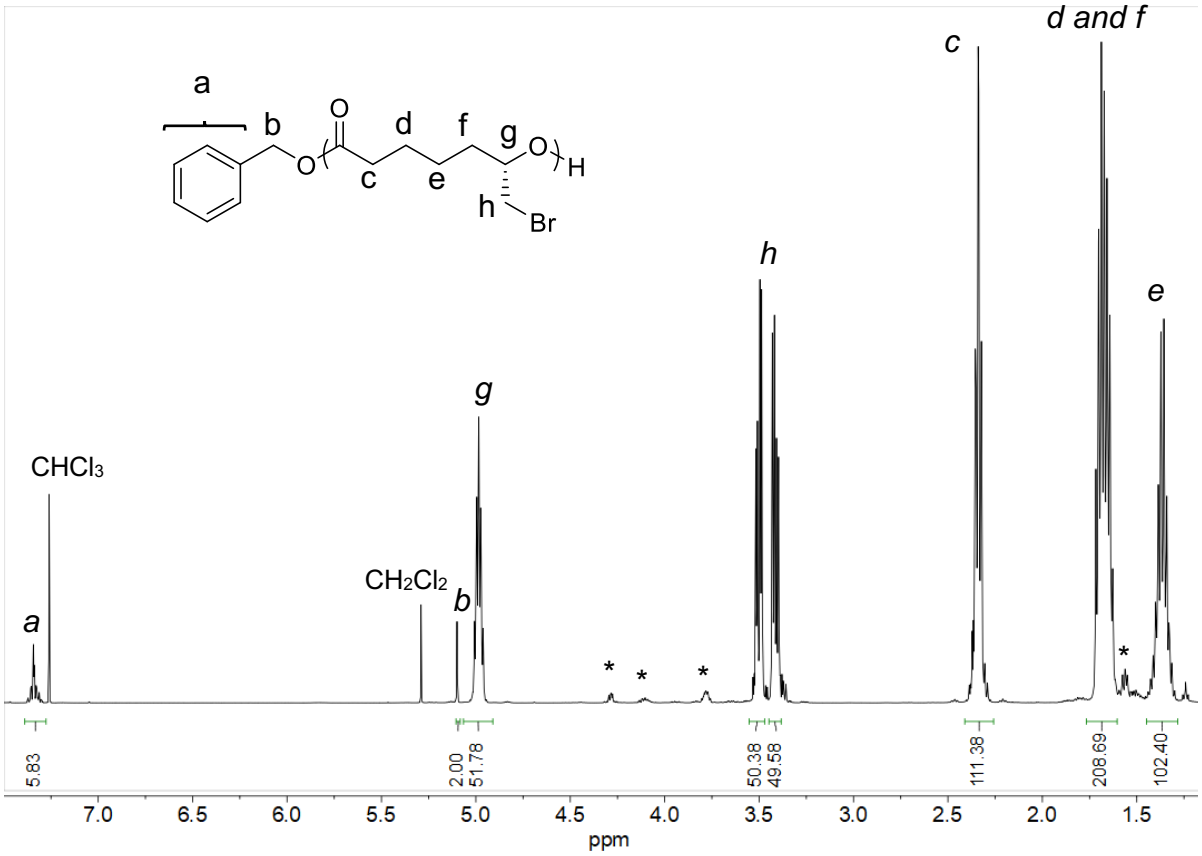

Figure 2.14. ^{1}H NMR spectrum of poly((*S*)-ε-methylbromo-ε-caprolactone) ($CDCl_3$, 500 MHz, 298 K). * indicates unprecipitated monomer.

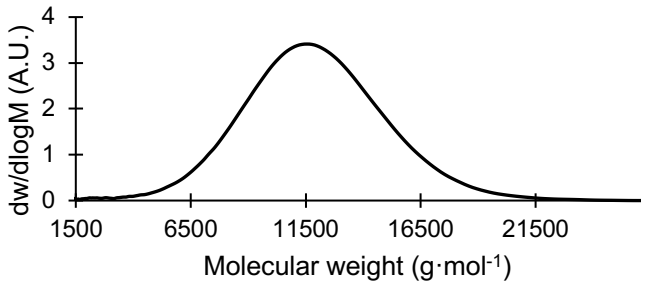

Figure 2.15. Size-exclusion chromatogram of poly((*S*)-ε-methylbromo-ε-caprolactone). Polymerisation was conducted at 45 °C in benzene-d_6 with [(*S*)-**5**]$_0$:[DPP]$_0$:[BnOH]$_0$ = 50:1:1 where [(*S*)-**5**]$_0$ = 1 M (M_n = 9,500 g·mol^{-1}, $Đ_M$ = 1.12) ($CHCl_3$, RI, calibrated against polystyrene standards).

Having produced a well-defined polymer, the thermal properties were then assessed by differential scanning calorimetry (DSC) using a heating and cooling rate of 10 $K \cdot min^{-1}$. The polymer only displayed a glass transition temperature of –28 °C, and no first order melting or crystallisation transitions, which suggested the sample was amorphous in nature. The lack of semi-crystallinity by DSC verified that an initial monomer *ee* of 85% most likely imparted enough stereoerrors into the polymer backbone to preclude crystallisation of the bulk sample.

2.3. Conclusions

With the aim to create a semi-crystalline poly(εSεL), (*S*)-ε-hydroxymethyl-ε-caprolactone was synthesised with an 85% *ee* through the asymmetric α-hydroxymethylation of cyclohexanone followed by a Baeyer-Villiger ring-expansion. After protection of the alcohol group *via* an acetylation reaction, the subsequent monomer was polymerised. Yet despite apparent first-order kinetics, the polymerisation shown to be uncontrolled with broad and multimodal distributions as a result of transesterification.

In efforts to overcome the transesterification side-reactions, the less electrophilic (*S*)-ε-methyl-*N*-hexylcarbamate-ε-caprolactone was synthesised. However, the resultant ROP was thought to be hindered by hydrogen bonding between the alcohol chain-end and carbonyl of the carbamate which led to a stoichiometric ring-opening reaction. Heating the reaction to 70 °C allowed for polymer propagation through the reduction in non-covalent side reactions, albeit with poor control.

Possessing a pendant group resistant towards nucleophilic attack, (*S*)-ε-methylbromo-ε-caprolactone was synthesised with an *ee* of 85% and subsequent

polymerisation with DPP was shown to proceed in a controlled manner. Yet despite an initial monomer *ee* of 85%, thermal analysis by DSC showed the polymer to be amorphous in nature, which suggested a high degree of stereo-irregularity along the polymer backbone and a result.

2.4. References

1. G. Wang, Y. Shi, Z. Fu, W. Yang, Q. Huang and Y. Zhang, *Polymer*, 2005, **46**, 10601-10606.
2. E. E. Smissman and J. V. Bergen, *J. Org. Chem.*, 1962, **27**, 2316-2318.
3. D. Mecerreyes, B. Atthoff, K. A. Boduch, M. Trollsås and J. L. Hedrick, *Macromolecules*, 1999, **32**, 5175-5182.
4. S. Lenoir, R. Riva, X. Lou, C. Detrembleur, R. Jérôme and P. Lecomte, *Macromolecules*, 2004, **37**, 4055-4061.
5. R. Riva, S. Schmeits, F. Stoffelbach, C. Jérôme, R. Jérôme and P. Lecomte, *Chem. Commun.*, 2005, 5334-5336.
6. C. Detrembleur, M. Mazza, O. Halleux, P. Lecomte, D. Mecerreyes, J. L. Hedrick and R. Jérôme, *Macromolecules*, 2000, **33**, 14-18.
7. C. Detrembleur, M. Mazza, X. Lou, O. Halleux, P. Lecomte, D. Mecerreyes, J. L. Hedrick and R. Jérôme, *Macromolecules*, 2000, **33**, 7751-7760.
8. B. Vroman, M. Mazza, M. R. Fernandez, R. Jérôme and V. Préat, *J. Controlled Release*, 2007, **118**, 136-144.
9. R. Riva, W. Lazzari, L. Billiet, F. Du Prez, C. Jérôme and P. Lecomte, *J. Polym. Sci., Part A: Polym. Chem.*, 2011, **49**, 1552-1563.
10. Y. Gao, T. Mori, S. Manning, Y. Zhao, A. d. Nielsen, A. Neshat, A. Sharma, C. J. Mahnen, H. R. Everson, S. Crotty, R. J. Clements, C. Malcuit and E. Hegmann, *ACS Macro Lett.*, 2016, **5**, 4-9.
11. A. Chen, J. Xu, W. Chiang and C. L. L. Chai, *Tetrahedron*, 2010, **66**, 1489-1495.
12. N. Zotova, A. Franzke, A. Armstrong and D. G. Blackmond, *J. Am. Chem. Soc.*, 2007, **129**, 15100-15101.

13. M. Trollsås, P. Löwenhielm, V. Y. Lee, M. Möller, R. D. Miller and J. L. Hedrick, *Macromolecules*, 1999, **32**, 9062-9066.

14. M. Liu, N. Vladimirov and J. M. J. Fréchet, *Macromolecules*, 1999, **32**, 6881-6884.

15. C. Béguin, K. K. Duncan, T. A. Munro, D. M. Ho, W. Xu, L. Liu-Chen, W. A. Carlezon Jr and B. M. Cohen, *Biorg. Med. Chem.*, 2009, **17**, 1370–1380.

16. M. Trollsås, V. Y. Lee, D. Mecerreyes, P. Löwenhielm, M. Möller, R. D. Miller and J. L. Hedrick, *Macromolecules*, 2000, **33**, 4619-4627.

17. L. Li and Z. Zhuang, *Molecules*, 2016, **21**, 1393.

3. Chapter three

Organocatalysed enantioselective ring-opening polymerisation of ε-substituted-ε-caprolactones

3.1. Introduction

One approach to achieve a semi-crystalline polymer is through the enantioselective ring-opening polymerisation (ROP) of a racemic monomer. However, most reports to date have focussed on metal-based catalysis[1-4] to achieve this leading to problems for biological applications.[5] A renewed interest in enantioselective organocatalysed ROP was inspired by Makiguchi *et al.* through the use of chiral binaphthol-derived (BINOL) phosphoric acids, reporting a highly enantioselective ROP of racemic lactide (Scheme X.1).[6] By leveraging the modularity of the chiral BINOL backbone it was found that the electronic nature of the backbone had a profound effect on enantioselectivity compared to steric hindrance. After quenching the polymerisation at a 50% monomer conversion, chiral high-performance liquid chromatography (HPLC) analysis of unreacted monomer showed that (*R*)-**1a** preferentially polymerised D-lactide at 75 °C to give an unreacted monomer enantiomeric excess (*ee*) of 80.6%. As expected, the polymerisation temperature strongly influenced the *ee* of the unreacted monomer and increasing the polymerisation temperature above 75 °C caused a slight decrease in *ee* to 74.9%. Interestingly, reducing the polymerisation temperature to 60 °C triggered a drastic decrease in *ee* of unreacted monomer to 24.4% which was thought to be a result of a heterogeneous polymerisation yielding low enantiomeric selectivity in addition to poor control over molecular weights.

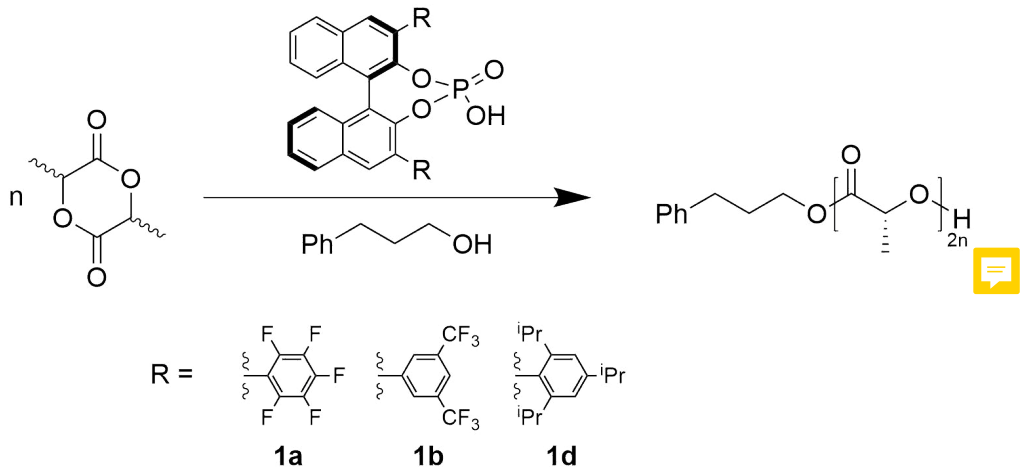

Scheme 3.1. Enantioselective polymerisation of *rac*-lactide by chiral BINOL-derived phosphoric acids. Adapted from Makiguchi *et al.*[6]

Inspired by the works of Makiguchi *et al.*, Wang and co-workers reported the first example of an organocatalysed enantioselective ROP of substituted ε-caprolactones.[7] In the hopes of synthesising a stereogradient polymer to improve upon the thermal properties of substituted poly(ε-caprolactone) *via* stereocomplexation, racemic α- and ε-benzyl-ε-caprolactone (αBnCL and εBnCL, respectively) were polymerised using the chiral (*R*)-TRIP BINOL phosphoric acid ((*R*)-**1d**) as an enantioselective ROP catalyst. Compared to αBnCL, reaction times for εBnCL were found to be increased as a result of the benzyl substituent present at the propagating position significantly hindering polymerisation rates. On the other hand, when polymerisations were conducted at 90 °C, the placement of the benzyl substituent was found to have little effect on enantioselectivity. Quenching the polymerisations at a 50% monomer conversion gave an unreacted monomer *ee* of 24% and 20% for αBnCL and εBnCL, respectively. Moreover, size-exclusion chromatography (SEC) analysis suggested the (*R*)-**1d** catalysed polymerisations proceeded in a controlled manner through moderate dispersities ($Đ_M$ = 1.12 – 1.22). However, the effects of catalyst structure and

polymerisation conditions such as temperature on enantioselectivity, and the thermal properties of the resulting polymers were not reported.

Despite the renewed interest experienced by enantioselective organocatalysed ROP within the last decade, little focus has gone beyond the ROP of lactide and simple substituted esters such as δ-valerolactone (δVL) and ε-caprolactone (εCL) leading to a limited monomer scope. Motivated by the works of Makiguchi *et al.* and Wang and co-workers, this chapter will focus on expanding the ε-substituted monomer scope of enantioselective organocatalysed ROP with the aim of synthesising a semi-crystalline polymer for crystalline-driven self-assembly applications.[6, 7] The specific placement of a substituent at the ε-position aids in overcoming transesterification side reactions, an inherent risk of ROP, through increased steric hindrance at the propagating centre.[8] Minimising transesterification during an enantioselective ROP creates a polymer possessing a narrow dispersity increasing the likelihood of a semi-crystalline polymer.

3.2. Results and Discussion

3.2.1. Catalyst Screening

Considering that chiral BINOL-based phosphoric acids have previously been shown to mediate the enantioselective polymerisation of racemic lactide, we chose to leverage the modularity of the chiral BINOL backbone for the enantioselective ROP of ε-substituted-ε-caprolactones (εSεLs).[6] Control over the electronic and steric nature of the BINOL backbone, and also catalyst acidity, allowed us to screen a variety of catalysts with three racemic εSεL monomers. Varying the substituent at the ε-position of ε-caprolactone, from a sterically small group such as methyl (Figure 3.1a) to a bulkier and more electron-rich group such as allyl (Figure 3.1b) and finally to an even further

sterically encumbered group such as butyl (Figure 3.1c) allowed us to explore how the nature of the ε-substituent also plays a role in enantioselectivity.

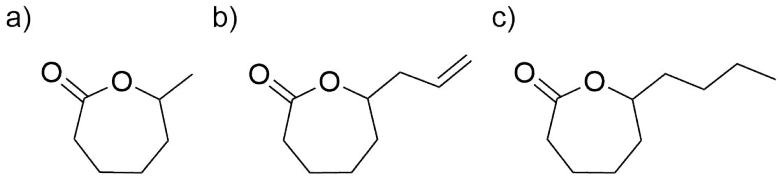

Figure 3.1. a) ε-heptalactone b) ε-allyl-ε-caprolactone c) ε-decalactone

3.2.1.1. Control

Diphenyl phosphate (DPP) is an inexpensive, commercially available organocatalyst that has previously been shown to efficiently mediate the ROP of cyclic esters to high monomer conversions under ambient conditions, with good control over molecular weights.[9-11] Furthermore, DPP displays no control over enantioselectivity during the polymerisation of racemic lactones to produce atactic polyesters. Accordingly, DPP was applied as the control catalyst for the ROP of our three racemic εSεL monomers, ε-heptalactone (*rac*-εHL), ε-allyl-ε-caprolactone (*rac*-εAL), and ε-decalactone (*rac*-εDL) at 70 °C (Scheme 3.2), using an initial $[\varepsilon S\varepsilon L]_0/[DPP]_0/[BnOH]_0$ ratio of 100:1:1 where $[\varepsilon S\varepsilon L]_0$ = 1 M in benzene-d_6 (Table 3.1 entries **1**, **2**, **3**).

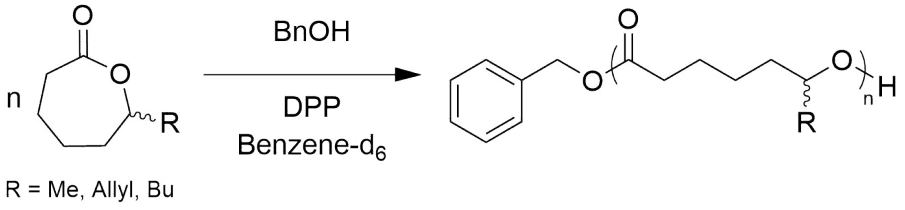

Scheme 3.2. ROP of racemic εSεL monomers catalysed by DPP. Polymerisations were conducted using benzyl alcohol as an initiator and an initial $[\varepsilon S\varepsilon L]_0/[DPP]_0/[BnOH]_0$ ratio of 100:1:1 where $[\varepsilon S\varepsilon L]_0$ = 1 M in benzene-d_6.

Polymerisations were followed by ^{1}H NMR spectroscopy through the reduction of the resonance attributable to C(O)OC*H*R of the monomer which coincided with the appearance of the corresponding proton in the PεSεLs. At 50% monomer conversion, polymerisations were quenched and following precipitation of the polymer, *ee* of recovered unreacted monomer was determined by chiral gas chromatography-mass spectrometry (GC-MS). As the least sterically hindered monomer, εHL was consumed most rapidly with subsequent reaction times lengthening as monomer steric hindrance increased. As expected, *ee*'s for all unreacted monomers were low (εHL 5.7%, εAL 3.3%, εDL 0.32%). Furthermore, after drying under vacuum, polymers were analysed by ^{1}H and ^{13}C NMR spectroscopy, differential scanning calorimetry (DSC), and size-exclusion chromatography (SEC). Previously reported for the ROP of lactones, DPP displayed good control over polymerisations, confirmed by the good agreement between theoretical molecular weights and molecular weights calculated from ^{1}H NMR spectra and size-exclusion chromatograms with narrow dispersities ($Đ_M$ = 1.02 – 1.06).[9] To determine the tacticity of the polymers, the carbonyl and methine region of quantitative ^{13}C NMR spectra of polymer samples were evaluated (Figure 3.2 and Figure 3.3, respectively). All three polymers displayed broad peaks for both the carbonyl and methine regions which confirmed their atactic microstructure, where no control is displayed over the distribution of stereocentres along the polymer backbone. Analysis of the polymers from DPP by DSC gave only one thermal transition which corresponded to the glass-transition temperature (T_g) confirming the polymers were amorphous in nature (−45 °C, −52 °C, and −53 °C for PεHL, PεAL, and PεDL, respectively). Combining results from chiral GC-MS, ^{13}C NMR spectroscopy, and DSC,

polymers obtained *via* DPP were confirmed as good controls for future enantioselective polymerisations as a result of their atactic and amorphous nature.

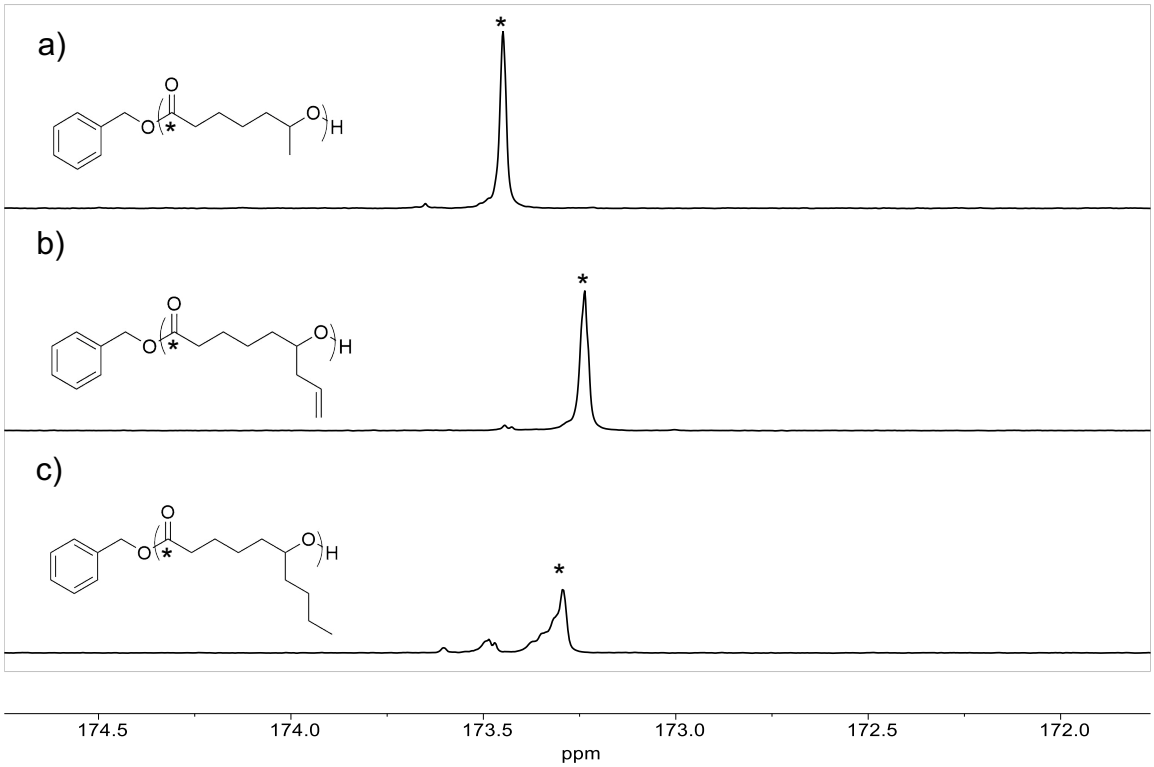

Figure 3.2. ^{13}C NMR spectra showing carbonyl region of a) PεHL b) PεAL and c) PεDL ($CDCl_3$, 150 MHz, 298 K).

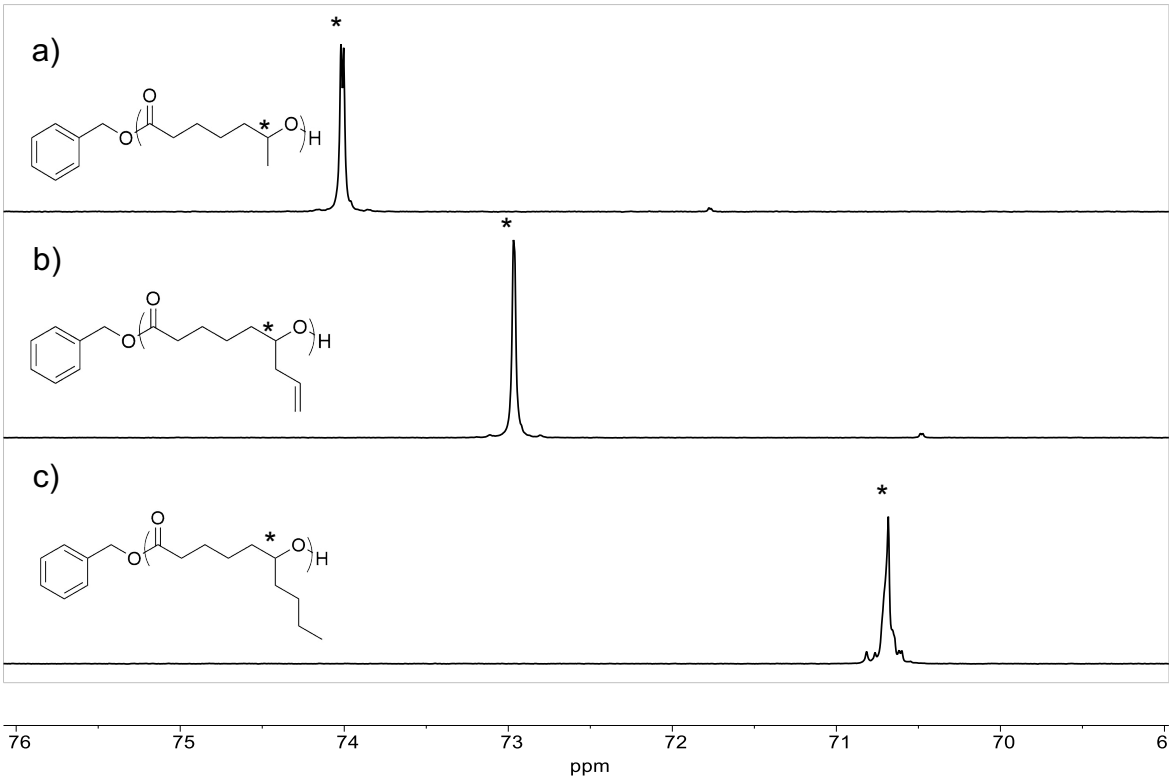

Figure 3.3. ^{13}C NMR spectra showing methine region of a) PεHL b) PεAL and c) PεDL ($CDCl_3$, 150 MHz, 298 K).

Table 3.1. Polymerisation data from DPP catalysed ROP of for *rac*-εSεL monomers using $[monomer]_0/[DPP]_0/[BnOH]_0$ ratio of 100:1:1 where $[monomer]_0$ = 1 M.

Entry	Monomer	Catalyst	Monomer conversion[a] (%)	*ee*[b] (%)	Temperature (°C)	Time (h)
1	*rac*-εHL	DPP	30	5.7	70	120
2	*rac*-εAL	DPP	89	3.3	70	340
3	*rac*-εDL	DPP	84	0.32	70	390

[a] Monomer conversion determined by ^1H NMR spectroscopy. [b] Enantiomeric excess determined by chiral GC-MS.

3.2.1.2. Investigating catalyst structure-function relationships

Recently, Zhang *et al.* reported an imidodiphosphorimidate as an efficient catalyst for the controlled ROP of δVL and εCL affording poly(δ-valerolactone) and poly(ε-caprolactone) with narrow dispersities and predictable molecular weights (Figure 3.4a).[12] Replacing the *N*-trifyl phosphoryl groups of an imidodiphosphorimidate with phosphoryl acid groups yields imidodiphosphoric acids such as **3** which possess a well-defined and narrow cavity (Figure 3.4b).[13] It was postulated that this narrow cavity may induce enantioselectivity during the ROP of the least sterically hindered monomer, *rac*-εHL. As such, the polymerisation of *rac*-εHL was conducted in benzene-d_6 using BnOH as an initiator and an initial *rac*-εHL concentration of 1 M and a [*rac*-εHL]$_0$/[**3**]$_0$/[BnOH]$_0$ ratio of 100:1:1 (Table 3.2 entry **10**). After 223 h at 70 °C, the polymerisation reached a 50% monomer conversion at which point the reaction was quenched and precipitated into cold hexanes. Despite the well-defined, narrow cavity found in **3**, chiral GC-MS analysis of unreacted monomer displayed a low *ee* of 25%. It was hypothesised that the increased acidity of **3** would strengthen hydrogen bonding interactions between catalyst, monomer, and initiator possibly leading to an increase in enantioselectivity and shorter polymerisation times. However, in comparison to other catalysts screen, **3** displayed a low catalytic activity with long polymerisation times thought to be a result of discrepancies between size of monomer and the narrow cavity found in **3** preventing adequate interactions between catalyst and monomer/initiator.

a) b)

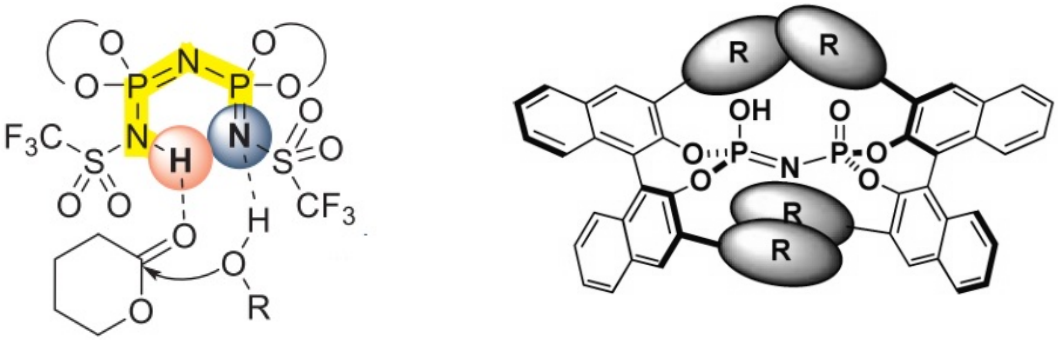

Figure 3.4. a) Proposed structure of dual activation of monomer and initiator by imidodiphosphorimidate. Adapted from Zhang *et al.*[12] b) Well-defined, narrow cavity found in imidodiphosphoric acids. Adapted from Liao *et al.*[13]

In recent years, chiral BINOL-derived phosphoric acids have emerged as powerful asymmetric organocatalysts as a result of their inherent modularity.[14-18] Careful selection of substituents at the 3,3'-positions of the BINOL-derived phosphoric acid catalysts is essential to obtain high enantioselectivities during polymerisations. We first evaluated the effect of the substituent (R) found in the chiral BINOL backbone through screening a variety of chiral BINOL-derived phosphoric acids, (*R*)-**1a-d**, with our three racemic εSεL monomers (Figure 3.5). Inspired by the strong influence of the electronic nature of the chiral BINOL backbone on the enantioselective ROP of *rac*-lactide, we first chose to screen (*R*)-**1a** with our racemic εSεL monomers.[6] Polymerisations were conducted using BnOH as the initiator with an initial $[\varepsilon S\varepsilon L]_0/[(R)\text{-}\mathbf{1a}]_0/[BnOH]_0$ ratio of 100:1:1 where $[\varepsilon S\varepsilon L]_0$ = 1 M in benzene-d_6 (Table 3.2 entries **1**, **3**, **4**). All polymerisations proceeded homogeneously at 70 °C with monomer conversions reaching approximately 50% before quenching and precipitating. Intriguingly, despite εDL possessing the highest steric hindrance, chiral GC-MS analysis of unreacted εDL

displayed the lowest *ee*, whilst εAL showed the highest *ee*, 21.4 and 38.4% respectively. This was hypothesised to be a consequence of the CH-π interactions between the electron-deficient aryl groups found in (*R*)-**1a** and the electron-rich terminal alkene found in εAL of the last inserted monomer unit within the growing polyester chain. In efforts to further increase *ee* whilst maintaining reasonable polymerisation times, the polymerisation of *rac*-εHL, as the least sterically hindered monomer, was repeated at a reduced polymerisation temperature of 25 °C from 70 °C (Table 3.2 entry **2**). After 72 h, a monomer conversion of 50% was achieved leading to a small increase in unreacted monomer *ee* from 29.6% to 38.2% (Table 3.2 entries **1** and **2**, respectively). SEC analysis of polymers produced by (*R*)-**1a** displayed monomodal distributions with narrow dispersities ($Đ_M \leq 1.15$). Moreover, theoretical molecular weights and those obtained from SEC and ^{1}H NMR spectroscopy were in agreement confirming (*R*)-**1a** displayed good control over the polymerisations. However, as a consequence of increased polymerisation times in correlation with monomer bulkiness, no other monomers were screened at this lower temperature. In efforts to find a universal catalyst, these results suggested that whilst electronegativity of the BINOL-backbone of the phosphoric acid catalyst had a small effect on the enantioselective ROP of *rac*-εAL, overall controlling electronegativity was not essential for optimising enantioselectivity.

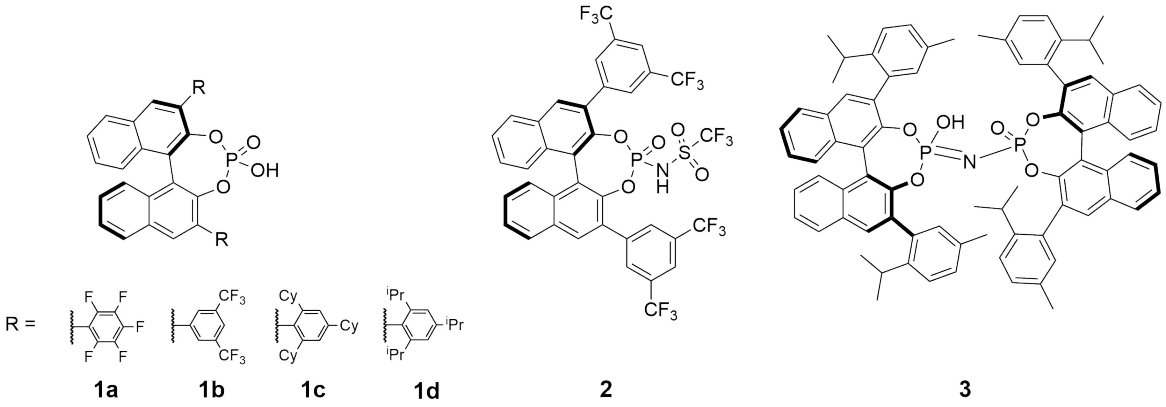

Figure 3.5. Chiral BINOL-derived phosphoric acids and *N*-phosphoramides screened as for the enantioselective polymerisation of εSεL monomers in the present work.

Phosphoric acid (*R*)-**1b** and *N*-phosphoramide (*R*)-**2** were investigated as enantioselective ROP catalysts to understand the effect of acidity on enantioselectivity. Possessing a 3,3'-BINOL substituent with comparable electron-withdrawing ability to **1a**, the polymerisation of *rac*-εHL was conducted screening (*R*)-**1b,** using BnOH as initiator with an initial [*rac*-εHL]$_0$/[(*R*)-**1b**)]$_0$/[BnOH]$_0$ ratio of 100:1:1 and an initial *rac*-εHL concentration of 1 M in benzene-d_6 (Table 3.2, entry **5**). At 70 °C the enantioselective polymerisation of *rac*-εHL took 122 h to reach a 45% monomer conversion. Analysis of the unreacted monomer confirmed (*R*)-**1b** to be a less effective enantioselective catalyst for the ROP of *rac*-εHL compared to (*R*)-**1a** (13.3% *vs*. 29.6% *ee*, respectively). This suggested that that the addition of increased steric hindrance at the 2,4-position of (*R*)-**1b** had a deleterious effect on enantioselectivity likely because of a lack of proximity to the active catalyst site.

Comparing pK_a's of phosphoric acids and *N*-phosphoramides in acetonitrile, *N*-phosphoramides were found to be considerably more acidic (12-14 and 6-7, respectively).[16] It was hypothesised that this increase in acidity moving from (*R*)-**1b** to

(*R*)-**2** would help increase the dual activation of monomer and initiator through strengthened hydrogen bonding during polymerisation. Overall, (*R*)-**2** was found to reduce the polymerisation time of εHL to 96 h (cf. 122 h) to achieve a 48% monomer conversion (Table 3.2 entry **9**) l as a result of the increased stronger hydrogen bonding. However, chiral GC-MS analysis of unreacted εHL showed a dramatic decrease in *ee* to just 6%, in line with the reactivity-selectivity principle as indicated by the inverse relationship between the reactivity of a species and the selectivity in the resulting reaction.[19]

Following low *ee*'s obtained from tuning the electronegativity and acidity of the chiral BINOL-based phosphoric acids, we turned our attention towards altering the steric environment around the chiral phosphoric acid framework, which has long been considered to be a dominant factor for chiral phosphoric acid catalysed reactions.[18] Possessing the most sterically demanding environment of the catalysts screened, the ROP of *rac*-εHL, *rac*-εAL, and *rac*-εDL were screened against (*R*)-2,4,6-tricyclohexyl BINOL phosphoric acid, (*R*)-**1c,** at 70 °C in benzene-d_6 using BnOH as initiator, and a $[monomer]_0/[(R)\text{-}\mathbf{1c}]_0/[BnOH]_0$ ratio of 100:1:1 at an initial 1 M monomer concentration (Table 3.2 entries **6**, **7**, **8**). Surprisingly, of all the catalysts screened for the ROP of *rac*-εSεLs, (*R*)-**1c** was shown to display the least selectivity during the polymerisation. Despite the expected need for large steric bulk around the active catalytic centre to obtain high enantioselectivity, the observed drop in selectivity for (*R*)-**1c** was hypothesised to be a result of a steric clash between both enantiomers of a monomer and the large steric bulk of the catalyst.

Focusing on the commercially available (*R*)-**1d**, previously shown to be highly isoselective for the synthesis of polyvinyl ethers, we investigated the enantioselective

ROP of εHL at 70 °C in benzene-d_6 using BnOH as initiator, an initial $[rac\text{-}\varepsilon HL]_0/[(R)\text{-}\mathbf{1d})]_0/[BnOH]_0$ ratio of 100:1:1 with a 1 M *rac*-εHL concentration (Table 3.2 entry **11**).[20] After 20 h at 70 °C, monomer conversion had reached 45% by ^{1}H NMR spectroscopy. After quenching and precipitating into cold hexanes, chiral GC-MS analysis of unreacted monomer gave an *ee* of 35%, comparable to that obtained *via* (*R*)-**1c** (36.1%) albeit with drastically reduced polymerisation times, 20 h compared to 96 h. The increase in *ee* of unreacted monomers when moving from (*R*)-**1c** to (*R*)-**1d**, despite the decrease in steric bulk at the 3,3' BINOL positions possibly highlights the dependence of the choice of substituents at these positions, and that they must not be too large nor too small, but just right, often referred to as "the Goldilocks Effect".[21] Polymers were analysed by ^{1}H and ^{13}C NMR spectroscopy, DSC, and SEC. Determination of polymer tacticity was achieved by analysis of quantitative ^{13}C NMR spectra. Polymers obtained from (*R*)-**1d** were shown to possess a more ordered microstructure than those from DPP, confirming that (*R*)-**1d** displayed stereocontrol during the polymerisation (Figures 3.6). However, thermal analysis *via* DSC displayed a T_g of −45 °C confirming the polymer was amorphous in nature, which indicates that a higher degree of stereocontrol is required to achieve a semi-crystalline polymer.

Overall, it was shown that the steric bulk of the aryl substituents at the 3,3'-position on the BINOL backbone is most influential on the enantioselectivity during the polymerisation. Furthermore, placing the steric bulk specifically in the *ortho*-position on the aryl ring is crucial to induce effective enantioselectivity. However, it has become clear that there is an optimum amount of steric bulk required to enhance selectivity.

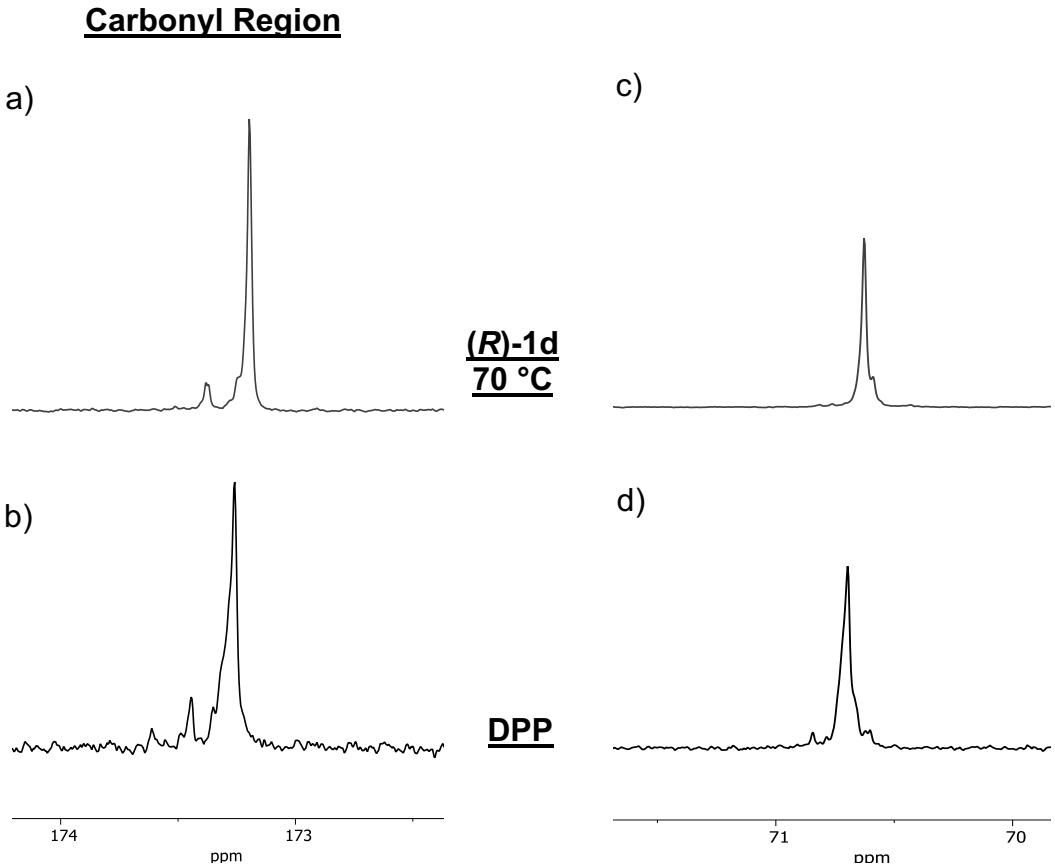

Figure 3.6. ^{13}C NMR spectra showing of a) carbonyl region PεHL from (*R*)-**1d** at 70 °C and b) carbonyl region PεHL from DPP, c) methine region PεHL from (*R*)-**1d** at 70 °C and d) methine region of PεHL from DPP ($CDCl_3$, 150 MHz, 298 K).

Table 3.2. Polymerisation data for *rac*-εSεL monomers using $[monomer]_0/[catalyst]_0/[BnOH]_0$ ratio of 100:1:1 where $[monomer]_0$ = 1 M

Entry	Monomer	Catalyst	Monomer conversion[a] (%)	*ee*[b] (%)	Temperature (°C)	Time (h)
1	*rac*-εHL	(*R*)-**1a**	49	29.6	70	14
2	*rac*-εHL	(*R*)-**1a**	50	38.2	25	72
3	*rac*-εAL	(*R*)-**1a**	54	38.4	70	98
4	*rac*-εDL	(*R*)-**1a**	53	21.4	70	336

5	*rac*-εHL	(*R*)-**1b**	45	1.56	70	122
6	*rac*-εHL	(*R*)-**1c**	50	2.96	70	96
7	*rac*-εAL	(*R*)-**1c**	50	45.2	70	216
8	*rac*-εDL	(*R*)-**1c**	56	2.12	70	410
9	*rac*-εHL	(*R*)-**2**	48	6.0	70	96
10	*rac*-εHL	**3**	55	37.6	70	223
11	*rac*-εHL	(*R*)-**1d**	45	35.0	70	20
12	*rac*-εAL	(*R*)-**1d**	47	39.0	70	96
13	*rac*-εDL	(*R*)-**1d**	50	21.6	70	340

[a] Monomer conversion determined by ^{1}H NMR spectroscopy. [b] Enantiomeric excess determined by chiral GC-MS.

3.2.2. Temperature optimisation

During a kinetic resolution polymerisation, one enantiomer is preferentially polymerised over the other despite the difference in activation energies between the two enantiomers often being extremely small.[22] One way to take advantage of this energetic difference is to reduce the polymerisation temperature to enhance the polymerisation of the favoured enantiomer versus the disfavoured enantiomer and thus increase the enantiomeric excess of unreacted monomer.[23] Encouraged by results from (*R*)-**1d** at 70 °C, and in attempts to further explore the effect of lowering temperature on the kinetic resolution of *rac*-εHL, *rac*-εAL, and *rac*-εDL during polymerisation, temperatures were reduced to 40 °C using BnOH as initiator, an initial $[\text{monomer}]_0/[(R)\text{-}\mathbf{1d}]_0/[\text{BnOH}]_0$ ratio of 100:1:1 with a 1 M monomer concentration in benzene-d_6 for all polymerisations (Table 3.3 entries **1**, **4**, **6**). Lowering the temperature

from 70 °C to 40 °C resulted in an increase in *ee* for all unreacted monomers alongside increased polymerisation times. After polymers were precipitated and dried under vacuum, they were analysed by ^{1}H and ^{13}C NMR spectroscopy, and SEC. Degree of polymerisation (DP) by ^{1}H NMR spectroscopy and theoretical DP were in good agreement for all samples, which indicates that polymerisations proceeded in a controlled manner. Moreover, molecular weights obtained *via* chloroform SEC analysis using polystyrene standards were in good correlation with theoretical molecular weights and those calculated *via* ^{1}H NMR spectroscopy. Additionally, SEC analysis gave monomodal distributions with narrow dispersities for all polymers ($Đ_M$ = 1.06 – 1.08). Interestingly, when further investigating the effect of the polymerisation temperature on *rac*-εAL and *rac*-εDL, lowering the temperature from 40 °C to 25 °C caused an drop in *ee* of unreacted monomers at an approximate 50% monomer conversion (Table 3.3 entries **5**, **7**). This observed drop in *ee,* in correlation with a drop in temperature below 40 °C, could be attributed to the inversion temperature of the enantioselective polymerisation, the temperature at which maximum enantioselectivity is observed.[24] Above and below the inversion temperature two different sets of activation parameters, $\Delta H^{\ddagger}$ and $\Delta S^{\ddagger}$, exist for each temperature range, which suggests that either there is a switch in enantioselectivity close to 40 °C and the other enantiomer is then favoured or, conversely, that the same enantiomer is favoured in both temperature ranges, but to varying degrees. Attempts were made to confirm the inversion temperature by further reducing polymerisation temperatures of εAL and εDL from room temperature to 5 °C, however as a consequence of drastically increased polymerisation times, slow catalyst death was observed with conversions plateauing at 5-10% after 400 h. Encouraged by the enhanced *ee* of unreacted monomers, PεAL

and PεDL from 40 °C polymerisations were evaluated by DSC after annealing at 25 °C for 4 weeks. DSC analysis revealed both PεAL and PεDL to be amorphous with only a glass transition temperature observed, T_g = −55 and −54 °C, respectively. To aid with investigating the tacticity of the polymer backbone, ^{13}C NMR spectroscopy analysis of the polymers, focussing on the carbonyl and substituted carbon peaks from (*R*)-**1d** at 40 °C were compared to those obtained *via* DPP (Figure 3.7). For a perfectly isoselective polymerisation, the ^{13}C NMR spectrum of the polymer would display only *meso* diad as a single, sharp peak in the carbonyl and substituted carbon regions, yet as shown in Figure 3.7a-d both the carbonyl and substituted carbon regions for PεAL samples from (*R*)-**1d** at 40 °C appear to be identical to the atactic PεAL obtained *via* DPP, the same was also observed for PεDL. These results in combination with DSC data confirm that a higher degree of enantioselectivity is required to obtain semi-crystalline isotactic PεAL and PεDL.

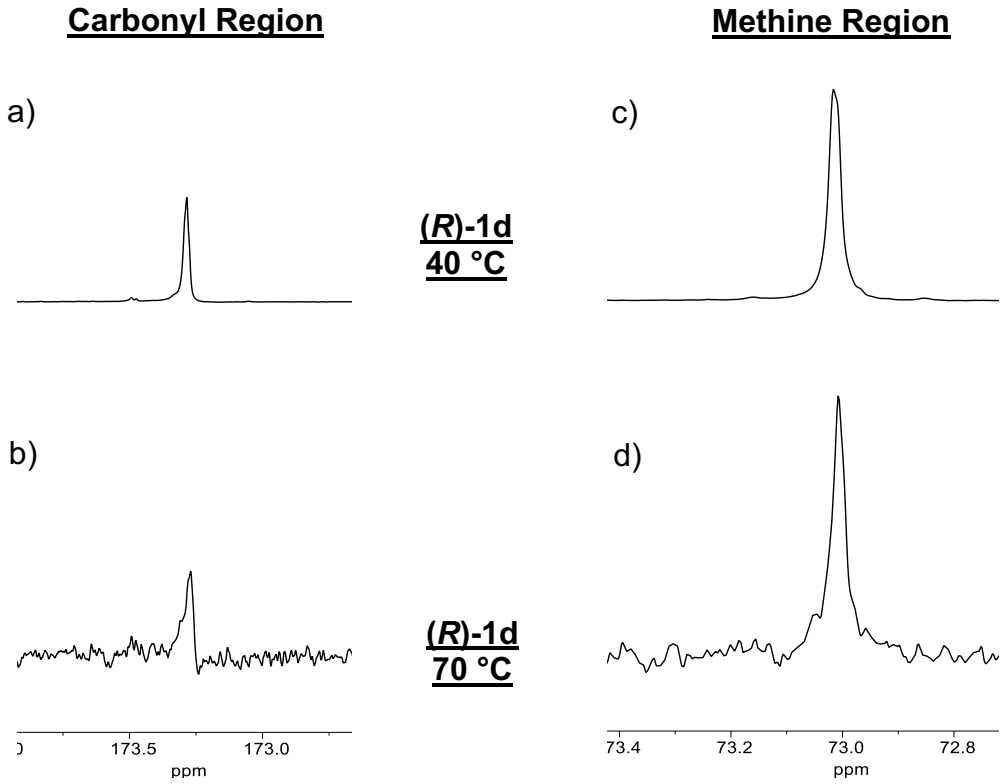

Figure 3.7. ^{13}C NMR spectra showing a) carbonyl region of PεAL from (*R*)-**1d** at 40 °C, b) carbonyl region of PεAL from DPP at 70 °C, c) allyl-substituted carbon region of PεAL from (*R*)-**1d** at 40 °C, d) allyl-substituted carbon region of PεAL from DPP at 70 °C ($CDCl_3$, 150 MHz, 298 K).

In contrast to the drop in *ee* with decreasing temperature observed for εAL and εDL, the enantioselective polymerisation of *rac*-εHL by (*R*)-**1d** gave an increase in *ee* of unreacted monomer from 46.2% to 58.6% as the polymerisation temperature was lowered from 40 °C to 5 °C (Table 3.3 entry **3**) which is a dramatic increase from the 18% *ee* at 40% monomer conversion achieved by Feijen *et al*. using an (*R*)-salen-AlO^{i}Pr complex.[4] After precipitation into cold hexanes, the polymer was dried under vacuum and subsequently analysed by ^1H and ^{13}C NMR spectroscopy, SEC, and DSC. Unlike as witnessed for *rac*-εAL and *rac*-εDL at lower temperatures, the

polymerisation of *rac*-εHL at 5 °C showed no signs of catalyst death indicated by the linear correlation between $\ln([M]_0/[M]_t)$ and time (Figure 3.8). This was likely a result of shortened reaction times owing to reduced steric bulk around the ring-opening centre found in *rac*-εHL compared to *rac*-εAL and *rac*-εDL.

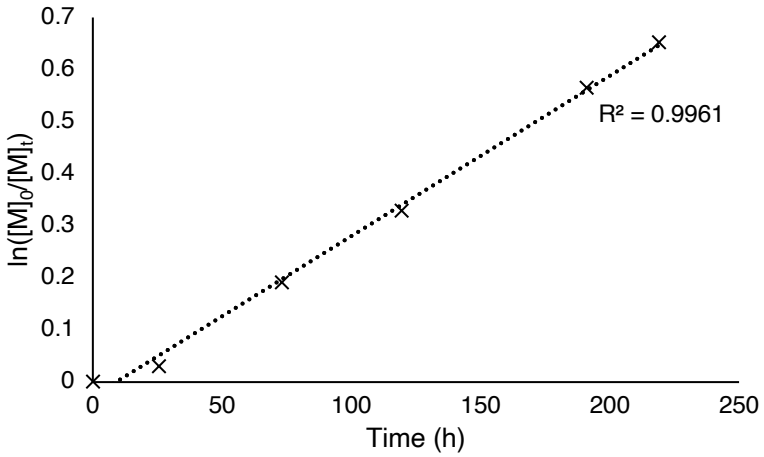

Figure 3.8. Kinetic plot for polymerisation of *rac*-εHL catalysed by (*R*)-**1d** at 5 °C with $[rac\text{-}\varepsilon HL]_0/[(R)\text{-}\mathbf{1d})]_0/[BnOH]_0$ ratio of 100:1:1 where $[rac\text{-}\varepsilon HL]_0$ = 1 M in benzene-d_6.

The polymerisation of *rac*-εHL at 5 °C by (*R*)-**1d** was shown to be controlled as evidenced by the good agreement between the theoretical molecular weight and those obtained *via* SEC (Figure 3.9) and ^{1}H NMR spectroscopy (Figure 3.10). Furthermore, the controlled nature of the polymerisation was confirmed by SEC with a monomodal distribution and a narrow dispersity ($Đ_M$ = 1.15).

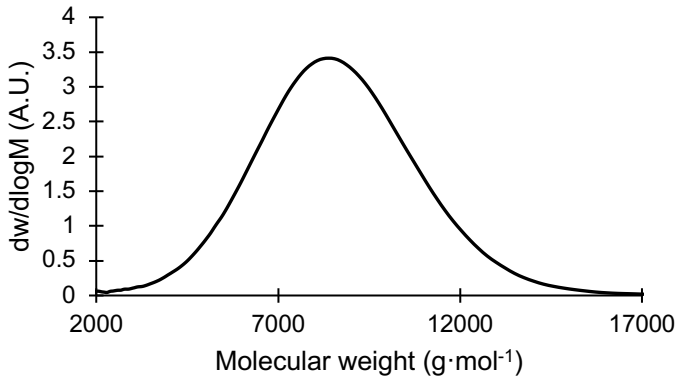

Figure 3.9. Size exclusion chromatogram of PεHL from [*rac*-εHL]$_0$/[(*R*)-**1d**)]$_0$/[BnOH]$_0$ ratio of 100:1:1 where [*rac*-εHL]$_0$ = 1 M at 5 °C in benzene-d_6. (M_n = 6.8 kg·mol^{-1}, $Đ_M$ = 1.15) ($CHCl_3$, RI, calibrated against polystyrene standards).

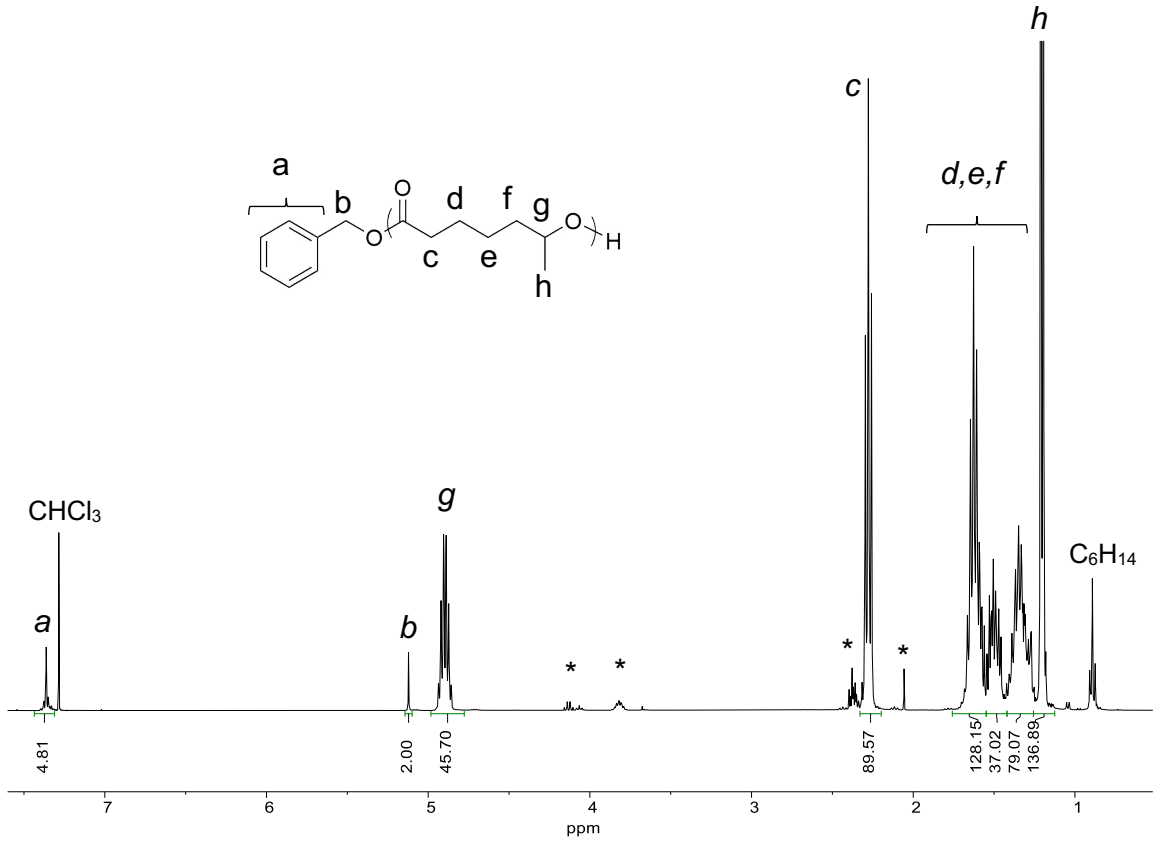

Figure 3.10. ^{1}H NMR spectrum of PεHL from (*R*)-**1d** at 5 °C. ($CDCl_3$, 500 MHz, 298 K). * = unprecipitated monomer.

The tacticity in PεHL from (*R*)-**1d** at 5 °C was assessed by examination of the carbonyl and methyl regions of the ^{13}C NMR spectra in comparison to PεHL obtained *via* DPP (Figures 3.11-12). When compared to Figure 3.11b and Figure 3.11e it is clear there are less diad resonances present in PεHL backbone from (*R*)-**1d** at 5 °C as both the carbonyl and methyl groups diads (δ = 173.3 and 70.7 ppm, respectively) start to converge to a single, sharp peak as would be expected for an isotactic polymer. As the polymerisation temperature is reduced from 70 °C to 5 °C, in line with an increase unreacted monomer *ee*, there is a sharpening of the diad peaks in the ^{13}C NMR spectra, as the kinetic resolution becomes more efficient (Figures 3.11-12a and c). However, it is clear there are still multiple diads present in the polymer backbone, as would be expected for an enantioselective polymerisation with an unreacted monomer

ee of 58.6%. Following ageing at 25 °C for 4 weeks, the thermal transitions of the polymer were then analysed by DSC. Despite promising results for unreacted monomer *ee* and improved isotacticity were obtained, only a T_g at −45 °C was observed which confirms polymer was still amorphous and further enantioselectivity is still required to obtain a semi-crystalline, isotactic PεHL.

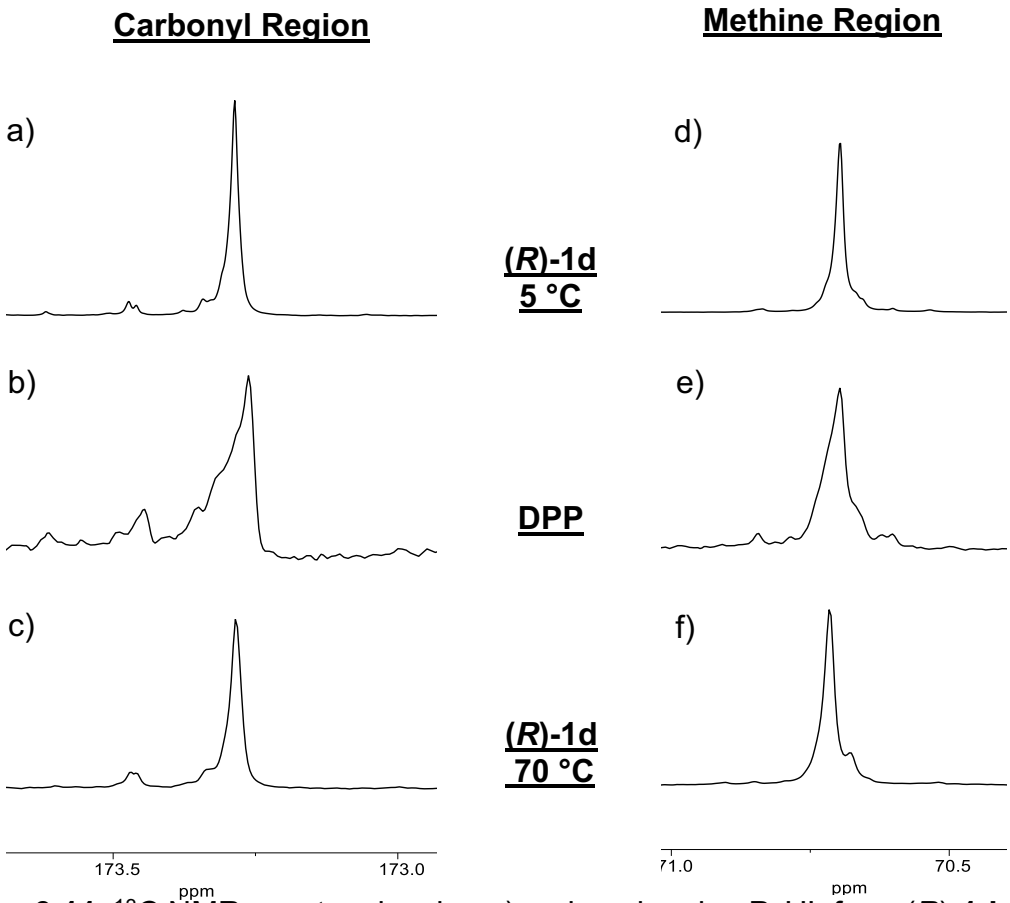

Figure 3.11. ^{13}C NMR spectra showing a) carbonyl region PεHL from (*R*)-**1d** at 5 °C, b) carbonyl region of PεHL from DPP at 70 °C, c) carbonyl region of PεHL from (*R*)-**1d** at 70 °C, d) methine region of PεHL from (*R*)-**1d** at 5 °C, e) methine region of PεHL from DPP at 70 °C and f) methine region of PεHL from (*R*)-**1d** at 70 °C ($CDCl_3$, 150 MHz, 298 K).

Table 3.3. Polymerisation data for *rac*-εSεL monomers using $[monomer]_0/[catalyst]_0/[BnOH]_0$ ratio of 100:1:1 where $[monomer]_0$ = 1 M

Entry	Monomer	Catalyst	Monomer conversion[a] (%)	*ee*[b] (%)	Temperature (°C)	Time (h)
1	*rac*-εHL	(*R*)-**1d**	51	46.2	40	27
2	*rac*-εHL	(*R*)-**1d**	47	45.4	25	100
3	*rac*-εHL	(*R*)-**1d**	58	58.6	5	220
4	*rac*-εAL	(*R*)-**1d**	51	52.8	40	265
5	*rac*-εAL	(*R*)-**1d**	55	46.2	25	1150
6	*rac*-εDL	(*R*)-**1d**	53	25.2	40	582
7	*rac*-εDL	(*R*)-**1d**	54	21.0	25	2500

[a] Monomer conversion determined by ^{1}H NMR spectroscopy. [b] Enantiomeric excess of unreacted monomer determined by chiral GC-MS.

3.3. Conclusion

Enantioselective control during a polymerisation is an essential tool for any polymer chemist for the synthesis of semi-crystalline polymers. To date the field enantioselective ROP has either been dominated by metal-based catalysts or limited to a narrow monomer scope. Here, we have made attempts to synthesise a semi-crystalline polymer through the application of an enantioselective organocatalyst whilst expanding on monomer scope.

Through control of substituents at the 3,3'-positions of the BINOL backbone, the chiral BINOL-based phosphoric acid catalysed polymerisation of a range of racemic εSεL monomers was demonstrated to be enantioselective over a series of temperatures. Overall, it was found that when catalysts were screened for enantioselective

polymerisation of *rac*-εHL, an increase in the acidity of the catalyst caused a decrease in polymerisation times because of increased monomer and initiator activation. However, an increase in acidity also appeared to cause a decrease in enantioselectivity during the polymerisation. Furthermore, no substantial improvement in enantioselectivity was observed when creating a sterically bulky pocket within the catalyst. This drop in enantioselectivity was thought to be a consequence of excessive steric bulk preventing efficient coordination between catalyst and monomer, regardless of monomer stereochemistry.

Investigation into the effect of the electronic and steric nature of the chiral BINOL-based backbone was found to be monomer dependent. The influence of an electronegative substituent on the BINOL backbone was found to be most influential for the enantioselective ROP the electron-rich *rac*-εAL, hypothesised to be a result of non-covalent interactions between substituents on the monomer and BINOL-backbone. Despite this, for all monomers it was found that the steric nature of the BINOL-backbone was most crucial for enantioselectivity. As a result, the ROP of *rac*-εHL, *rac*-εAL, and *rac*-εDL preferentially proceeded at 70 °C using (*R*)-**1d**. To enhance the kinetic resolution the polymerisation temperature was gradually reduced. As the polymerisation temperature was reduced below 40 °C, it was thought that an inversion temperature was reached for the polymerisations leading to a drop in enantioselectivity. Conversely, lowering the polymerisation temperature for the ROP of *rac*-εHL using (*R*)-**1d** from 70 °C to 5 °C saw an increase in enantioselectivity. Despite the increase in enantioselectivity, polymers were shown to be amorphous as a result of a high distribution of stereoerrors found along the polymer backbone. Future studies

will focus on further optimising polymerisation conditions to obtain semi-crystalline PεSεLs.

3.4. References

1. R. Ligny, S. M. Guillaume, J. F. Carpentier, *Angew. Chem. Int. Ed.*, 2017, **56**, 10388-10393.
2. C.-X. Cai, A. Amgoune, C. W. Lehmann and J.-F. Carpentier, *Chem. Commun.*, 2004, 330-331.
3. N. Spassky, M. Wisniewski, C. Pluta and A. Le Borgne, *Macromol. Chem. Phys.*, 1996, **197**, 2627-2637.
4. M. R. T. Breteler, Z. Zhong, P. J. Dijkstra, A. R. A. Palmans, J. Peeters and J. Feijen, *J. Polym. Sci., Part A: Polym. Chem.*, 2006, **45**, 429-436.
5. A. C. Albertsson and I. K. Varma, *Biomacromolecules*, 2003, **4**, 1466-1486.
6. K. Makiguchi, T. Yamanaka, T. Kakuchi, M. Terada and T. Satoh, *Chem. Commun.*, 2014, **50**, 2883-2885.
7. C. Lv, R. Yang, G. Xu, L. Zhou and Q. Wang, *Eur. Polym. J.*, 2020, **133**, 109792.
8. J. A. Wilson and A. P. Dove, *Biomacromolecules*, 2015, **2015**, 10.
9. K. Makiguchi, T. Satoh and T. Kakuchi, *Macromolecules*, 2011, **44**, 1999 - 2005.
10. J. Zhao and N. Hadjichristidis, *Polym. Chem.*, 2015, **6**, 2659-2668.
11. P. Bexis, A. W. Thomas, C. A. Bell and A. P. Dove, *Polym. Chem.*, 2016, **7**, 7126-7134.
12. X. Zhang, Y. Jiang, Q. Ma, S. Hu, Q. Wang and S. Liao, *Eur. Polym. J.*, 2020, **123**, 109449.
13. S. Liao, I. Čorić, Q. Wang and B. List, *J. Am. Chem. Soc.*, 2012, **134**, 10765-10768.
14. T. Akiyama, *Chem. Rev.*, 2007, **107**, 5744-5758.
15. M. Terada, *Synthesis*, **2010**, 1929-1982.

16. D. Parmar, E. Sugiono, S. Raja and M. Rueping, *Chem. Rev.*, 2014, **114**, 9047-9153.

17. J. P. Reid and J. M. Goodman, *Chem. Eur. J.*, 2017, **23**, 14248-14260.

18. R. Maji, S. C. Mallojjala and S. E. Wheeler, *Chem. Soc. Rev.*, 2018, **47**, 1142-1158.

19. A. Pross, in *Adv. Phys. Org. Chem.*, ed. V. Gold, Academic Press, 1977, vol. 14, pp. 69-132.

20. A. J. Teator and F. A. Leibfarth, *Science*, 2019, **363**, 1439-1443.

21. J. P. Reid and J. M. Goodman, *J. Am. Chem. Soc.*, 2016, **138**, 7910-7917.

22. G. Xu, Q. Mahmood, C. Lv, R. Yang, L. Zhou and Q. Wang, *Coord. Chem. Rev.*, 2020, **414**, 213296.

23. R. E. Gawley and J. Aubé, in *Principles of Asymmetric Synthesis (Second Edition)*, eds. R. E. Gawley and J. Aubé, Elsevier, Oxford, 2012, DOI: https://doi.org/10.1016/B978-0-08-044860-2.00002-7, pp. 63-95.

24. R. E. Gawley and J. Aubé, in *Principles of Asymmetric Synthesis (Second Edition)*, eds. R. E. Gawley and J. Aubé, Elsevier, Oxford, 2012, DOI: 10.1016/B978-0-08-044860-2.00001-5, pp. 1-62.

4. Chapter four

Temporally controlled ring-opening polymerisation of lactones using donor-acceptor Stenhouse adducts

4.1. Introduction

The development of sequence- and spatio-controlled synthetic polymers, *i.e.* rational manipulation of stereochemistry, composition and chain length, is a fundamental aim in polymer chemistry. Over the last several decades, there has been an explosion of synthetic polymers with well-defined microstructures that have resulted from the development of sophisticated polymerisation methods such as controlled radical polymerisation (CRP)[1] or ring-opening polymerisation (ROP)[2]. However, acquiring temporal control in polymer synthesis has proved more challenging, although there have been some recent advancements for photoinitiated CRPs.[3] Nevertheless, the ability to command the progress of polymerisation in a reversible manner presents an unparalleled opportunity to fabricate innovative materials. Switchable catalysis provides unique temporal control of polymerisation through the application of an external stimulus, either by switching between two distinct catalytic species or dictating an ON/OFF states of chain propagation. This manipulation of reactivity can be achieved through the incorporation of a responsive functionality into a catalytic system where possible external triggers include a range of photo, thermal, chemical, and mechanical stimuli to enable “on-demand” polymerisation.[4-7]

4.1.1. Photo-triggered switchable catalysts

Remotely controlling polymerisations *via* a photo-triggered switchable catalyst provides several advantages, including non-invasive methodologies, tuneable wavelength control, and the potential for modulation over the spatial and temporal domains. The activation of a photoswitchable catalyst typically involves modification of the steric environment or a change in the electronic properties of the catalytic system

to toggle the catalyst between the ON and OFF state. There are largely two main pathways associated with photoswitchable catalysis, photocyclisation and photoisomerisation.

Neilson and Bielawksi reported the first photoswitchable N-heterocyclic carbene (NHC) organocatalyst for the ROP of lactones (Scheme 4.1).[4] Although NHCs were already established as ROP catalysts, the incorporation of a photochromic diarylethene moiety permitted a ring-cyclisation of the NHC by UV light exposure. The ring closure resulted in a subsequent reduction of electron density at the carbene centre as a result of extended conjugation along the backbone of the cyclic moiety; this led to an inactive catalyst for polymer initiation/propagation. However, upon exposure to a visible light source, the ring-closed structure was reversibly ring-opened to regenerate the active ROP catalyst. Under visible light and in the presence of an initiator, the ring-opened NHC successfully catalysed the ROP of δ-valerolactone (δVL) and ε-caprolactone (εCL). Simply switching between UV and visible light afforded good control over the ON and OFF states of the polymerisation. However, it is worth noting that catalyst decomposition (*ca*. 13 %) occurred for each ON/OFF cycle, thus limiting the long-term value of the system.

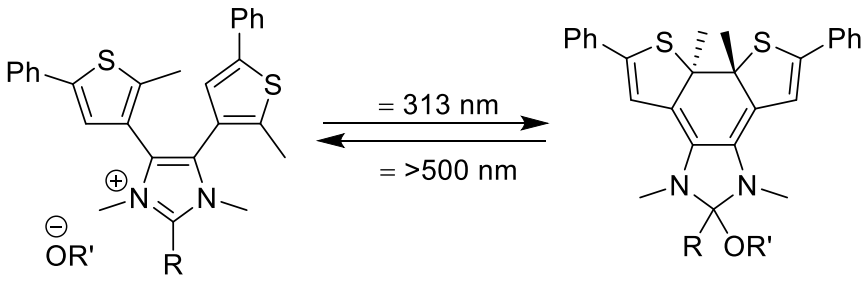

Scheme 4.1. Active (left) and inactive (right) structures of the photoswitchable *N*-heterocyclic carbene ring-opening polymerisation catalyst reported by Neilson and Bielawksi.[4]

The application of a diarylethene-bearing photoswitchable catalyst for the ROP of cyclic esters was also reported by Hecht and co-workers focussing on reversible hydrogen bonding between a phenolic proton on the catalyst and the carbonyl group of the cyclic ester monomer (Scheme 4.2).[8] It was found that upon exposure to UV light a keto-enol tautomerization could be triggered that eliminated the hydrogen bond-donating capability of the catalyst, thus rendering it inactive towards ROP, although this was found to be reversible under visible light. In the presence of a base co-catalyst for initiator activation, the dual-catalyst system showed an enhanced activity for the ROP of cyclic esters when compared to the base alone. Furthermore, by cycling between visible and UV light, it was possible to pause and recover catalytic activity without any change in polymerisation rates. Polymerisations proceeded in a controlled manner as evidenced by narrow dispersities ($Đ_M$ = 1.08 – 1.14) and reasonable agreement between theoretical molecular weights and experimentally determined molecular weights. However, it is worth noting that a small degree of initiation was caused by the phenolic group on the catalyst which led to loss of control over chain-end fidelity and chain propagation.

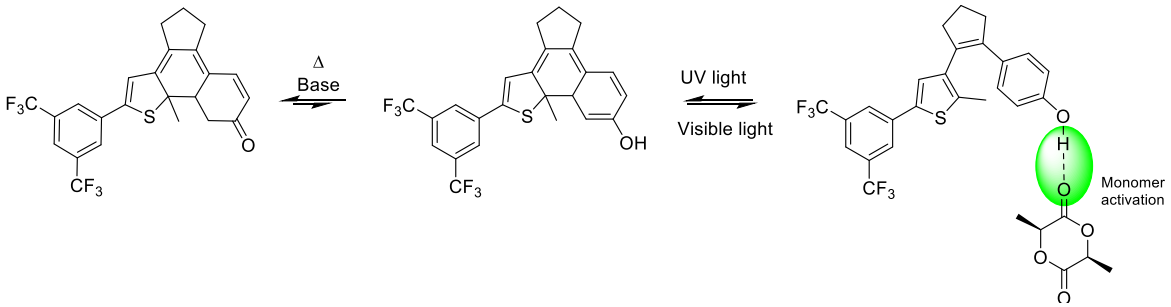

Scheme 4.2. Reversible keto-enol tautomerization of diarylethene-bearing photoswitchable catalyst for the ring-opening polymerisation of cyclic esters. Adapted from Hecht and co-workers.[8]

In addition to dynamic photocyclisation, it is also possible to leverage *E/Z* alkene photoisomerisation to toggle between a catalytic ON and OFF state. Through the application of host-guest chemistry, Harada and co-workers showed that 2-*O*-*trans*-cinnamoyl-α-cyclodextrin could mediate the switchable ROP of δVL in bulk at 100 °C by a photocontrolled *E/Z* isomerisation.[9] It was found that the *E*-isomer could efficiently catalyse the ROP of δVL, yet under the same conditions, the *Z*-isomer (afforded from UV irradiation) was significantly less active as a result of unfavourable steric interactions that prevented the δVL monomer from entering the cyclodextrin cavity.

Viehmann *et al.* functionalised a guanidine species with the isomerisable azobenzene group to afford a photoswitchable catalyst for the ROP of lactide (Scheme 4.3a).[10] It was hypothesised that the *E*-isomer would be catalytically active towards ROP as a result of monomer activation *via* hydrogen bonding between the free guanidine N–H group and the carbonyl unit of the cyclic monomer. Subsequent photoisomerisation to the *Z*-isomer would prevent monomer coordination and activation as a result of intramolecular hydrogen bonding (Scheme 4.3a). However, in the presence of lactide,

after 48 h at room temperature no significant polylactide formation was observed for either isomer. The inactivity of the catalyst was thought to be a consequence of reduced basicity related to electron delocalisation between the aromatic residues and the guanidine unit. However, a structurally similar azobenzene-based thiourea was reported as an active photoswitchable catalyst for the ROP of lactide (Scheme 4.3b).[11] The authors hypothesised that the *E*-isomer would allow for sufficient interaction between the thiourea and lactide monomer, whereas the *Z*-isomer would promote intramolecular hydrogen bonding and inhibit coordination between the catalytic site and monomer. In the presence of pentamethyldiethylenetriamine as a co-catalyst, lactide was successfully polymerised to yield high molecular weight polymers with narrow dispersities as the catalytic *E*-isomer was the thermodynamic species (M_n = 26,000 g·mol^{-1} and $Đ_M$ = 1.03 – 1.05). It was possible to slow down the rate of polymerisation *via* formation of the catalytic *Z*-isomer, although complete termination of the polymerisation was not attainable which suggested that monomer coordination was still competing with intramolecular H-bonding.

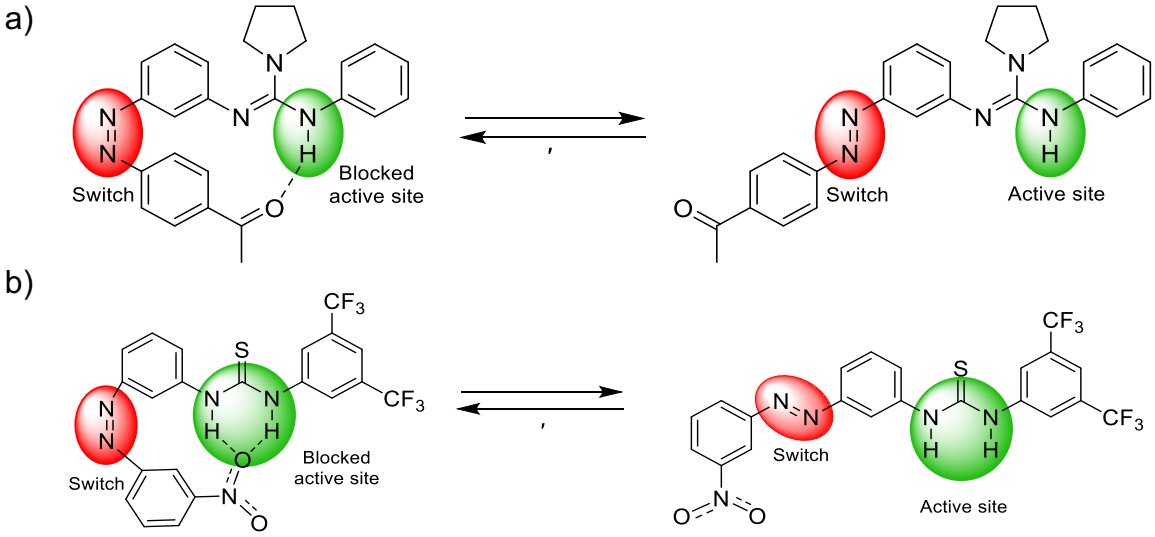

Scheme 4.3. a) Photoswitching *E/Z* isomerisation of a guanidine-based ring-opening polymerisation catalyst. Adapted from Viehmann *et al.*[10] b) Photoswitching *E/Z* isomerisation of a thiourea ROP catalyst. Adapted from Dai *et al.*[11]

4.1.2. Thermally-triggered switchable catalysts

Thermal activation is arguably the most conventional approach to catalyst activation. However, thermal activation is intrinsically more complicated than light activation, as all chemical bonds absorb energy whereas photon energy can only be absorbed by a photochromic moiety. In addition, thermal catalytic activation generally relies on bond rupture to release the active catalyst, however excessive heat can also lead to unwanted side reactions.[12] Thermally latent NHCs were first explored by Coulembier *et al.* as thermally switchable catalysts for the alcohol initiated ROP of lactide (Figure 4.1).[13] At room temperature the NHC and alcohol formed an adduct that was inactive towards ROP, yet upon heating to 90 °C the catalytically active "free" carbene was reversibly generated *in situ* to afford polylactide with controlled molecular weights and narrow dispersities. Through modulation of the reaction temperature, the

polymerisation could be reversibly terminated which led to excellent temporal control over the reaction.

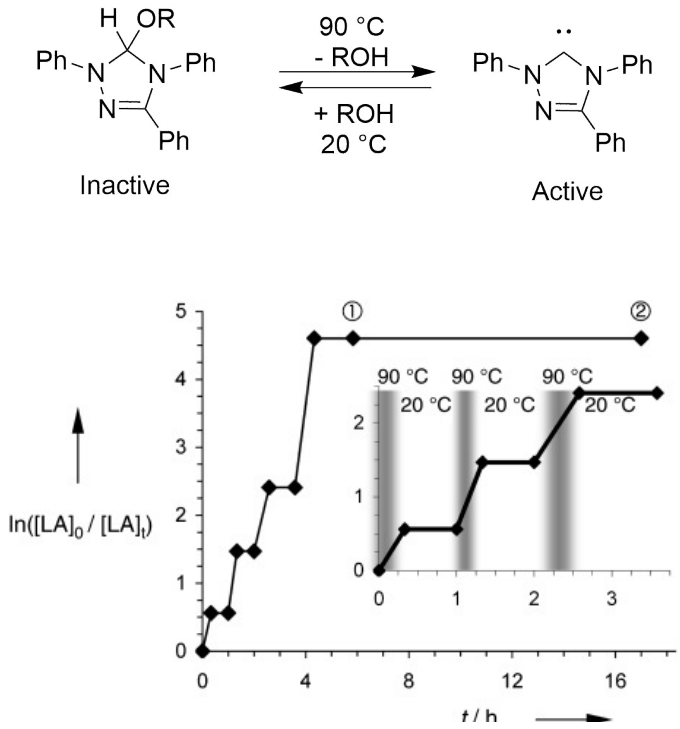

Figure 4.1. Temporally controlled ROP of lactide using a thermally switchable latent NHC catalyst. Adapted from Coulembier *et al.*[13]

4.1.3. Donor-acceptor Stenhouse adducts

In search of a more orthogonally-switchable ROP catalyst, our attention was drawn to donor-acceptor Stenhouse adducts (DASA) which have recently emerged as a versatile class of switchable compounds as a consequence of their modular nature and ease of synthesis.[14-18] Through the application of two discrete orthogonal stimuli, light and heat, it is possible to reversibly shift between a linear, coloured conjugated triene and a cyclic, colourless zwitterionic cyclopentenone structure (Scheme 4.4).

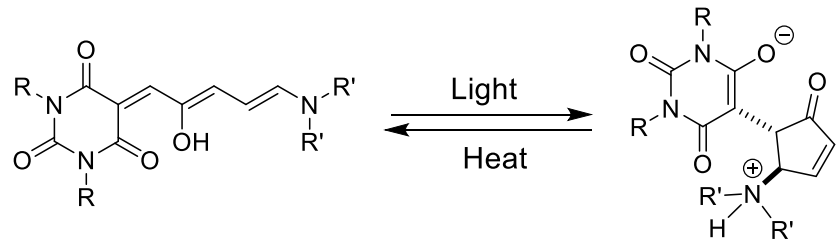

Hydrophobic and coloured Hydrophillic and colourless

Scheme 4.4. Photoswitching and thermal reversion from the triene to the zwitterionic cyclopentenone of a generic DASA compound.

With this in mind, we hypothesised that the linear triene would be inactive towards the ROP of cyclic esters through a lack of monomer activation *via* strong hydrogen bonding. However, exposure to light would reveal an active, zwitterionic ROP catalyst possibly capable of following an activated monomer mechanism where the monomer is activated through hydrogen bonding between the ammonium N-H and carbonyl of cyclic ester. Subsequent heating should again yield the deactivated linear species to reversibly terminate the polymerisation. Herein, we describe the use of DASA compounds as switchable catalysts for the dual-orthogonal temporally controlled ROP of various cyclic esters.

4.2. Results and discussion

4.2.1. Donor-acceptor Stenhouse adduct synthesis

Inspired by facile multi-gram scale synthesis using commercially available starting materials, DASA compound **3** was synthesised following an adapted procedure by Helmy *et al.* (Scheme 4.5).[14] The reaction of *N*-hexylamine with an equimolar ratio of *N*-hexyl isocyanate and, subsequently, malonyl chloride yielded the cyclic intermediate **1**. The addition of 2-furaldehyde to **1** generated the condensation product **2** as a yellow

solid in moderate yield (65%). Finally, the addition of diethylamine to **2** induced the ring opening of the furan moiety to afford a conjugated triene structure **3** that was isolated as a dark-pink solid in 62% yield.

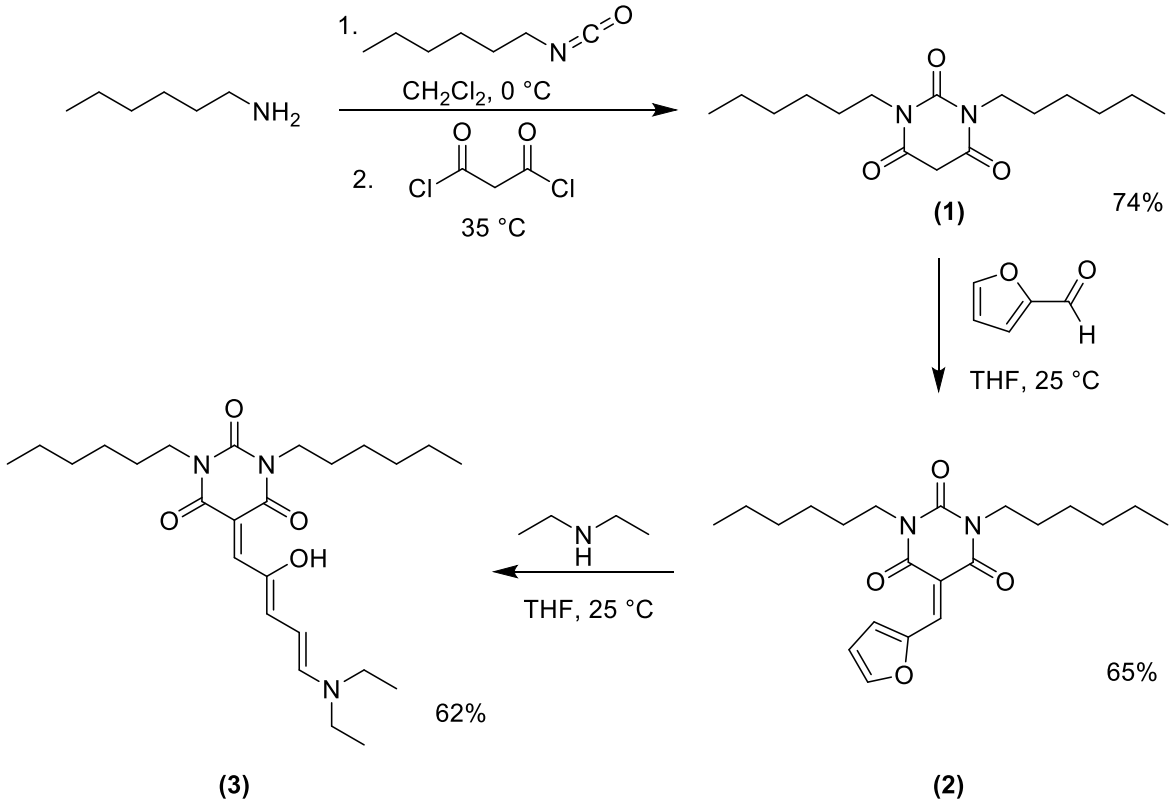

Scheme 4.5. The 3-step synthesis of the triene DASA substrate **3** from commercially available precursors.

The formation of **3** was confirmed by ^{1}H and ^{13}C NMR spectroscopy. The resulting ^{1}H NMR spectrum showed a proton signal at δ = 3.48 ppm, attributable to $N(C\underline{H_2}CH_3)_2$, which confirmed the successful addition of diethylamine (Figure 4.2). Moreover, the appearance of vinylic resonances (δ = 6.05 – 7.19 ppm) suggested a triene species and the appearance of a deshielded (due to conjugation effects) enol proton (δ = 12.61 ppm) corroborated the ring-opened structure of **3**.

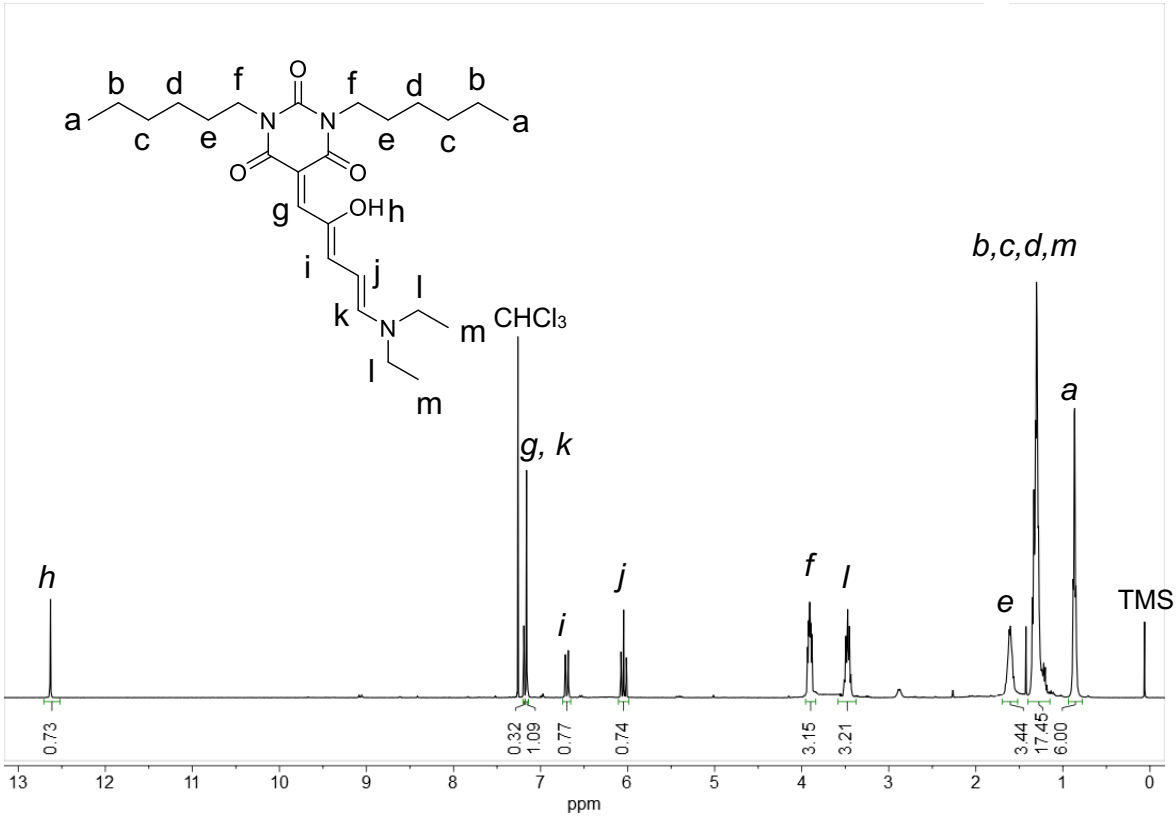

Figure 4.2. ^{1}H NMR spectrum of DASA compound **3** ($CDCl_3$, 400 MHz, 298 K)

4.2.2. Investigating solvatochromatic relationship

Upon exposure to light, DASA compounds undergo a significant structural rearrangement which involves an intramolecular cyclisation of the triene **3**, to form the zwitterionic cyclopentenone **4** (Scheme 4.6). It is proposed that this occurs through a light-triggered *E/Z* isomerisation of **3** to yield **3'**, which is then quickly followed by a conrotatory, thermally-allowed 4π-electrocyclisation.[16] However, many cyclopentenones possess poor thermal stability and lifetimes, usually reverting back to their corresponding linear species within minutes at ambient temperature.[19] The cyclopentanone can however, be stabilised in polar protic solvents (such as methanol or water) and thermal reversion to the triene is significantly mitigated. On the other

hand, it has also been reported that halogenated solvents (such as dichloromethane or chloroform) favour the triene form, and efficient photoisomerisation to the zwitterion is hindered in these solvents.[14] Alternatively, aromatic solvents (toluene, benzene, and xylenes) have been found to be suitable solvents for both photocyclisation and thermal reversion reactions and thus were hence selected for later experiments (Scheme 4.6).[14]

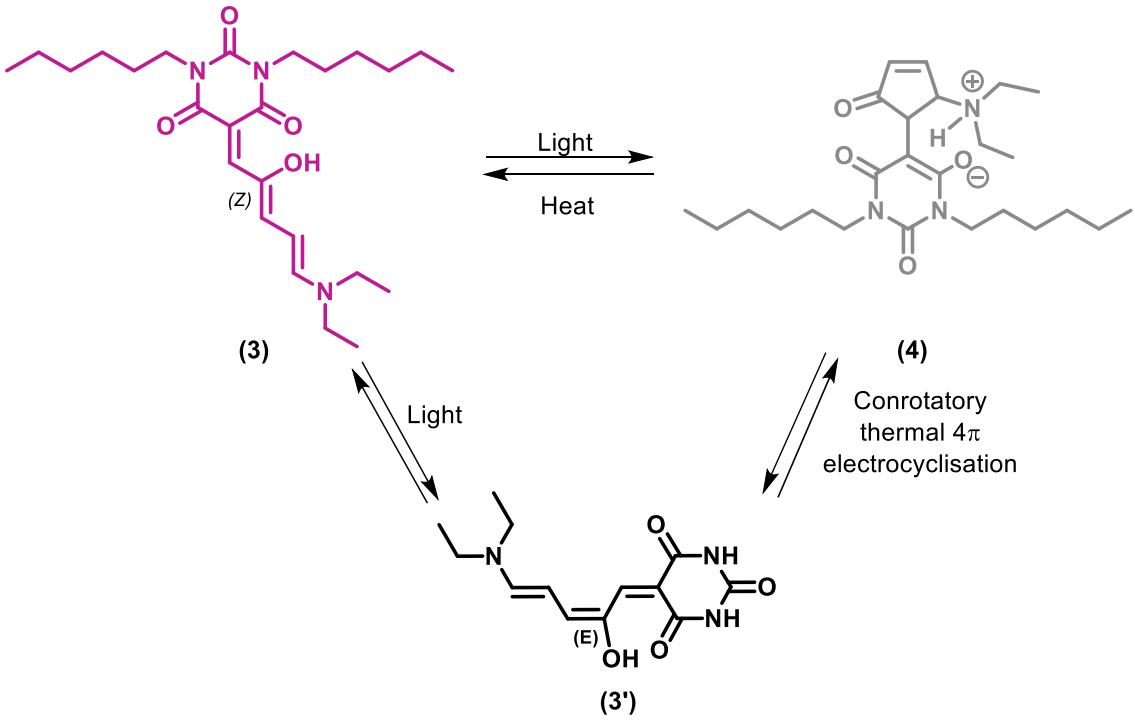

Scheme 4.6. Photoswitching and thermal reversion of coloured triene **3** to colourless cyclopentenone **4** through the intermediate *E*-isomer **3'**.

To this end, the absorption profile of **3** was investigated to discern the wavelength of maximum absorption (λ_{max}) in a variety of solvents. Dilute solutions of **3** [0.35 μM] were prepared in methanol (polar, protic), acetonitrile (polar, aprotic), dichloromethane (halogenated), and toluene (aromatic). Their corresponding absorption profiles were

analysed using UV-Vis spectroscopy (Figure 4.3). A prominent π-π* transition was observed in all solvents between λ = 500-600 nm which can be attributed to the triene chromophore of **3**.[18] Changes to the absorption shape and λ_{max} were observed among the solutions which suggested that the DASA displayed solvatochromatic behaviour. The compound was most blue-shifted and displayed significant band broadening in the polar protic solvent methanol (λ_{max} = 545 nm), which has been previously reported as a common phenomenon in other DASA substrates.[18] Furthermore, the toluene (λ_{max} = 575 nm) and dichloromethane (λ_{max} = 570 nm) solutions were red-shifted. Exposure of the prepared solutions to a λ = 430-540 nm light source triggered a colour change from pale pink to colourless for both methanol and toluene solutions which indicated efficient conversion of the triene to the cyclopentenone isomer. Analysis of the colourless, irradiated solutions by UV-Vis spectroscopy confirmed that no appreciable absorption was witnessed from λ = 350-700 nm. Conversely, when the solutions prepared in dichloromethane and acetonitrile (λ_{max} = 560 nm) were exposed to the same light source, a colour change from pale pink to orange was observed which suggested only partial isomerisation from the triene to the cyclopentenone isomer. Such behaviour was expected and is likely a consequence of the poor stabilisation of the zwitterion in aprotic and halogenated solvents.

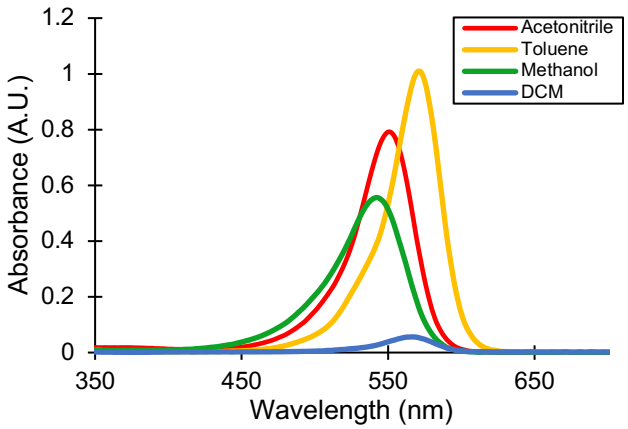

Figure 4.3. Absorption spectra of **3** [0.35 μM] in methanol, acetonitrile, dichloromethane, and toluene.

4.2.3. Switchable DASA catalysis for ring-opening polymerisation

The linear triene **3** was postulated to be incapable of mediating the ROP of cyclic esters and carbonates as a result of insufficient hydrogen bonding moieties capable of effective monomer activation. Moreover, it was hypothesised that the weakly nucleophilic enol found in **3** would lead complications with regards to polymer initiation, similar to the report by Hecht and co-workers[10] where initiation by the phenol moiety was witnessed, which led to poor control over the polymerisation. Instead, we predicted that the zwitterionic cyclopentenone species **4**, formed upon irradiation of **3**, would be an active ROP catalyst. It was predicated that the active catalyst would follow an activated monomer mechanism as a result of efficient monomer activation *via* hydrogen bonding between the monomer carbonyl and the charged moieties found in **3** (Scheme 4.7). The application of heat would terminate the polymerisation through the isomerisation of the DASA compound to form the “inactive” linear triene. Cycling of

the DASA catalyst between the ON and OFF states would then be possible through the judicious control of light and heat in a decoupled manner.

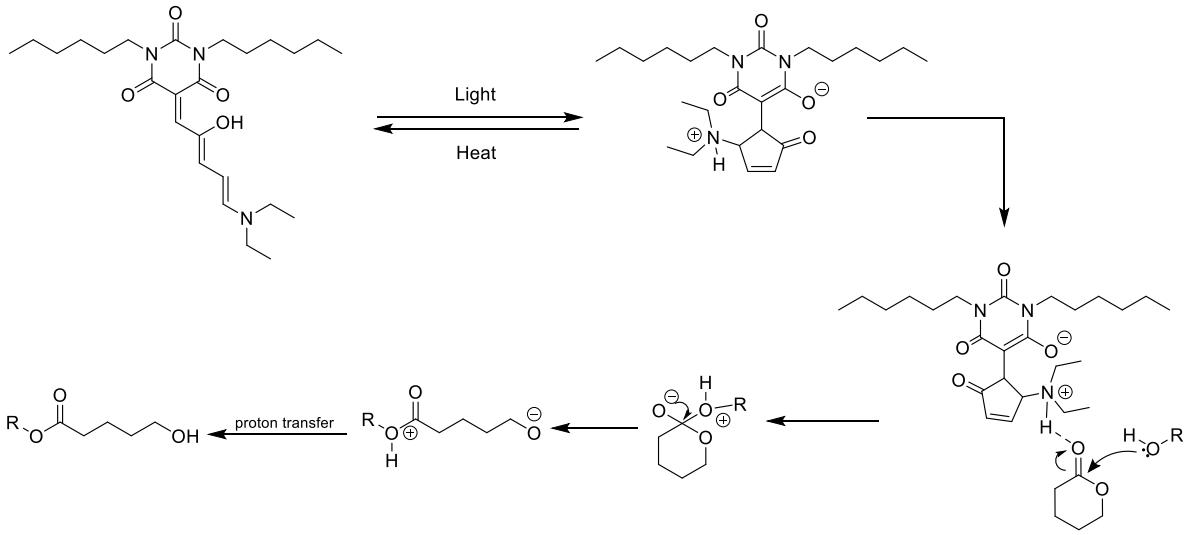

Scheme 4.7. Possibly activated monomer mechanism for DASA catalysed ROP of δVL.

As such, **3** was investigated as a switchable ROP catalyst for a range of cyclic esters and carbonates (Figure 4.4). A 3 M monomer solution using a DASA loading of 1 mol% in benzene-d_6 was irradiated for 72 h after which no polymer formation could be seen by ^{1}H NMR spectroscopy. This confirmed that the weakly nucleophilic enol found in **3** was incapable of polymer initiation. As highlighted earlier, cyclic zwitterionic DASA compounds are readily stabilised in protic solvents, whereas aromatic solvents allow for reversible switching upon irradiation, which is followed by a fast, thermally induced reversion to the linear form. Recently, Alves *et al.* reported that through the addition of a thiol, in the presence of light, it was possible to "trap" the activated zwitterionic DASA species through a thiol-Michael addition.[20] Inspired by this, we postulated that the addition of a thiol to would serve to "trap" and stabilise the activated DASA species **4**

to yield a thiol-Michael addition adduct such as **5** (Scheme 4.8). This would ensure complete “activation” and maintenance of the catalytic species, as the zwitterionic isomer would be unable to isomerise back to the linear triene under standard polymerisation conditions and would lead to efficient chain propagation. Afterwards, increasing the reaction temperature would promote the reversible thiol-Michael addition to regenerate the thiol and deactivated DASA catalyst **3**, effectively terminating the polymerisation.[21-24]

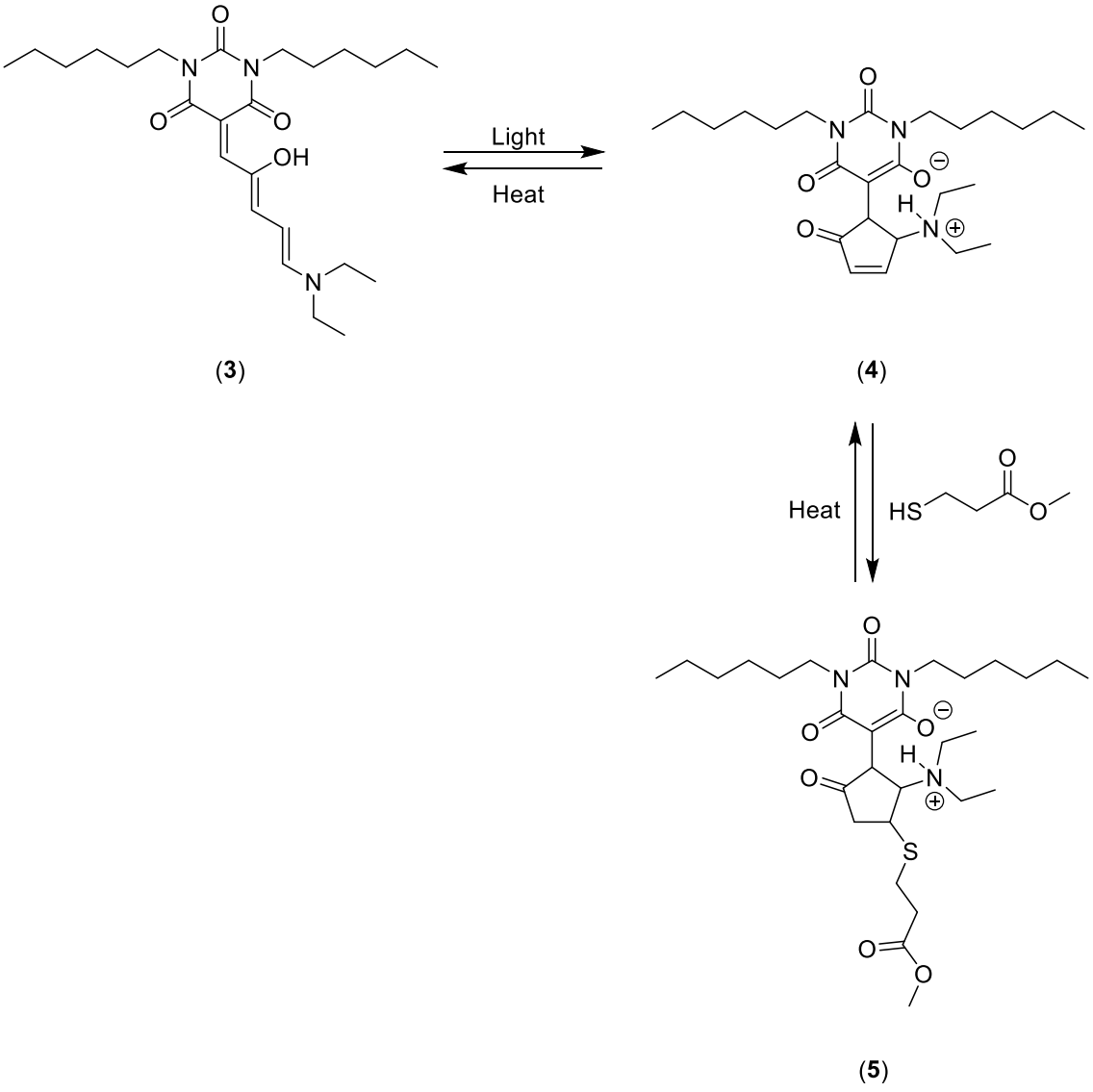

(**3**) (**4**) (**5**)

Scheme 4.8. Addition of thiol to DASA to "trap" in the zwitterionic state, as found by Alves *et al*.[20]

To test this idea, **3** was irradiated in the presence of methyl 3-mercaptopropionate and various cyclic (di)ester and carbonate monomers (Figure 4.4) in benzene-d_6, using a $[monomer]_0/[initiator]_0/[\mathbf{3}]_0$ ratio of 30:1:0.01 where $[monomer]_0$ = 3 M. Irradiation of the reaction mixture failed to yield any polymer when using lactide (LA) or methyl allyl carbonate (MAC). Yet **3** was found to facilitate the ROP of δVL and εCL, albeit to low

conversions after extended reaction times (17.4% and 9% in 144 h, respectively). As δVL was found to polymerise more rapidly than εCL under these conditions, additional studies focussed on optimising the DASA-catalysed ROP of δVL.

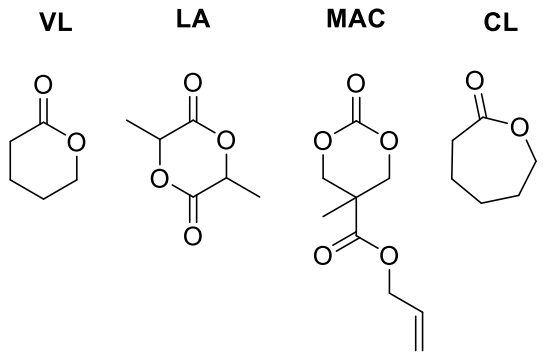

Figure 4.4. Monomers screened against **3** as a potential ROP catalyst.

Polymerisations were initially conducted in benzene-d_6 to leverage the efficient switching capabilities of DASA compounds in aromatic solvents. To induce switching between the ON and OFF catalyst state, it was necessary to heat the catalyst to high temperatures (> 110 °C) to trigger a retro-Michael addition reaction and deactivate the DASA catalyst to the OFF state. However, these efforts were hindered by the low boiling point of benzene-d_6 (80 °C); therefore the reversible switching behaviour was investigated using tetrachloroethane-d_2 (TCE-d_2), a halogenated solvent which possesses a high boiling point (147 °C). Although the switching of DASA compounds in halogenated solvents is not as efficient as polar protic solvents or aromatic solvents, **3** still has a sufficient molar absorptivity in halogenated solvents (Figure 4.3) and it was predicted that the lifetime of the active zwitterionic cyclopentenone catalyst could be suitably increased by thiol-Michael addition “trapping” after isomerisation.

The polymerisation of δVL, initiated by methyl 3-mercaptopropionate, was repeated in TCE-d_2 to investigate the capability of **3** as a switchable ROP catalyst, using a $[\delta VL]_0/[initiator]_0/[\mathbf{3}]_0$ ratio of 30:1:0.1 where $[\delta VL]_0$ = 3 M. In the absence of light, no polymerisation was observed, yet irradiation of the reaction mixture triggered the polymerisation (Figure 4.5, sections *i* and *ii,* respectively). Interestingly, monomer conversion continued to increase for many hours after irradiation was paused, which indicated that the catalyst was still active (Figure 4.5, section *iii*). This continuation of propagation supported the formation of the trapped thiol-DASA compound, as zwitterionic cyclic pentenones such as **4** are known to convert back to the linear triene on the time-scale of seconds to minutes and this process is even more favourable in halogenated solvents such as TCE-d_2.[19] After suspending irradiation, heating the system to 110 °C halted conversion and this paused state persisted even after cooling to room temperature, which further suggested successful reversion to the inactive triene **3** *via* a plausible retro-Michael addition pathway (Figure 4.5, sections *iv* and *v*). Interested by the ON/OFF switching capabilities of the catalytic system displayed thus far, irradiation was resumed (Figure 4.5, section *vi*). Intriguingly, the increase in conversion also resumed and it was shown that the system could be repeatedly paused and re-initiated over several cycles to ultimately achieve a high conversion (78%) (Figure 4.5, sections *vii* – *ix*).

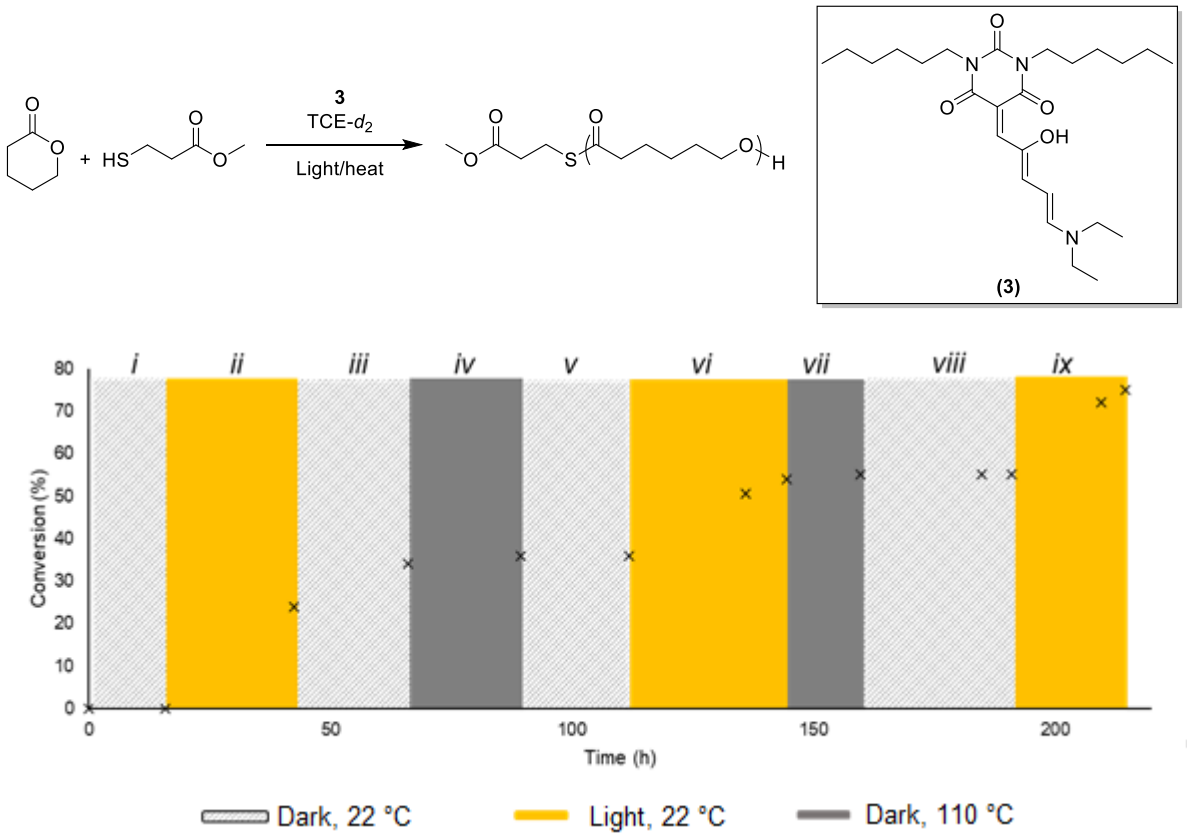

Figure 4.5. Kinetic plot for the switchable ROP of δVL catalysed by **3** (inserted scheme). Polymerisation was conducted in TCE-d_2 with $[\delta VL]_0/[\mathbf{3}]_0/[Thiol]_0$ = 30:0.1:1 where $[\delta VL]_0$ = 3 M.

As monomer conversion approached 80%, the polymerisation was quenched through precipitation into cold hexanes to reduce the risk of chain-transfer reactions (such as transesterification) that are more favourable at higher polymer concentrations. The isolated polymer sample was analysed by ^{1}H NMR spectroscopy and size-exclusion chromatography (SEC). Surprisingly, only three multiplet signals were detected in the ^{1}H NMR spectrum, attributable to the aliphatic polymer backbone (δ = 1.64, 2.30, and 4.04 ppm), with no apparent chain-end signals (Figure 4.6). In addition to this, SEC analysis showed a broad, monomodal distribution with a high molecular weight tail ($Đ_M$

= 1.71) along with poor correlation between theoretical molecular weight ($M_{n\ Theor}$ = 3,000 g·mol^{-1}) and that obtained by SEC analysis ($M_{n\ SEC}$ = 10,500 g·mol^{-1}) (Figure 4.6, insert). The apparent absence of polymer chain-ends by ^{1}H NMR spectroscopy is sometimes observed for ultra-high molecular weight polymers ($M_n > 10^5$ g·mol^{-1}), *i.e.* poor signal to noise, however the molecular weight of the isolated polyvalerolactone (PVL) was modest according to SEC analysis. Alternatively, it is also possible for chain-end signals to overlap with polymer or monomer resonances and thus be indistinguishable in the spectrum. To further investigate this possibility, the polymerisation was repeated using benzyl thiol as initiator which would present diagnostic, non-overlapping aromatic signals for the polymer chain-end. However, no chain-end aromatic resonances were visible and the spectrum was comparable to the alkyl thiol-initiated polymer. At this point, the data was consistent with a cyclic polymer structure for both thiol-initiated polymerisations. However, the possibility of a linear polymer was not ruled out, it was postulated that the formation of a linear polymer without visible thiol chain-ends could be the result of thiol-water exchange, or water initiation. Future works will focus on determination of either the formation of a cyclic or linear polymer through the application of matrix-assisted laser desorption ionisation (MALDI). Moreover, the formation of a cyclic polymer can be confirmed by SEC through the synthesis of a linear sample of PVL with the same theoretical molecular weight. Thus comparison of the molecular weights determined by SEC will aid in the confirmation of either a linear or cyclic polymer by DASA catalysis as a cyclic polymer will possess a larger hydrodynamic radius leading to decreased retention times.

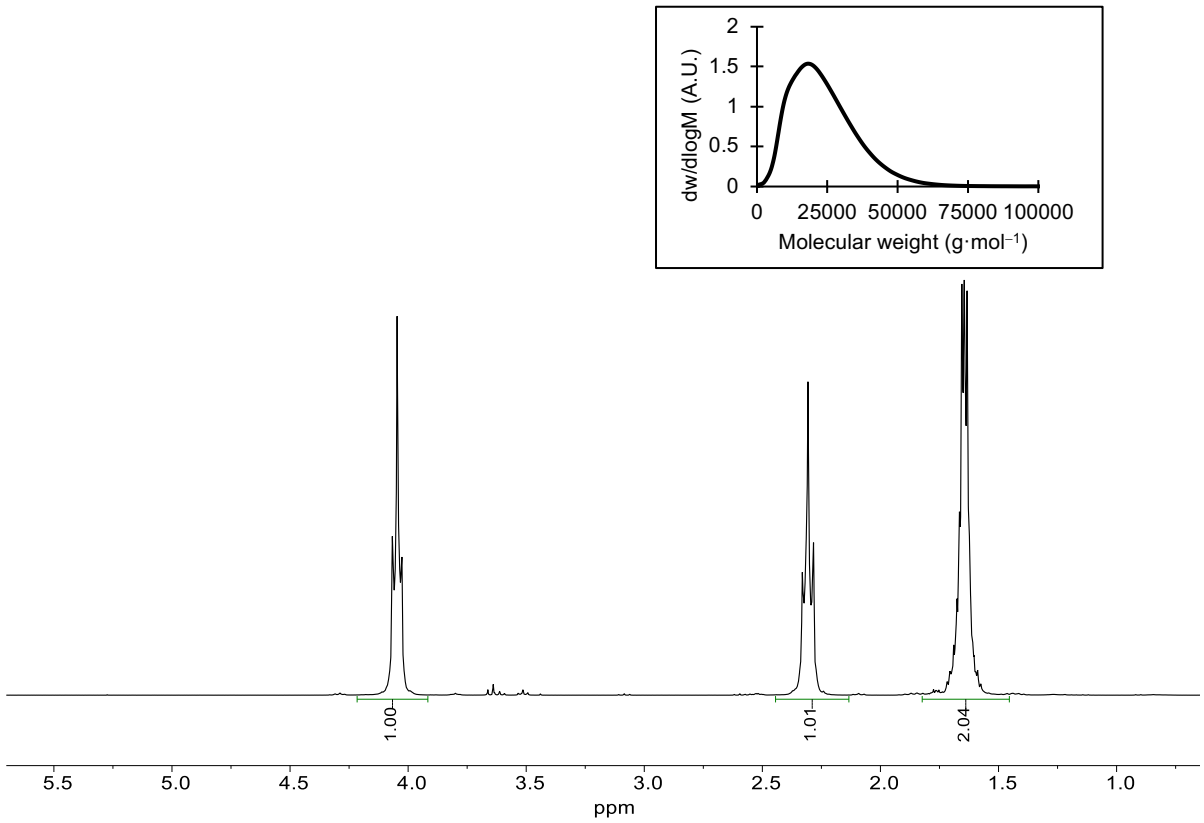

Figure 4.6. ^{1}H NMR spectrum of precipitated PVL (400 MHz, 298 K, $CDCl_3$). Polymerisation was conducted in TCE-d_2 with $[\delta VL]_0/[\mathbf{3}]_0/[Thiol]_0$ = 30:0.1:1 where $[\delta VL]_0$ = 3 M. Inset is size-exclusion chromatogram of PVL (M_n = 10,500 g·mol^{-1}, $Đ_M$ = 1.71) ($CHCl_3$, RI, calibrated against polystyrene standards).

4.2.4. Investigating effect of initiators

Searching for a more effective initiator that could yield a diagnostic chain-end signal by ^{1}H NMR spectroscopy we instead turned our attentions towards benzyl alcohol (BnOH) for the controlled ROP of δVL. In general, alcohols are less nucleophilic than thiols as a result of their increased electronegativity, however, it was hypothesised that the alcohol would still be able to "trap" the DASA in its activated zwitterionic form through an oxo-Michael addition reaction. The BnOH initiated ROP of δVL catalysed

by DASA **3** was monitored by ^{1}H NMR spectroscopy, and the evolution of a polymer structure with a definable end-group was apparent, as evidenced by the disappearance of free initiator (singlet, δ = 4.47 ppm) with concomitant increase of a singlet δ = 5.98 ppm, characteristic of the benzyl chain-end (Figure 4.7).

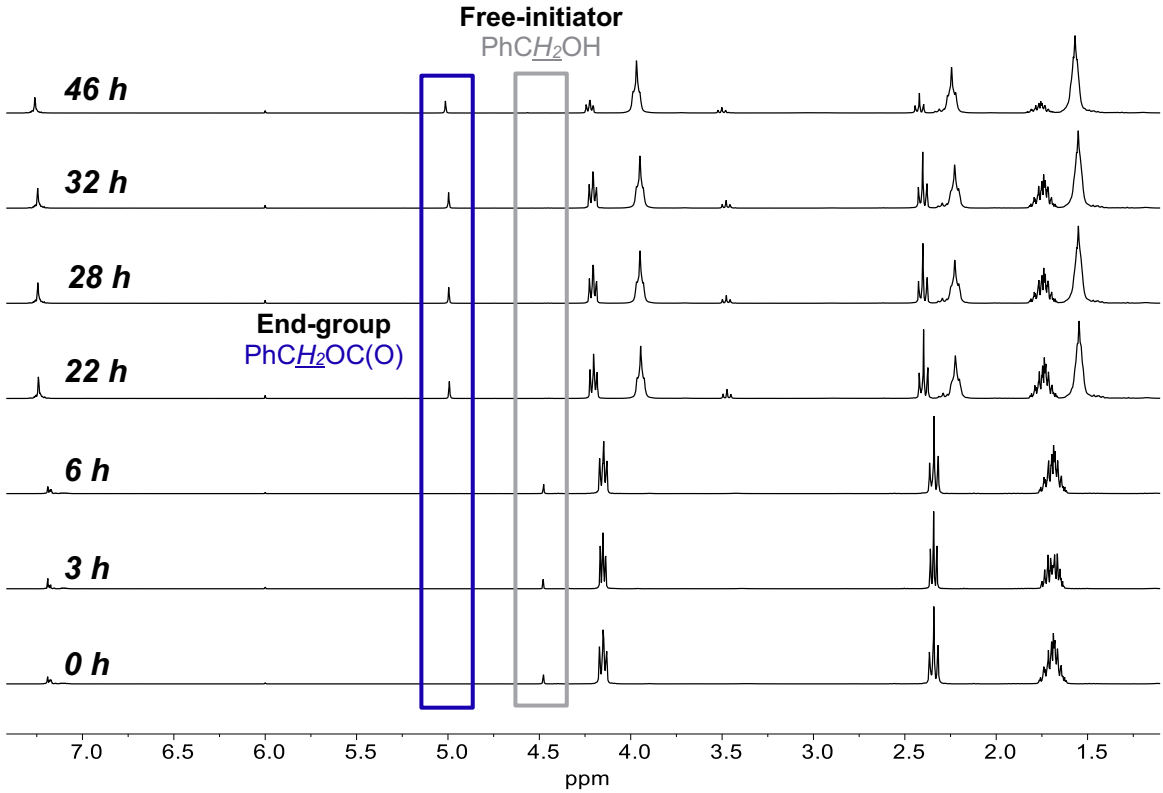

Figure 4.7. ^{1}H NMR spectra of δVL polymerisation catalysed by DASA **3** and initiated by BnOH (300 MHz, $Cl_2CDCDCl_2$, 298 K).

Once it was confirmed that BnOH could initiate the DASA catalysed polymerisation of δVL, we then focussed on the switching capability of the system. Initially, the reaction was monitored in the absence of light, during which time no polymerisation was noted, similar to the thiol-initiated reactions (Figure 4.8, section *i*). After irradiating the reaction mixture to generate the catalytically active DASA species, the polymerisation of δVL

was successfully initiated by BnOH as indicated by an increase in conversion (Figure 4.8, section *ii*). After it was established that the polymerisation could be orthogonally photoinitiated, it was essential to the determine reversible switching capability. Removing the light source and heating the mixture to 110 °C resulted in a dramatic decrease in rate of conversion, only a 4% increase in conversion was witnessed over a 10-hour period (Figure 4.8, section *iii*). Once cooled to room temperature, subsequent re-exposure to the light source caused an increase in conversion rate (Figure 4.8, section *iv*), confirming the active switching behaviour of the system between the ON and OFF states. It was noted that this second initiation appeared to be slower than the first step upon comparing the relative rates of change (slope), however this was assumed to be a consequence of low monomer concentration as the reaction approached high conversion (> 80%).

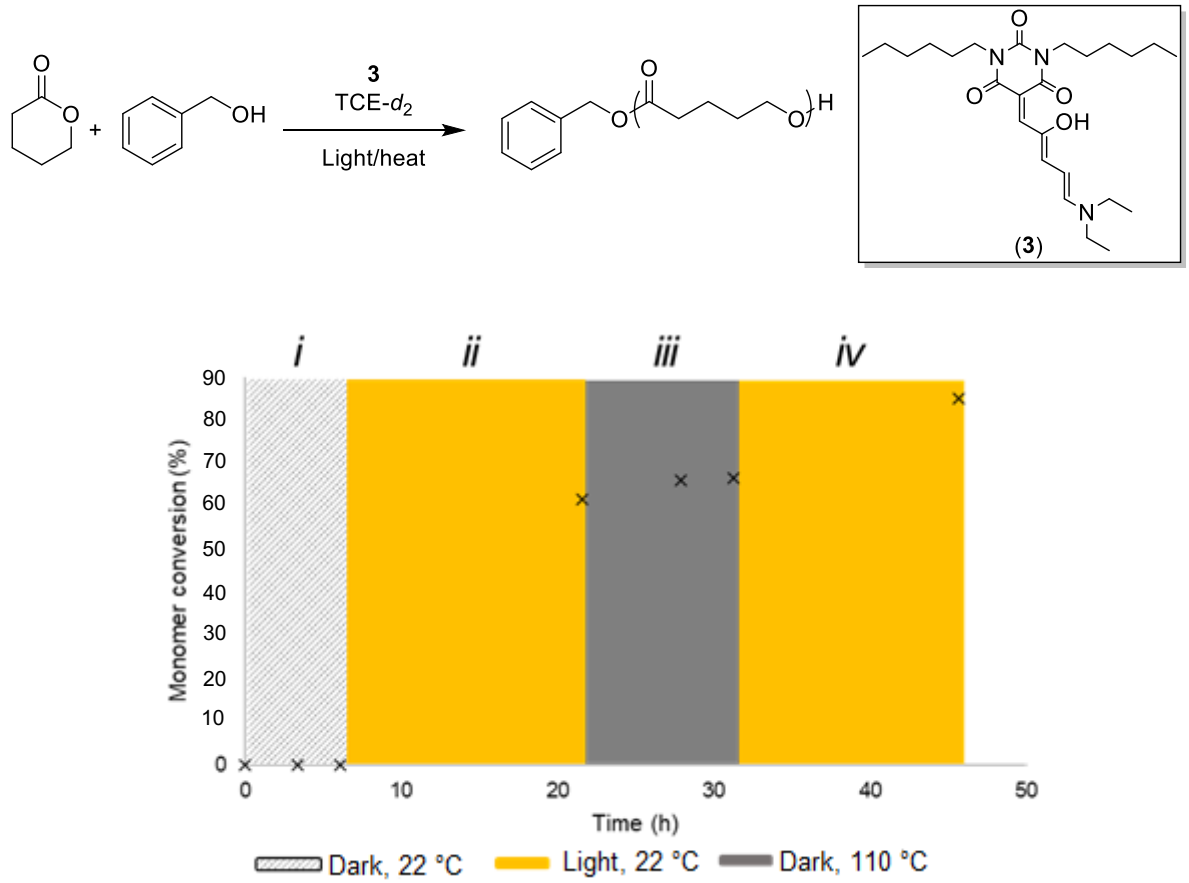

Figure 4.8. Kinetic plot for the DASA catalysed ROP of δVL initiated by BnOH (inset scheme). Polymerisation was conducted in TCE-d_2 with $[\delta VL]_0/[\mathbf{3}]_0/[BnOH]_0$ = 30:0.1:1 where $[\delta VL]_0$ = 3 M.

The polymerisation was then terminated through precipitation into cold hexanes and analysed by ^{1}H NMR spectroscopy and SEC. In contrast to the samples obtained from thiol-based initiators, the aromatic polymer chain-ends (δ = 7.34 ppm) from BnOH were visible by ^{1}H NMR spectroscopy (Figure 4.9), the formation of a well-defined, linear polymer. Moreover, theoretical molecular weights ($M_{n\ Theor}$ = 2,700 g·mol^{-1}) and molecular weights calculated from ^{1}H NMR spectroscopy ($M_{n\ NMR}$ = 2,900 g·mol^{-1}) and SEC ($M_{n\ SEC}$ = 3,900 g·mol^{-1}) were in good agreement. However, SEC analysis also

indicated a broad monomodal distribution ($Đ_M$ = 1.60) which suggests inefficient control over the polymerisation (Figure 4.10). Comparing results from ^{1}H NMR spectroscopy and SEC from both thiol and BnOH initiated samples, the BnOH-initiated polymerisations proceeded in a more-controlled fashion which resulted in PVL with comparatively narrow dispersities and predictable molecular weights.

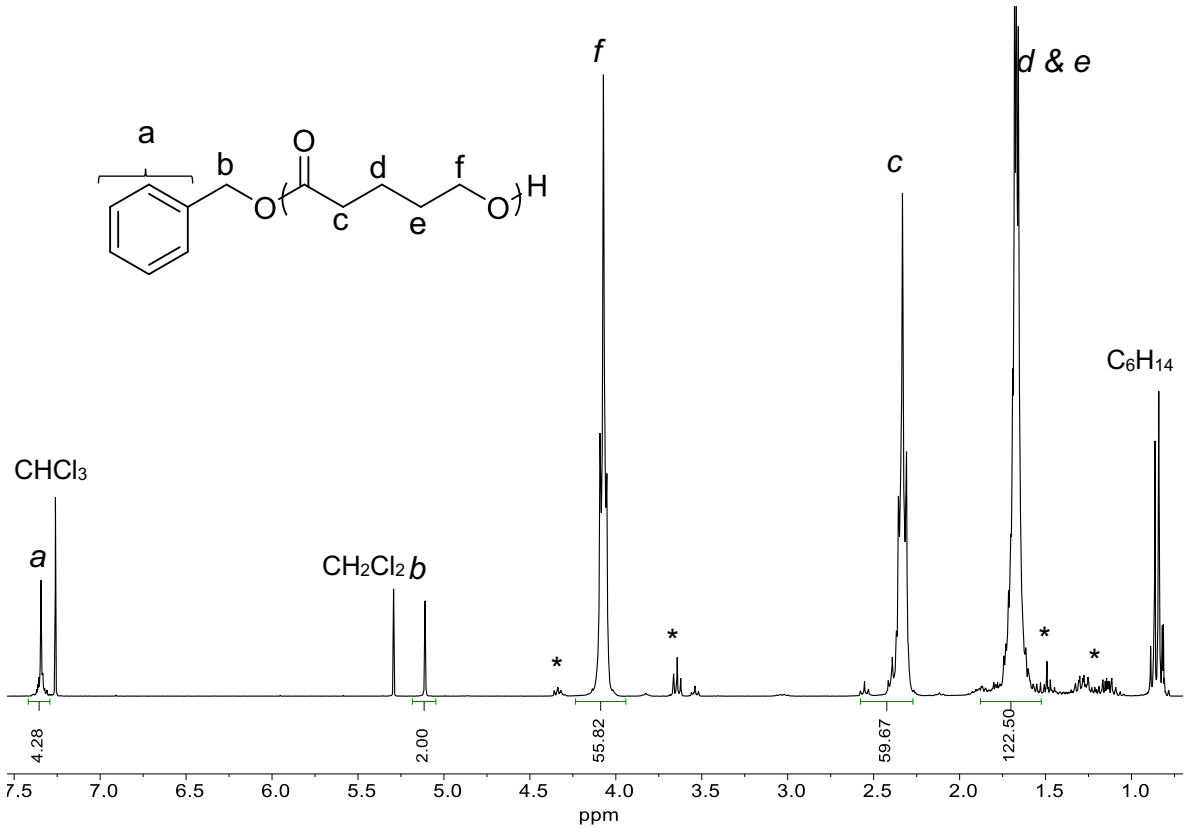

Figure 4.9. ^{1}H NMR spectrum of precipitated PVL from the BnOH initiated ROP of δVL. * indicates unprecipitated monomer (300 MHz, 298 K, $CDCl_3$).

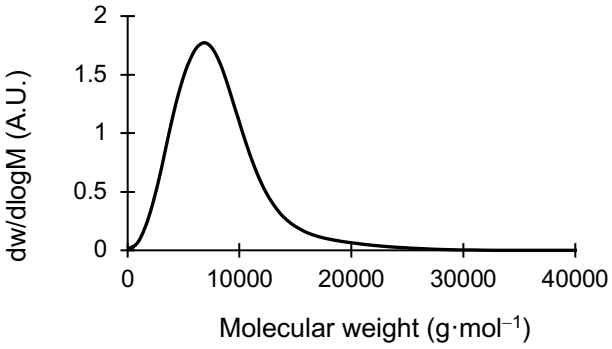

Figure 4.10. Size-exclusion chromatogram of PVL obtained from the BnOH-initiated reaction. Polymerisation was conducted in TCE-d_2 with $[\delta VL]_0/[\mathbf{3}]_0/[BnOH]_0$ = 30:0.1:1 where $[\delta VL]_0$ = 3 M (M_n = 3,900 g·mol^{-1}, $Đ_M$ = 1.60) ($CHCl_3$, RI, calibrated against polystyrene standards).

4.3. Conclusions

In conclusion, utilising the well-known chemistry of DASA compounds, **3** was successfully synthesised and screened as a ROP catalyst for a variety of cyclic (di)esters and carbonates. Upon irradiation, **3** was found to be an efficient catalyst for the ROP of δVL and εCL, however no polymer was produced when employing lactide or methyl allyl carbonate. For thiol-initiated polymerisations, poor control over the final polymer properties, such as end-group fidelity and molecular weight, was observed. However, better control over polymer properties was afforded when switching to an alcohol-based initiator which led to a controlled polyester with high end-group fidelity. Judicious control over light and temperature provided command over the ON and OFF state of the polymerisation for multiple cycles without any obvious loss of catalytic activity.

Switchable catalysis for ROP offers unique opportunities for complete and orthogonal control over polymerisation, though reports to date only utilise a single trigger such as temperature or light. Moreover, these previous approaches often required rigorous control over reaction conditions, such as a precise wavelength and/or power, to toggle the catalytic ON/OFF state. Here, we have demonstrated a new approach towards switchable catalysis for ROP through the application of two distinct external stimuli to exert good control over the catalytic ON and OFF state without the need for a co-catalyst. This approach opens up the opportunity to new orthogonally controlled polymerisations.

4.4. References

1. M. Ouchi, T. Terashima and M. Sawamoto, *Acc. Chem. Res.*, 2008, **41**, 1120-1132.

2. S. M. Guillaume, E. Kirillov, Y. Sarazin and J. F. Carpentier, *Chem. Eur. J.*, 2015, **21**, 7988-8003.

3. S. Shanmugam, J. Xu and C. Boyer, *Macromol. Rapid Commun.*, 2017, **38**, 1700143.

4. B. M. Neilson and C. W. Bielawski, *Chem. Commun.*, 2013, **49**, 5453-5455.

5. C. K. A. Gregson, V. C. Gibson, N. J. Long, E. L. Marshall, P. J. Oxford and A. J. P. White, *J. Am. Chem. Soc.*, 2006, **128**, 7410-7411.

6. H. J. Yoon, J. Kuwabara, J.-H. Kim and C. A. Mirkin, *Science*, 2010, **330**, 66-69.

7. A. Piermattei, S. Karthikeyan and R. P. Sijbesma, *Nat. Chem.*, 2009, **1**, 133-137.

8. F. Eisenreich, M. Kathan, A. Dallmann, S. P. Ihrig, T. Schwaar, B. M. Schmidt and S. Hecht, *Nat. Chem.*, 2018, **1**, 516-522.

9. M. Osaki, Y. Takashima, H. Yamaguchi and A. Harada, *Org. Bio. Chem.*, 2009, **7**, 1646-1651.

10. P. Viehmann and S. Hecht, *Belstein J. Org. Chem.*, 2012, **8**, 1825-1830.

11. Z. Dai, Y. Cui, C. Chen and J. Wu, *Chem. Commun.*, 2016, **52**, 8826-8829.

12. Y. Yağci and I. Reetz, *Prog. Polym. Sci.*, 1998, **23**, 1485-1538.

13. O. Coulembier, A. P. Dove, R. C. Pratt, A. C. Sentman, D. A. Culkin, L. Mespouille, P. Dubois, R. M. Waymouth and J. L. Hedrick, *Angew. Chem. Int. Ed.*, 2005, **44**, 4964-4968.

14. S. Helmy, F. A. Leibfarth, S. Oh, J. E. Poelma, C. J. Hawker and J. Read de Alaniz, *J. Am. Chem. Soc.*, 2014, **136**, 8169-8172.

15. S. Helmy, S. Oh, F. A. Leibfarth, C. J. Hawker and J. Read de Alaniz, *J. Org. Chem.*, 2014, **79**, 11316-11329.

16. M. Di Donato, M. M. Lerch, A. Lapini, A. D. Laurent, A. Iagatti, L. Bussotti, S. P. Ihrig, M. Medved', D. Jacquemin, W. Szymański, W. J. Buma, P. Foggi and B. L. Feringa, *J. Am. Chem. Soc.*, 2017, **139**, 15596-15599.

17. M. M. Lerch, M. Medved′, A. Lapini, A. D. Laurent, A. Iagatti, L. Bussotti, W. Szymański, W. J. Buma, P. Foggi, M. Di Donato and B. L. Feringa, *J. Phys. Chem. Part A*, 2018, **122**, 955-964.

18. M. M. Lerch, W. Szymański and B. L. Feringa, *Chem. Soc. Rev.*, 2018, **47**, 1910-1937.

19. M. M. Lerch, S. J. Wezenberg, W. Szymanski and B. L. Feringa, *J. Am. Chem. Soc.*, 2016, **138**, 6344-6347.

20. J. Alves, S. Wiedbrauk, D. Gräfe, S. L. Walden, J. P. Blinco and C. Barner-Kowollik, *Chem. Eur. J.*, 2020, **26**, 809.

21. C. F. H. Allen and W. J. Humphlett, *Can. J. Chem.*, 1966, **44**, 2315-2321.

22. N. Kuhl, R. Geitner, R. K. Bose, S. Bode, B. Dietzek, M. Schmitt, J. Popp, S. J. Garcia, S. van der Zwaag, U. S. Schubert and M. D. Hager, *Macromol. Chem. Phys.*, 2016, **217**, 2541-2550.

23. N. Kuhl, R. Geitner, J. Vitz, S. Bode, M. Schmitt, J. Popp, U. S. Schubert and M. D. Hager, *J. Appl. Polym. Sci.*, 2017, **134**.

24. B. Zhang, P. Chakma, M. P. Shulman, J. Ke, Z. A. Digby and D. Konkolewicz, *Org. Biomol. Chem.*, 2018, **16**, 2725-2734.

25. B. A. Laurent and S. M. Grayson, *Chem. Soc. Rev.*, 2009, **38**, 2202-2213.

5. Chapter five

Conclusions and future work

UNIVERSITY OF BIRMINGHAM

5.1. Conclusions

This thesis describes strategies for the synthesis of stereoenriched poly(ε-subsituted-ε-caprolactones) (PεSεLs) which are promising approaches to achieve new functional semi-crystalline materials. The first approach investigated the synthesis of a stereoenriched alcohol-functionalised monomer capable of post-polymerisation modifications. The synthesis of the alcohol monomer from cyclohexanone, following a Baeyer-Villiger ring expansion provided a functional lactone which possessed a high degree of enantioselectivity. To prevent unwanted side-reactions and produce well-defined linear polymers, it was necessary to protect the alcohol before polymerisation. It was found that the susceptibility of the new functional pendant group to nucleophilic attack was a crucial factor towards achieving control over the polymerisation using the organocatalyst diphenylphosphate (DPP), and any presence of a carbonyl moiety led to increased side-reactions and a loss of control over the polymerisation. Instead, with retention of stereochemistry, conversion of the alcohol into a bromide functionality led to a moderately controlled polymerisation to yield a polymer with narrow dispersities and predictable molecular weights. Thermal analysis confirmed the polymer to be amorphous in nature with only a glass-transition temperature witnessed.

The second approach towards the synthesis of a semi-crystalline polymer involved the stereoselective polymerisation from a racemic monomer to control the polymer microstructure. Initially, a variety of substituted chiral binapthol (BINOL) phosphoric acid catalysts, previously demonstrated to be effective stereoselective ring-opening polymerisation (ROP) catalysts, with varying degrees of steric bulk and electronegativities were screened against a range of ε-substituted-ε-caprolactone (εSεL) monomers at 70 °C. Overall, steric bulk in close proximity to the active site of

the catalyst was found to be the most influential on stereoselectivity during the polymerisation. As such, a tris(*iso*-propyl) substituted catalyst displayed modest stereoselectivities, particularly in combination with the least sterically bulky monomer, ε-heptalactone (εHL), with stereoselectivities decreasing as monomer bulk increased. The temperature of the polymerisation was found to be highly effective towards exerting control over stereoselectivity, and decreasing the temperature corresponded to an increase in stereoselectivities. This led to a considerable increase in stereoselectivity for the ROP of εHL giving the highest stereoselectivities ever reported for this family of monomers. However, an inversion point was witnessed for some monomers as a result of a switch in favourable thermodynamics. Thermal analysis of the most stereoenriched polymer presented only a glass-transition temperature confirming the sample was completely amorphous and devoid of any semi-crystallinity.

Obtaining remote control over the ON/OFF states of a polymerisation *via* an external stimuli overs unprecedented opportunity to fabricate innovative materials. Chapter four described the orthogonal control the ROP of δ-valerolactone (δVL) using a unique combination of light and heat in combination with a donor-acceptor Stenhouse adduct (DASA) as a switchable catalyst. Exposure to light triggered a cyclisation to provide the active DASA catalyst, and in the presence of δVL and suitable initiator, the polymerisation was initiated. The OFF state of the polymerisation was achieved through heating the system, in the absence of irradiation, and was found to be sustainable even after cooling the system to ambient temperatures. Subsequent re-exposure to light triggered the ON state of the polymerisation, and propagation continued. Judicious control over light and heat allowed for cycling between the ON and OFF state for multiple rounds. In hopes of “trapping” the polymerisation in the ON

state *via* a Michael addition, a thiol-based initiator was initially investigated for the switchable ROP of δVL. Whilst the switching capabilities were retained, analysis of the resultant polymer displayed no assignable chain-ends by ^{1}H NMR spectroscopy and size-exclusion chromatography (SEC) displayed molecular weights lower than expected. It was hypothesized that this was a result of either the formation of a cyclic polymer or initiation by residual water present in the reaction, or labile thiol chain-ends leading to a linear polymer with no discernible chain-ends. Changing to an alcohol-based initiator provided a polymer with detectable chain-ends by ^{1}H NMR spectroscopy, and with moderate control over molecular weights, with retention of the switchable behaviour of the system.

5.2. Future works

The methodologies developed towards the synthesis of semi-crystalline stereoenriched PεSεLs provides the opportunity for the synthesis of new functional materials. Chapter two described the enantioenriched synthesis of a functional monomer and its subsequent polymerisation. In order to achieve a semi-crystalline material, it is necessary to reduce stereoerrors in the polymer backbone. One way to achieve this is through the combination of the enantioenriched monomer with a stereoselective catalyst that is selective for the most enriched stereoisomer found in the monomer mixture. Terminating the polymerisation at a conversion before the less-favoured isomer starts to become consumed should promote the formation of a polymer with less stereoerrors than seen from catalysts such as DPP. Through the reduction of stereoerrors, this should promote the formation of long-range order in the sample which would lead to semi-crystallinity within the material.

Conversely, chapter three described the application of stereoselective organocatalysts for the stereoselective ROP of racemic εSεLs. It was found that the steric bulk of the BINOL substituent on the phosphoric acid catalyst was most effective towards gaining stereoselectivity during the polymerisation. Therefore, finding a substituent that is more sterically bulky the tris(isopropyl), whilst still allowing monomer approach could allow for an increase in stereoselectivity during the polymerisation. Moreover, as showed, lowering the polymerisation temperature was influential in increasing stereoselectivity, and the highest stereoselectivities were obtain in benzene-d_6 at 5 °C; yet benzene possesses a freezing point of 5.5 °C meaning further lowering the polymerisation temperature whilst using benzene-d_6 is not possible. One way to overcome this is to exchange benzene-d_6 with toluene-d_8 which has a freezing point of –95 °C which would allow for the reduction of polymerisation temperature, albeit at the cost of increased polymerisation times.

The DASA system investigated in chapter four as a switchable catalyst for the ROP of δVL proved to be effective in obtaining control over the ON and OFF states of the polymerisation. Chain-ends from polymers obtained using a thiol-based initiator were difficult to detect by ^{1}H NMR spectroscopy, as such analysis of the polymer samples by matrix-assisted laser desorption ionisation (MALDI) would be helpful to determine the formation of cyclic or linear polymers and help to identify the functionality of chain-ends in the case of a linear polymer. Moreover, comparison of SEC data obtained from a linear poly(δ-valerolactone) (PVL) sample of equal theoretical molecular weight would further aid in the identification of a cyclic polymer. As a consequence of increased hydrodynamic radius associated with cyclic polymers this would lead to an increased apparent molecular weight by SEC through an increased retention time

compared to its linear counterpart. As a result of its modular synthesis, it is possible to create a varied library of potential DASA catalysts to screen against cyclic esters to see how the properties of the catalyst effect the polymerisation. Furthermore, changing the amine during the final stages of DASA synthesis can change the final colour of the DASA product allowing you to change the wavelength at which the catalyst activation occurs leading to more control over the catalytic system.

6. Chapter Six

Experimental

6.1. Materials

All chemicals and solvents, unless otherwise stated, were purchased from Sigma-Aldrich, Strem, Apollo Scientific and Fisher Scientific and used without further purification. (*R*)-3,3′-Bis(2,3,4,5,6-pentafluorophenyl)-1,1′-binaphthyl-2,2′-diyl hydrogenphosphate ((*R*)-pentafluoro), (*R*)-3,3′-Bis(3,5-bis(trifluoromethyl)phenyl)-1,1′-binaphthyl-2,2′-diyl hydrogenphosphate ((*R*)-bis trifluoro), (*R*)-3,3′-Bis(2,4,6-tricyclohexylphenyl)-1,1′-binaphthyl-2,2′-diyl hydrogenphosphate ((*R*)-cyclohexyl), N-((4S)-2,6-bis(3,5-bis(trifluoromethyl)phenyl)-4-oxidodinaphtho[2,1-d:1',2'-f][1,3,2]dioxaphosphepin-4-yl)-1,1,1-trifluoromethanesulfonamide ((*R*)-bis trifluoro trif), 8-(((4R)-4-hydroxy-2,6-bis(2-isopropyl-5-methylphenyl)-4l5-dinaphtho[2,1-d:1',2'-f][1,3,2]dioxaphosphepin-4-ylidene)amino)-10-(5-isopropyl-2-methylphenyl)-6-(2-isopropyl-5-methylphenyl)dinaphtho[2,1-d:2',3'-f][1,3,2]dioxaphosphepine 8-oxide (imido) were synthesized by the Leibfarth group, Department of Chemistry, University of North Carolina, NC US. Benzyl alcohol (BnOH), ε-heptalactone (εHL), ε-allyl-ε-caprolactone (εAL), ε-decalactone (εDL), δ-valerolactone (δVL), ε-caprolactone (εCL), were dried over CaH_2, distilled, and stored under an inert atmosphere. (*S*)-ε-Methylbromo-ε-caprolactone, (*S*)-ε-methyl acetate-ε-caprolactone, (*S*)-ε-methyl hexylcarbamate-ε-caprolactone, diphenyl phosphate (DPP), (*R*)-3,3′-Bis(2,4,6-triisopropylphenyl)-1,1′-binaphthyl-2,2′-diyl hydrogenphosphate ((*R*)-TRIP), ((*R*)-pentafluoro), ((*R*)-bis trifluoro), ((*R*)-bis trifluoro trif), 8-oxide (imido), 5-((2*Z*,4*E*)-5-(diethylamino)-2-hydroxypenta-2,4-dien-1-ylidene)-1,3-dihexylpyrimidine-2,4,6(1*H*,3*H*,5*H*)-trione were dried over P_2O_5 in a vacuum desiccator for 3 days, in which the P_2O_5 was replaced every day, and then stored under an inert atmosphere. Benzyl thiol, chloroform-*d* and tetrachloroethane-d_2 were

dried and stored over 3 Å molecular sieves under an inert atmosphere. Benzene-d_6 was dried over sodium benzophenone, distilled, and stored under an inert atmosphere. L-Lactide (L-LA, Purac) was dissolved in CH_2Cl_2 and passed through a silica plug. The solution was transferred to a Schlenk flask and concentrated under vacuum. The resultant solid was recrystallised twice from dry hot toluene (70 °C), sublimed and stored under an inert atmosphere. Silica gel (pore size = 40 Å) was obtained from Fisher Scientific and used as received. Dry solvents were obtained by purification over an Innovative Technology SPS alumina solvent column and degassed by repeated freeze-pump-thaw cycles prior to use.

6.2. Characterisation techniques

6.2.1. Nuclear Magnetic Resonance (NMR) spectroscopy

NMR spectra were recorded on a Bruker Avance III HD 300, 400 or 500 MHz spectrometer at 298 K. Chemical shifts are reported as δ in parts per million (ppm) and referenced to the residual solvent signal ($CDCl_3$: ^1H, δ = 7.26 ppm, ^{13}C, δ = 77.2 ppm, C_6D_6, ^1H, δ = 7.16 ppm, ^{13}C, δ = 128.1 ppm $Cl_2CDCDCl_2$: ^1H, δ = 6.00 ppm, ^{13}C, δ = 73.8 ppm). Multiplicities are reported as s = singlet, brs = broad singlet, d = doublet, t = triplet, q = quartet, quin = quintuplet, m = multiplet. Multiplicity is followed by coupling constant (J) in Hz, and integration.

6.2.2. Size-exclusion chromatography (SEC)

SEC analysis was performed on a system composed of an Agilent 1260 Infinity II LC system equipped with an Agilent guard column (PLGel 5 μM, 50 × 7.5 mm) and two Agilent Mixed-C columns (PLGel 5 μM, 300 × 7.5 mm). The mobile phase used was HPLC grade $CHCl_3$ with 2% Et_3N at 40 ºC at flow rate of 1.0 mL·min^{-1}. SEC samples were calibrated against linear polystyrene standards (162 – 2.4 × 10^5 g·mol^{-1}).

6.2.3. Flash chromatography

Flash chromatography was performed on a Teledyne ISCO CombiFlash Rf+ Lumen equipped with two UV detectors (254 nm and 280 nm) and an internal evaporative light scattering detector (ELSD). Samples were purified with RediSep RF normal phase columns.

6.2.4. Gas-chromatography mass-spectrometry (GCMS)

GCMS was performed on a Shimadzu GCMS QP2010 SE system with a CP-Chirasil-Dex CB 25 × 0.25 column. The temperature programming was set to 90 °C for 10 min then a gradient to 200 °C at 2 °C·min^{-1}. The injector temperature was 170 °C with 1.0 µL injection volume. The helium carrier gas flow rate was set at 1 mL·min^{-1}. MS detection was used selective ion scanning m/z 1.5-1000 amu. The EI source temperature was 200 °C.

6.2.5. High-resolution mass-spectrometry (HRMS)

HRMS spectra were recorded by the MS Analytical Facility Service at the University of Birmingham on a Waters Xevo G2-XS Quadrupole Time-of-Flight mass spectrometer.

6.2.6. Fourier-transform infrared (FTIR) spectroscopy

FTIR spectra were recorded on an Agilent Technologies Cary 630 FTIR spectrometer. 16 Scans from 600 to 4000 cm^{-1} were taken at a resolution of 4 cm^{-1}, and the spectra were corrected for background absorbance.

6.2.7. UV/Vis spectroscopy

UV/Vis spectroscopy was performed on Evolution 350 UV-Vis spectrophotometer equipped with Xenon Flash Lamp light source and Dual Matched Silicon Photodiodes detector. Quartz cells (path length 1 cm, 170 - 2000 nm) from Hellma were used.

6.2.8. Differential scanning calorimetry (DSC)

DSC data was obtained from using a Mettler Toledo DSC1 star system. DSC heating and cooling curves were run in triplicate in series between −100 and 150 °C under a nitrogen atmosphere at a heating rate of ±10 °C·min^{-1} in a 40 µL aluminium crucible.

6.3. Experimental procedures for Chapter two

6.3.1. *Synthesis of (*S)-2-hydroxymethyl cyclohexanone

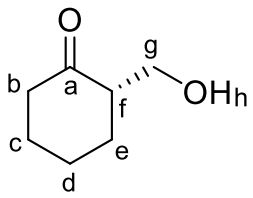

Using a modified version of a previously reported procedure,[1] L-threonine (1.49 g, 12.5 mmol, 0.1 equiv.) was dissolved in formalin (9.5 mL, 125 mmol, 1 equiv.). The mixture was then diluted with THF (250 mL) and cooled to 5 °C to form a clear, colourless, uniform solution. Then, cyclohexanone (20 mL, 190 mmol, 1.5 equiv.) and anhydrous $MgSO_4$ (15 g, 125 mmol, 1 equiv.) were added. The temperature was then held at 5 °C for 3 months. Afterwards, solids were removed and washed with EtOAc (3 × 20 mL). To the combined organics was added sat. NH_4Cl (40 mL) and stirred for 20 min. Solids were removed and the organic layer was dried with $MgSO_4$, and volatiles were removed under a reduced pressure. Vacuum distillation of the crude product provided (*S*)-2-hydroxymethyl cyclohexanone (10.6 g, 82.4 mmol, 66% yield) as a pale yellow, clear, and viscous liquid in 86% *ee*. Characterisation was consistent with previous reports.[1]

^{1}H NMR (300 MHz, 298 K, $CDCl_3$): δ = 3.72 (dd, J = 11.6, 7.4 Hz, 1H, H^g), 3.59 (dd, J = 11.6, 3.7 Hz, 1H, $H^{g'}$), 2.63 (brs, 1H, H^h), 2.58 – 2.41 (m, 1H, H^f) , 2.41 – 2.24 (m, 2H, H^b), 2.18 – 1.82 (m, 3H, H^c, H^d, H^e), and 1.75 – 1.38 (m, 3H $H^{c'}$, $H^{d'}$, $H^{e'}$) ppm.

^{13}C NMR (100 MHz, 298K, $CDCl_3$): δ = 214.7 (C^a), 62.2 (C^g), 52.3 (C^b), 42.6 (C^f), 30.1 (C^e), 27.5 (C^c), and 24.3 (C^d) ppm.

6.3.2. Synthesis of (S)-ε-hydroxymethyl-ε-caprolactone

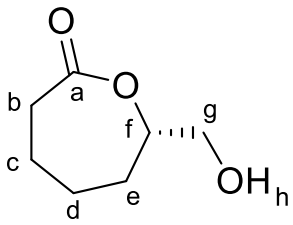

Following a previously reported procedure,[1] a 100 mL round-bottomed flask (dried overnight in the oven and under a N_2 atmosphere) was charged with a solution of (*S*)-hydroxymethyl cyclohexanone (2 g, 15.6 mmol, 1 equiv.) in dry CH_2Cl_2 (40 mL) was cooled using an ice bath. To this, $NaHCO_3$ was added (1.96g, 23.4 mmol, 1.5 equiv.), followed by *m*-chloroperoxybenzoic acid <77% (4.18 g, 18.7 mmol, 1.2 equiv.) in small aliquots. The mixture was warmed to room temperature and stirred overnight. The reaction was then diluted with CH_2Cl_2 (15 mL) and solid sodium thiosulfate (1.23 g, 7.8 mmol, 0.5 equiv.) The mixture was stirred for 20 min after which the solids were removed and washed with CH_2Cl_2 (80 mL). Volatiles were removed *in vacuo* and the crude product was purified *via* flash chromatography using hexane/EtOAc (100:0 to 0:100) as eluent to provide (*S*)-ε-hydroxymethyl-ε-caprolactone (1.25 g, 15.6 mmol, 56% yield) as a clear, colourless, viscous liquid in 85% *ee*. Characterisation was consistent with previous reports.[1]

^{1}H NMR (300 MHz, 298 K, $CDCl_3$): δ = 4.35 (m, 1H, H^f), 3.82-3.58 (m, 2H, H^g), 2.87 – 2.54 (m, 2H, H^b), 2.15 (brs, 1H, H^h), 2.04 – 1.82 (m, 3H, H^c, H^d, H^e), 1.73 – 1.49 (m, 3H, $H^{c'}$, $H^{d'}$, $H^{e'}$) ppm.

^{13}C NMR (100 MHz, 298 K, $CDCl_3$): δ = 175.0 (C^a), 81.2 (C^g), 65.0(C^b), 34.7 (C^b), 30.4 (C^c), 27.7 (C^e), 22.8 (C^d) ppm.

*6.3.3. Synthesis of (*S*)-ε-methylacetyloxy-ε-caprolactone*

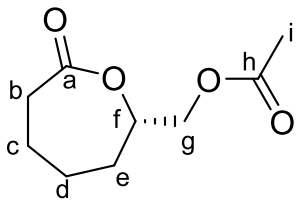

To a solution of (*S*)-ε-hydroxymethyl-ε-caprolactone (2.25 g, 15.6 mmol, 1 equiv.) in CH_2Cl_2 (30 mL) acetic anhydride (1.75 mL, 18.4 mmol, 1.18 equiv.) and triethylamine (1.86 g, 18.4 mmol, 1.18 equiv.) were added to form a uniform, colourless solution. The mixture was left to stir at room temperature overnight. Then, 4-dimethylaminopyridine (95.3 mg, 0.78 mmol, 0.05 equiv.) was added and the mixture left to stir for 4 h. After the removal of volatiles *in vacuo*, the crude product was purified *via* silica gel chromatography using a CH_2Cl_2/MeOH eluent (95:5) to yield (S)-ε-methylacetyloxy-ε-caprolactone (800 mg, 4.3 mmol, 27.5% yield).

^{1}H NMR (400 MHz, 298 K, $CDCl_3$): δ = 4.52 – 4.43 (m, 1H, H^f), 4.19 (dd, J = 11.9, 7.1 Hz, 1H, H^g), 4.14 (dd, J = 11.6, 4.8 Hz, 1H, $H^{g'}$), 2.72 (dd, J = 14.4, 7.3 Hz, 1H, H^b), 2.66 – 2.51 (m, 1H, $H^{b'}$), 2.09 (s, 3H, H^i), 2.05 – 1.91 (m, 3H, H^c, H^d, H^e), and 1.85 – 1.48 (m, 3H, $H^{c'}$, $H^{d'}$, $H^{e'}$) ppm

^{13}C NMR (125 MHz, 298 K, $CDCl_3$): δ = 175.7 (C^a), 170.2 (C^h), 74.6 (C^f), 65.2 (C^g), 35.1 (C^b), 31.6 (C^e), 28.8 (C^c), 24.0 (C^d), and 20.7 (C^i) ppm.

HRMS (ESI-TOF): m/z calculated for $C_9H_{14}O_4Na$ $[M+Na]^+$ 209.0979, found 209.0856

*6.3.4. Synthesis of (*S*)-ε-methyl-*N*-hexylcarbamate-ε-caprolactone*

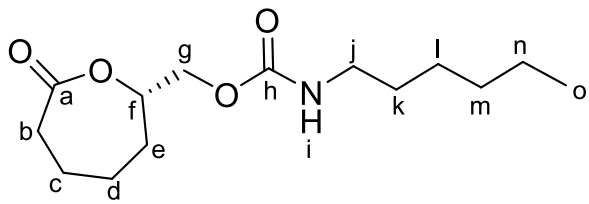

To a 100 mL round-bottomed flask (dried in oven overnight and under N_2 atmosphere) (*S*)-ε-hydroxymethyl-ε-caprolactone (0.90 g, 6.25 mmol, 1 equiv.) was dissolved in dry THF (15 mL). To this, hexyl isocyanate (2.5 mL, 31.3 mmol, 5 equiv.) and dibutylitin dilaurate (0.037 mL,

0.063 mmol, 0.01 equiv.) were added, and the mixture was left to stir at room temperature overnight. Volatiles were removed and crude product was purified *via* neutral alumina column chromatography using hexane/EtOAc as eluent (50:50) to provide (*S*)-ε-methyl-*N*-hexylcarbamate-ε-caprolactone (1.05 g, 3.87 mmol, 62% yield) as a white solid.

^{1}H NMR (400 MHz, 298 K, $CDCl_3$): δ = 5.05 (brs, 1H, H^i), 4.48 – 4.35 (m, 1H, H^f), 4.16 – 3.93 (m, 2H, H^g), 3.15 – 2.98 (m, 2H, H^j), 2.70 – 2.46 (m, 2H, H^b), 2.00 – 1.79 (m, 3H, H^c, H^d, H^e), 1.60 – 1.46 (m, 3H, $H^{c'}$, $H^{d'}$, $H^{e'}$), 1.46 – 1.35 (m, 2H, H^j), 1.28 – 1.12 (m, 6H, H^l, H^m, H^n), and 0.87 – 0.71 (m, 3H, H^o) ppm.

^{13}C NMR (125 MHz, 298 K, $CDCl_3$): δ = 175.0 (C^a), 156.1 (C^h), 78.1 (C^f), 66.2 (C^g), 41.0 (C^j), 34.7 (C^b), 31.4 (C^m), 30.8 (C^e), 29.7 (C^k), 27.7 (C^d), 26.3 (C^l), 22.8 (C^c), 22.5 (C^n), and 13.9 (C^o) ppm.

HRMS (ESI-TOF): m/z calculated for $C_{14}H_{25}NO_4Na$ $[M+Na]^+$ 294.0679, found 294.0687.

6.3.5. Synthesis of (S)-ε-methylbromo-ε-caprolactone

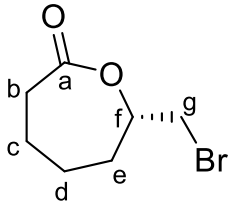

Following a previously reported procedure,[1] a 250 mL round-bottomed flask (dried in oven overnight and under a N_2 atmosphere) was charged with a solution of (*S*)-ε-hydroxymethyl-ε-caprolactone (430 mg, 2.98 mmol, 1 equiv.) in dry CH_2Cl_2 (15 mL), which was then cooled using an ice bath. Once cool, triphenylphosphine (1.578 g, 6.01 mmol, 2 equiv.), followed by the slow addition of carbon tetrabromide (1.99 g, 6.00 mmol, 2 equiv.). The reaction was warmed to room temperature and stirred for 4 h. After the removal of volatiles *in vacuo*, the crude product was purified *via* flash chromatography using DCM/MeOH as

eluent (100:0 to 90:10) to yield (*S*)-ε-methylbromo-ε-caprolactone (300 mg, 1.45 mmol, 49% yield) as a clear, yellow, viscous liquid with 85% *ee*. Characterisation was consistent with previous reports.[1]

^{1}H NMR (300 MHz, 298 K, $CDCl_3$): δ = 4.55 – 4.31 (m, 1H, H^f), 3.52 (dd, J = 10.6, 5.7 Hz, 1H, H^g), 3.40 (dd, J = 10.6, 6.1 Hz, 1H, $H^{g'}$), 2.79 – 2.47 (m, 2H, H^b), 2.27 – 2.09 (m, 1H, H^e), 2.08 – 1.81 (m, 2H, H^c), and 1.76 – 1.47 (m, 3H, $H^{e'}$, H^d) ppm.

^{13}C NMR (100 MHz, 298 K, $CDCl_3$): δ = 174.1 (C^a), 79.3 (C^f), 34.8(C^b), 34.2 (C^g), 33.0 (C^e), 27.9 (C^c), and 22.8 (C^d) ppm.

FT-IR υ_{max} (cm^{-1}): 2938 (υ C–H), 1724 (υ C=O), 743 (υ C–Br).

6.3.6. General procedure for ROP of (S)-substituted-ε-caprolactone

Within a glovebox, in a vial the appropriate (*S*)-ε-substituted-ε-caprolactone (0.6 mmol, 100 equiv.) was dissolved in C_6D_6 (550 µL). In a separate vial, a stock solution of BnOH (0.006 mmol, 1 equiv.) and DPP (0.006 mmol, 1 equiv.) was dissolved in C_6D_6 (500 µL). The stock solution (50 µL) was added to the monomer solution to start the polymerisation. The polymerisation was transferred to a J Youngs tube, removed from the glovebox and heated to the appropriate temperature. At the appropriate monomer conversion, the polymerisation was quenched by the addition of basic Amberlyst 21 and purified by precipitation into cold hexanes to provide the corresponding polymer as a clear, viscous polymer.

<u>P((*S*)-ε-methylacetyloxy-ε-caprolactone)</u>

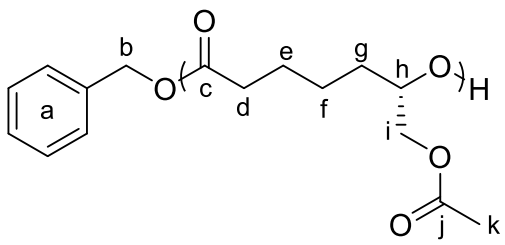

Polymerisation performed at room temperature.

^{1}H NMR (400 MHz, 298 K, $CDCl_3$): δ = 7.40 – 7.29 (m, H^a), 5.06 (s, H^b), 5.01 (dt, J = 9.4, 5.1

Hz, H^h), 4.18 (dd, J = 12.0, 3.3 Hz, H^i), 3.96 (dd, J = 12.0, 6.6 Hz, $H^{i'}$), 2.27 (t, J = 7.5 Hz, H^d), 2.01 (s, H^k), 1.73 – 1.47 (m, H^e, H^g), and 1.41 – 1.23 (m, H^f) ppm.

^{13}C NMR (100 MHz, 298 K $CDCl_3$): δ = 173.0 (C^c), 170.5 (C^j), 128.6(C^a), 128.2 (C^a), 128.1 (C^a), 75.6 (C^h), 68.7 (C^b), 64.9 (C^i), 33.8 (C^d), 30.5 (C^e), 24.7 (C^g), 24.5 (C^f), and 21.1 (C^k) ppm.

SEC ($CHCl_3$, RI): M_n = 9,350 g·mol^{-1}, M_w = 10,900 g·mol^{-1}, $Đ_M$ = 1.16

P((*S*)-ε-methyl-*N*-hexylcarbamate-ε-caprolactone)

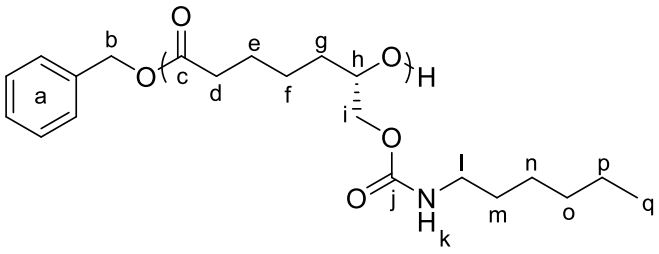

^{1}H NMR (400 MHz, 298 K, $CDCl_3$): δ = 7.40 – 7.31 (m, H^a), 5.10 (s, H^b), 4.77 (s, H^k), 4.46 (m, H^h), 4.15 (qt, J = 11.7, 5.5 Hz, H^i), 3.16 (td, J = 7.1, 5.9 Hz, H^l), 2.78 – 2.53 (m, H^g), 2.10 – 1.84 (m, H^d), 1.74 – 1.53 (m, H^e, H^f), 1.53 – 1.40 (m, H^m), 1.39 – 1.20 (m, H^n, H^o, H^p), and 0.94 – 0.78 (m, H^q) ppm.

^{13}C NMR (125 MHz, 298 K, $CDCl_3$): δ = 174.2 (C^c), 160.0 (C^j), 128.7(C^a), 128.3 (C^a), 128.3 (C^a), 74.1 (C^h), 64.8 (C^b), 62.3 (C^i), 40.3 (C^l), 39.7 (C^d), 32.2 (C^g), 31.9 (C^m), 28.4 (C^n), 28.4 (C^o), 25.6 (C^e), 24.2 (C^f), 22.9 (C^p), and 17.4 (C^q) ppm.

SEC ($CHCl_3$, RI): M_n = 13,400 g·mol^{-1}, M_w = 12,900 g·mol^{-1}, $Đ_M$ = 1.07

P((*S*)-ε-methylbromo-ε-caprolactone)

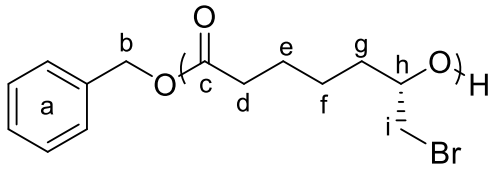

^{1}H NMR (500 MHz, 298 K, $CDCl_3$): δ = 7.42 – 7.28 (m, H^a), 5.10 (s, H^b), 4.98 (ddd, J = 11.3, 6.3, 4.6 Hz, H^h), 3.55 – 3.45 (m, H^i), 3.41 (dd, J = 10.9, 5.4 Hz, $H^{i'}$), 2.35 (qd, J = 7.6, 7.2, 2.3 Hz, H^d), 1.78 – 1.60 (m, H^e, H^g), and 1.45 – 1.27 (m, 1H^f) ppm.

^{13}C NMR (125 MHz, 298 K, $CDCl_3$): δ = 172.8 (C^c), 136.1 (C^a), 128.7 (C^a), 128.3 (C^a), 72.2 (C^h) , 70.9 (C^b), 34.3 (C^d), 34.2 (C^i), 32.3 (C^e), 32.3 (C^g), and 24.71 (C^f) ppm.

SEC ($CHCl_3$, RI): M_n = 9,500 g·mol^{-1}, M_w = 8,750 g·mol^{-1}, $Đ_M$ = 1.12

6.4. Experimental procedures for Chapter three

6.4.1. General procedure for Baeyer-Villiger ring-expansion of substituted cyclohexanones

Using a modified version of the previously reported procedure,[1] a 250 mL round-bottomed flask (dried overnight in the oven and under a N_2 atmosphere), was charged with the appropriate substituted cyclohexanone (35.7 mmol, 1.0 equiv.) in dry CH_2Cl_2 (150 mL) and cooled using an ice-bath. To this, $NaHCO_3$ (53.6 mmol, 1.5 equiv.) was added to form a heterogenous mixture. *m*-Chloroperoxybenzoic acid <77% (42.8 mmol, 1.2 equiv.) was added in small aliquots and allowed to warm to room temperature overnight to form a viscous white liquid. The solution was diluted with CH_2Cl_2 (50 mL) and solid sodium thiosulfate (17.9 mmol, 0.5 equiv.) was added and left to stir at room temperature for 20 min. Solids were removed and washed with CH_2Cl_2 (200 mL). Organics were combined and volatiles were removed. Product was purified *via* flash chromatography using hexane/EtOAc (100:0 to 0:100) as eluent to provide the corresponding ε-substituted-ε-caprolactone as a colourless, viscous liquid.

<u>εHL</u>:

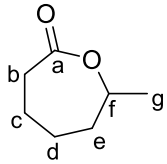

2.50 g, 19.5 mmol, 55% yield. Characterisation was consistent with previous reports.[2]

^{1}H NMR (400 MHz, 298 K, $CDCl_3$): δ = 4.42 (m, 1H, H^f), 2.60 (m, 2H, H^b), 1.87 and 1.57 (m, 6H, H^c, H^d, H^e), 1.30 (d, 3H, H^g) ppm.

^{13}C NMR (125 MHz, 298 K, $CDCl_3$): δ = 175.8 (C^a), 76.9 (C^f), 36.3 (C^b), 35.1 (C^e), 28.3 (C^c), 22.9 (C^d) and 22.6 (C^g) ppm.

εAL:

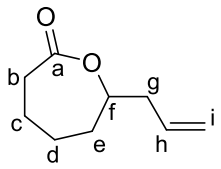

2.26 g, 14.7 mmol, 51% yield. Characterisation was consistent with previous reports.[3]

^{1}H NMR (400 MHz, 298 K, $CDCl_3$): δ = 5.91-5.77 (m, 1H, H^h), 5.18-5.08 (m, 2H, H^i), 4.34-2.45 (m, 1H, H^f), 2.75-2.55 (m, 2H, H^b), 2.54-2.44 (m, 1H, H^g), 2.38-2.29 (m, 1H, $H^{g'}$), 2.03-1.88 (m, 3H, H^c, H^d, H^e), and 1.67-1.51 (m, 3H, $H^{c'}$, $H^{d'}$, $H^{e'}$) ppm.

^{13}C NMR (125 MHz, 298 K, $CDCl_3$): δ = 175.6 (C^a), 133.3 (C^h), 118.5 (C^i), 79.9 (C^f), 40.5 (C^g), 22.94 (C^d) 34.9 (C^e), 33.6 (C^b), 28.2 (C^d) and 22.9 (C^c) ppm.

6.4.2. General procedure for ROP of ε-substituted-ε-caprolactone

Within a glovebox, in a vial the appropriate ε-substituted-ε-caprolactone (0.6 mmol, 100 equiv.) was dissolved in C_6D_6 (550 µL). In a separate vial, a stock solution of BnOH (6.2 µL, 0.006 mmol, 1 equiv.) and appropriate phosphoric acid catalyst (0.006 mmol, 1 equiv.) was dissolved in C_6D_6 (500 µL). The stock solution (50 µL) was added to the monomer solution to start the polymerisation. The polymerisation was transferred to a J-Youngs tube, removed from the glovebox and heated at the appropriate temperature (Tables 6.1-3.). At a 50% monomer conversion the polymerisation was quenched by the addition of basic Amberlyst 21 and purified by precipitation into cold hexanes to provide the corresponding polymer as a clear, viscous polymer.

PεHL:

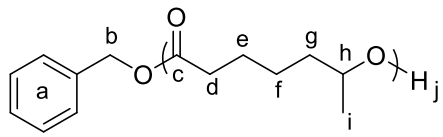

^{1}H NMR (500 MHz, 298 K, $CDCl_3$): δ = 7.33 – 7.22 (m, H^a), 5.04 (s, H^b), 4.87 – 4.77 (m, H^h), 2.20 (t, J = 7.5 Hz, H^d), 1.61 – 1.36 (m, H^e, H^g), 1.35 – 1.17 (m, H^f), and 1.12 (d, J = 6.1 Hz, H^i) ppm.

^{13}C NMR (125 MHz, 298 K, $CDCl_3$): δ = 173.3,128.7 (C^a), 128.3 (C^a), 128.3 (C^a), 70.7 (C^h), 35.7 (C^b), 34.6 (C^g), 25.1 (C^d), 25.0 (C^e), 24.9 (C^f), and 20.08 (C^i) ppm.

Table 6.1. SEC data for PεHL

Catalyst	Temperature (°C)	Conversion[a] (%)	$M_{n,\,theor}$[b] (g·mol^{-1})	$M_{n,\,SEC}$[c] (g·mol^{-1})	$Đ_M$[c]
DPP	70	30	3,950	4,200	1.07
(*R*)-pentafluoro	70	49	6,400	6,500	1.05
(*R*)-pentafluoro	25	50	6,500	6,550	1.02
(*R*)-bis trifluoro	70	45	5,900	5,750	1.11
(*R*)-cyclohexyl	70	50	6,500	6,750	1.09
(*R*)-bis trifluoro trif	70	48	6,650	6,900	1.14
Imido	70	55	7,150	8,300	1.18
(*R*)-TRIP	70	45	5,850	5,900	1.03
(*R*)-TRIP	40	51	6,600	6,550	1.04
(*R*)-TRIP	25	47	6,100	6,100	1.02
(*R*)-TRIP	5	54	7,000	7,000	1.02

[a] Determined by ^{1}H NMR spectroscopy. [b] $M_{n,theor} = ([\varepsilon HL]_0/[BnOH]_0) \times MW_{(\varepsilon HL)} \times$ (% conv.) + $MW_{(BnOH)}$. [c] Determined by $CHCl_3$ SEC using polystyrene standards and a RI detector.

PεAL:

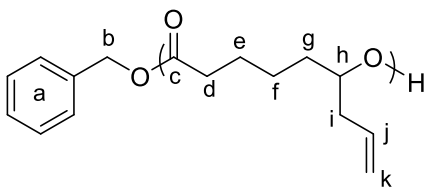

^{1}H NMR (500 MHz, 298 K, $CDCl_3$): δ = 7.41 – 7.28 (m, H^a), 5.72 (ddt, J = 17.2, 10.3, 7.0 Hz, H^j), 5.10 (s,

H^b), 5.08 – 5.00 (m, H^k), 4.89 (m, H^h), 2.31 – 2.20 (m, H^d), 1.75 – 1.44 (m, H^e, H^f, H^g), and 1.43 – 1.19 (m, H^e, H^f, H^g) ppm.

^{13}C NMR (125 MHz, 298 K, $CDCl_3$): δ = 173.2 (C^c), 133.8 (C^j), 128.7 (C^a), 128.3 (C^a) 128.3 (C^a), 117.8 (C^k), 73.0 (C^h), 38.7 (C^b), 34.5 (C^g), 33.4 (C^d), 33.3 (C^i), 25.02 (C^e), and 25.01 (C^f) ppm.

Table 6.2. SEC data for PεAL

Catalyst	Temperature (°C)	Conversion[a] (%)	$M_{n,\,theor}$[b] (g·mol^{-1})	$M_{n,\,SEC}$[c] (g·mol^{-1})	$Đ_M$[c]
DPP	70	89	13,800	13,950	1.08
(*R*)-pentafluoro	70	54	8,400	8,550	1.05
(*R*)-bis trifluoro	70	50	7,800	8,000	1.09
(*R*)-TRIP	70	47	7,350	7,400	1.04
(*R*)-TRIP	40	51	7,950	7,900	1.04
(*R*)-TRIP	25	55	8,500	8,300	1.06

[a] Determined by ^{1}H NMR spectroscopy. [b] $M_{n,theor} = ([\varepsilon AL]_0/[BnOH]_0) \times MW_{(\varepsilon AL)} \times (\%\ conv.) + MW_{(BnOH)}$. [c] Determined by $CHCl_3$ SEC using polystyrene standards and a RI detector.

PεDL:

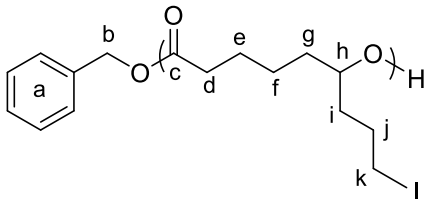

^{1}H NMR (500 MHz, 298 K, $CDCl_3$): δ = 7.41 – 7.29 (m, H^a), 5.11 (s, H^b), 4.91 – 4.78 (m, H^h), 2.27 (t, J = 7.6 Hz, H^d), 1.71 – 1.44 (m, H^e, H^f, H^g, H^i, H^j, H^k), 1.40 – 1.16 (m, $H^{e'}$, $H^{f'}$, $H^{g'}$,$H^{i'}$, $H^{j'}$, $H^{k'}$), and 0.88 (t, J = 7.0 Hz, H^l) ppm.

^{13}C NMR (125 MHz, 298 K, $CDCl_3$): δ = 173.4 (C^c), 128.7 (C^a), 128.3 (C^a), 128.3 (C^a), 74.0 (C^h), 34.6 (C^b), 34.0 (C^g), 33.9 (C^d), 27.6 (C^i), 25.2 (C^e), 25.1 (C^f), 25.1 (C^j), 22.7 (C^k), and 14.2 (C^l) ppm.

Table 6.3 SEC data for PεDL

Catalyst	Temperature (°C)	Conversion[a] (%)	$M_{n,\,theor}$[b] (g·mol^{-1})	$M_{n,\,SEC}$[c] (g·mol^{-1})	$Đ_M$[c]
DPP	70	84	14,400	14,200	1.05
(*R*)-pentafluoro	70	53	9,100	9,350	1.06
(*R*)-cyclohexyl	70	56	9,600	9,450	1.07
(*R*)-TRIP	70	50	8,600	8,900	1.09
(*R*)-TRIP	40	53	9,100	9,050	1.02
(*R*)-TRIP	25	54	9,300	9,450	1.06

[a] Determined by ^{1}H NMR spectroscopy. [b] $M_{n,theor} = ([\varepsilon DL]_0/[BnOH]_0) \times MW_{(\varepsilon DL)} \times (\%\ conv.) + MW_{(BnOH)}$. [c] Determined by $CHCl_3$ SEC using polystyrene standards and a RI detector.

6.5. Experimental procedures for Chapter four

*6.5.1. Synthesis of 1,3-dihexylpyrimidine-2,4,6(1*H*,3*H*,5*H*)-trione*

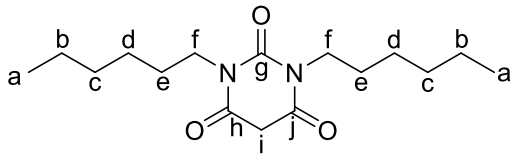

Following an adapted procedure,[4] to a 100 mL round-bottomed flask (dried in oven overnight and under an N_2 atmosphere) was added *N*-hexylamine (2 g, 15.48 mmol, 1 equiv.) in dry CH_2Cl_2 (100 mL) and cooled using an ice bath. In a separate dry and air-free round-bottomed flask, *N*-hexyl isocyanate (2.25 mL, 15.48 mmol, 1 equiv.) was dissolved in CH_2Cl_2 (30 mL). The isocyanate solution was added to the amine solution dropwise. The mixture was warmed to room temperature and left to stir for 1 h after which malonyl dichloride (1.51 mL, 15.48 mmol, 1 equiv.) was added and the reaction was heated to reflux for 1 h. Once cooled to room temperature, the reaction was quenched by the addition of 1 M HCl (60 mL). The aqueous phase was extracted with CH_2Cl_2 (2 × 50 mL) and the combined organic phases were washed with H_2O (50 mL). The organic phase was dried with anhydrous $MgSO_4$, and after solids and volatiles were removed the crude product was purified by flash chromatography using hexane/EtOAc as eluent (90:10 to 80:20) to yield 1,3-

dihexylpyrimidine-2,4,6(1*H*,3*H*,5*H*)-trione (3.20 g, 10.8 mmol, 69% yield) as a yellow oil.

^{1}H NMR (400 MHz, 298 K, $CDCl_3$): δ = 3.89 – 3.79 (m, 4H, H^f), 3.63 (s, 2H, H^i), 1.63 – 1.50 (m, 4H, H^e), 1.36 – 1.26 (m, 12H, H^b, H^c, H^d), and 0.94 – 0.81 (m, 6H, H^a) ppm.

^{13}C NMR (125 MHz, $CDCl_3$): δ 164.7 (C^h, C^j) , 151.5 (C^g), 42.2 (C^f), 39.8 (C^i), 31.5 (C^e), 28.0 (C^d), 26.6 (C^c), 22.6 (C^b), and 14.2 (C^a) ppm.

HRMS (ESI-TOF): m/z calculated for $C_{16}H_{28}N_2O_3Na$ $[M+Na]^+$ 320.2182, found 320.2178.

*6.5.2. Synthesis of 5-(furan-2-ylmethylene)-1,3-dihexylpyrimidine-2,4,6(1*H*,3*H*,5*H*)-trione*

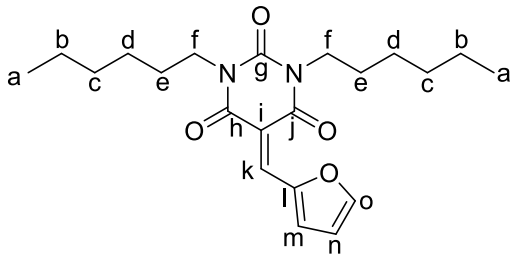

Following an adapted procedure,[4] to a solution of 1,3-dihexylpyrimidine-2,4,6(1*H*,3*H*,5*H*)-trione (3.20 g, 10.8 mmol, 1 equiv.) in CH_2Cl_2 (50 mL) was added furfural (0.89 mL, 10.8 mmol, 1 equiv.) to form a deep yellow solution which was left to stir at room temperature for 5 h. The mixture was then washed with H_2O (3 × 15 mL). The organic layer was then dried with anhydrous $MgSO_4$. After the removal of solids and volatiles 5-(furan-2-ylmethylene)-1,3-dihexylpyrimidine-2,4,6(1*H*,3*H*,5*H*)-trione (2.98 g, 7.96 mmol, 73% yield) was provided as a yellow powder.

^{1}H NMR (300 MHz, 298 K, $CDCl_3$): δ = 8.62 (d, J = 3.8 Hz, 1H, H^o), 8.42 (s, 1H, H^k), 7.83 (d, J = 1.6 Hz, 1H, H^m), 6.72 (dd, J = 3.8, 1.6 Hz, 1H, H^n), 4.31 – 3.68 (m, 4H, H^f), 1.75 – 1.50 (m, 4H, H^e), 1.33 (h, J = 6.5, 5.5 Hz, 12H, H^b, H^c, H^c), and 0.90 (d, J = 6.6 Hz, 6H, H^a) ppm.

^{13}C NMR (100 MHz, 298 K, $CDCl_3$): δ = 162.2 (C^h, C^j), 151.3 (C^g), 151.0 (C^l), 150.1 (C^k), 140.9 (C^o), 127.7 (C^n), 114.9 (C^m), 111.9 (C^i), 42.5 (C^h), 41.7(C^f)31.4 (C^e), 28.1 (C^d), 26.6 (C^c), 22.3 (C^b), and 14.1 (C^a) ppm.

HRMS (ESI-TOF): m/z calculated for $C_{21}H_{30}N_2O_4Na$ $[M+Na]^+$ 398.2290, found 398.2284.

*6.5.3. Synthesis of 5-((2Z,4*E*)-5-(diethylamino)-2-hydroxypenta-2,4-dien-1-ylidene)-1,3-dihexylpyrimidine-2,4,6(1*H*,3*H*,5*H*)-trione (DEA DASA)*

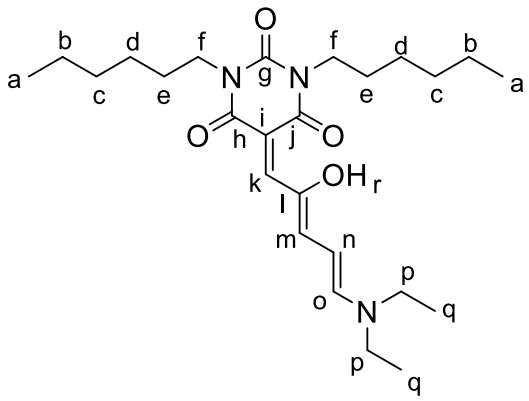

DEA DASA was synthesised adapting a reported procedure.[4] To a solution of 5-(furan-2-ylmethylene)-1,3-dihexylpyrimidine-2,4,6(1*H*,3*H*,5*H*)-trione (375 mg, 1 mmol, 1 equiv.) in THF (10 mL) was added diethyl amine (103 µL, 1 mmol, 1 equiv.) to form a dark-pink solution. The reaction was left to stir at room temperature for 1 h. After the removal of volatiles, DEA DASA (395 mg, 882 µmol, 88% yield) was afforded as a dark-pink solid.

^{1}H NMR (400 MHz, 298 K, $CDCl_3$): δ = 12.65 – 12.61 (brs, 1H, H^r), 7.19 (s, 1H, H^k), 7.16 (s, 1H, H^o), 6.70 (dd, J = 12.3, 1.4 Hz, 1H, H^m), 6.05 (t, J = 12.3 Hz, 1H, H^n), 3.97 – 3.87 (m, 4H, H^f), 3.47 (dq, J = 9.3, 7.1 Hz, 4H, H^p), 1.67 – 1.56 (m, 4H, H^e), 1.39 – 1.16 (m, 18H, H^b, H^c, H^d, H^q), and 0.96 – 0.80 (m, 6H, H^a) ppm.

^{1}H NMR (125 MHz, 298 K, $CDCl_3$): δ = 165.2 (C^l), 163.3 (C^i), 156.0 (C^k), 151.7 (C^g), 150.2 (C^o), 146.7 (C^h, C^j), 140.0 (C^n), 102.4 (C^m), 68.2 (C^p), 51.8 (C^f), 44.1 (C^e), 42.0 (C^d), 41.8 (C^c), 31.7 (C^b), 28.3 (C^a), (C^l), and 22.8 (C^q) ppm.

HRMS (ESI-TOF): m/z calculated for $C_{25}H_{41}N_3O_4Na$ $[M+Na]^+$ 471.3179, found 398.3175.

6.5.4. General procedure for switchable DASA catalysed ROP of δVL

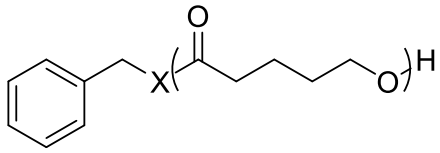

X = O or S

Within a glovebox, in a vial the appropriate δVL (0.180 g, 1.8 mmol, 30 equiv.) was dissolved in $Cl_2CDCDCl_2$ (500 µL). In a separate vial, a stock solution of DEA DASA (13.4 mg, 0.03 mmol, 0.5 equiv.) was dissolved in $Cl_2CDCDCl_2$ (500 µL) to form a deep pink solution. The stock solution (100 µL, 0.1 equiv. of DEA DASA) was added to the δVL solution, after which either BnSH or BnOH (0.06 mmol, 1 equiv.) was added. The polymerisation was transferred to a J-Youngs tube and removed from the glovebox kept in the dark at room temperature for 24 h. To begin initiation the J-Youngs tube was illuminated using an OmniCure Series 1500 UV Spot Curing System with 320-500nm bandpass filter. After an appropriate monomer conversion was reached, the J-Youngs tube was heated to 110 °C for at least 12 h to pause propagation. To ensure a pause in propagation, the J-Youngs tube was cooled to room temperature and kept in the dark for a minimum of 12 h. Further control over light and temperature allowed for command over the ON and OFF state of polymerisation until an appropriate monomer conversion was reached. The polymer was then quenched and purified through multiple precipitations into cold hexanes

<u>PδVL – BnOH initiated</u>

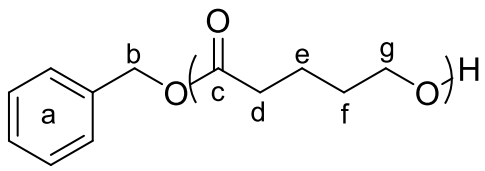

^{1}H NMR (300 MHz, 298 K, $CDCl_3$): δ = 7.44 – 7.29 (m, H^a), 5.11 (s, H^b), 4.22 – 3.94 (m, H^g), 2.46 – 2.23 (m, H^d), and 1.82 – 1.57 (m, H^e, H^f) ppm.

SEC ($CHCl_3$, RI): M_n = 3,900 g·mol^{-1}, M_w = 6,200 g·mol^{-1}, $Đ_M$ = 1.60

PδVL – BnSH initiated

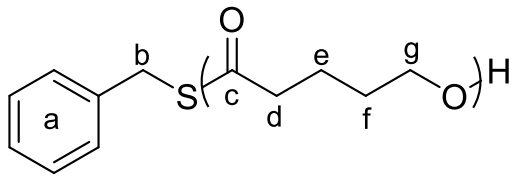

^{1}H NMR (300 MHz, 298 K, $CDCl_3$): δ = 4.19 – 3.90 (m, H^g), 2.49 – 2.19 (m, H^d), and 1.78 – 1.58 (m, H^e, H^f) ppm. *Note*, *aromatic peaks (H^a and H^b) were not visible by ^{1}H NMR spectroscopy.*

SEC ($CHCl_3$, RI): M_n = 10,400 g·mol^{-1}, M_w = 17,900 g·mol^{-1}, $Đ_M$ = 1.71

6.6. References

1. A. Chen, J. Xu, W. Chiang and C. L. L. Chai, *Tetrahedron*, 2010, **66**, 1489-1495.
2. L. van der Mee, F. Helmich, R. de Bruijn, J. A. J. M. Vekemans, A. R. A. Palmans and E. W. Meijer, *Macromolecules*, 2006, **39**, 5021-5027.
3. X. Just-Baringo, J. Clark, M. J. Gutmann and D. J. Procter, *Angew. Chem. Int. Ed.*, 2016, **55**, 12499-12502.
4. S. Helmy, F. A. Leibfarth, S. Oh, J. E. Poelma, C. J. Hawker and J. Read de Alaniz, *J. Am. Chem. Soc.*, 2014, **136**, 8169-8172.